

The Texas Medical Center Library

DigitalCommons@TMC

The University of Texas MD Anderson Cancer
Center UTHealth Graduate School of
Biomedical Sciences Dissertations and Theses
(Open Access)

The University of Texas MD Anderson Cancer
Center UTHealth Graduate School of
Biomedical Sciences

12-2010

14-3-3SIGMA NEGATIVELY REGULATES THE STABILITY AND SUBCELLULAR LOCALIZATION OF COP1

Chun-Hui Su

Follow this and additional works at: https://digitalcommons.library.tmc.edu/utgsbs_dissertations

 Part of the [Biology Commons](#)

Recommended Citation

Su, Chun-Hui, "14-3-3SIGMA NEGATIVELY REGULATES THE STABILITY AND SUBCELLULAR LOCALIZATION OF COP1" (2010). *The University of Texas MD Anderson Cancer Center UTHealth Graduate School of Biomedical Sciences Dissertations and Theses (Open Access)*. 101.
https://digitalcommons.library.tmc.edu/utgsbs_dissertations/101

This Dissertation (PhD) is brought to you for free and open access by the The University of Texas MD Anderson Cancer Center UTHealth Graduate School of Biomedical Sciences at DigitalCommons@TMC. It has been accepted for inclusion in The University of Texas MD Anderson Cancer Center UTHealth Graduate School of Biomedical Sciences Dissertations and Theses (Open Access) by an authorized administrator of DigitalCommons@TMC. For more information, please contact digitalcommons@library.tmc.edu.

The
TMC LIBRARY
Health Sciences Resource Center

14-3-3SIGMA NEGATIVELY REGULATES THE STABILITY AND
SUBCELLULAR LOCALIZATION OF COP1

By
Chun-Hui Su, M.S.

APPROVED:

Mong-Hong Lee, Supervisory Professor

Randy J. Legerski, Ph.D.

Pierre D. McCrea, Ph.D.

Lei Li, Ph.D.

Hui-Kuan Lin, Ph.D.

APPROVED:

George M. Stancel, Ph.D.

Dean, The University of Texas

Health Science Center at Houston

Graduate School of Biomedical Sciences at Houston

14-3-3SIGMA NEGATIVELY REGULATES THE STABILITY AND
SUBCELLULAR LOCALIZATION OF COP1

A

DISSERTATION

Presented to the Faculty of

The University of Texas

Health Science Center at Houston

And

The University of Texas

M.D. Anderson Cancer Center

Graduate School Biomedical Sciences

in Partial Fulfillment

of the Requirements

for the Degree of

DOCTOR OF PHILOSOPHY

by

Chun-Hui Su, B.S., M.S.

Houston, Texas

December, 2010

ACKNOWLEDGEMENTS

I am appreciative of Dr. Mong-Hong Lee for his guidance and support on the path to pursue my Ph.D. at Graduate School of Biomedical Sciences at Houston, the University of Texas. This work was facilitated by his inspiration, advice, and discussion. He provided me with a conducive environment for integrating the multi-disciplinary knowledge in cancer biology, cell biology and biochemistry for my projects. Many thanks go to my second mentor Dr. Sai-Ching J Yeung. He always patiently gives me critical opinions, and teaches me basic statistical analysis to help my projects move forward.

I also appreciate my supervisory committee members, Dr. Randy J. Legerski, Dr. Pierre D. McCrea, Dr. Lei Li, and Dr. Hui-Kuan Lin. They give my critical opinions and wonderful suggestions in science and in my processes toward my Ph.D. degree. I truly appreciate my advisory and examining committee members, Dr. Sandy Chang, Dr. Khandan Keyomarsi, and Dr. Dos D. Sarbassov for their comments and corrections to make this work more improved and advanced.

I am appreciative to all the current and alumni members in Dr. Mong-Hong Lees' lab, especially Dr. Ruiying Zhao and Dr. Jian Chen, who provide many creative ideas and detailed explanations in methodology. I will always remember the suggestions that Edward Wang, Guermarie Velazquez-Torres, and Colin Carlock gave to finish the dissertation writing.

Thanks to our core facilities. The DNA sequencing core lab and immunohistochemistry core lab provided great services.

Thanks to staff and friends in Department of Molecular and Cellular Oncology. Especially Dr. Zhenbo Han and Bill Spohn give me microscopy support anytime. They provide me enjoyable learning process.

I finally thank my parents. Without their support I could not even come to the U.S. to start my research. My daughter, Shannon, always cheers me up when I feel down. Definitely I appreciate my husband, Tsai-Wei Shen, for his company and sacrifice to support me in this journey.

14-3-3SIGMA NEGATIVELY REGULATES THE STABILITY AND SUBCELLULAR LOCALIZATION OF COP1

Publication No. _____

Chun-Hui Su, B.S., M.S.

Supervisory Professor: Mong-Hong Lee, Ph.D.

Mammalian constitutive photomorphogenic 1 (COP1), a p53 E3 ubiquitin ligase, is a key negative regulator for p53. DNA damage leads to the translocation of COP1 to the cytoplasm, but the underlying mechanism remains unknown. We discovered that 14-3-3 σ controlled COP1 subcellular localization and protein stability. Investigation of the underlying mechanism suggested that, upon DNA damage, 14-3-3 σ bound to phosphorylated COP1 at S387, resulting in COP1 translocation to the cytoplasm and cytoplasmic COP1 ubiquitination and proteasomal degradation. 14-3-3 σ targeted COP1 for degradation to prevent COP1-mediated p53 degradation, p53 ubiquitination, and p53 transcription repression. COP1 expression promoted cell proliferation, cell transformation, and tumor progression, attesting to its role in cancer promotion. 14-3-3 σ negatively regulated COP1 function and prevented tumor growth in cancer xenografts. COP1 protein levels were inversely correlated with 14-3-3 σ protein levels in human breast and pancreatic cancer specimens. Together, these results define a novel, detailed mechanism for the posttranslational regulation of COP1 upon DNA damage and provide a mechanistic

explanation of the correlation of COP1 overexpression with 14-3-3 σ downregulation during tumorigenesis.

TABLE OF CONTENTS

APPROVAL FORM	i
TITLE PAGE	ii
ACKNOWLEDGEMENTS	iii
ABSTRACT	v
TABLE OF CONTENTS	vii
LIST OF FIGURES	xi
LIST OF TABLES	xv
LIST OF ABBREVIATIONS	xvi
Chapter 1: Introduction	1
1.1 Introduction of 14-3-3 proteins	1
1.2 Introduction of 14-3-3 σ	5
1.3 The E3 ligase EFP for 14-3-3 σ	6
1.4 14-3-3 σ regulations on p53 in a positive feedback loop in response to DNA damage	7
1.5 14-3-3 σ negative regulation on a p53 E3 ligase MDM2	8
1.6 The discovery of COP1 and its role in Arabidopsis	9
1.7 Introduction of mammalian COP1	10
1.8 Substrates of COP1 E3 ligase	11
1.9 COP1 upstream regulators: COP9 signalosome	14
1.10 The role of COP1 in response to DNA damage	15
1.11 The role of COP1 in cancer	16

1.12	Rationale and hypothesis	17
Chapter 2: Materials and Methods		19
2.1	Cell Culture and Reagents	19
2.2	Antibodies and reagents	19
2.3	Construction of expression plasmid	22
2.4	Immunoprecipitation and immunoblotting	22
2.5	<i>In vitro</i> binding assay	24
2.6	<i>In vivo</i> ubiquitination assay	24
2.7	<i>In vitro</i> ubiquitination assay	25
2.8	Quantitative-PCR	25
2.9	Luciferase reporter gene assay	26
2.10	Generation of stable transfectants	27
2.11	Live-cell imaging	27
2.12	Cell fractionation	28
2.13	Soft agar colony formation	28
2.14	Foci formation assay	28
2.15	MTT assay	29
2.16	Cell cycle analysis	29
2.17	Nude mice experiment	29
2.18	Immunohistochemistry	30
Chapter 3: Results		32
3.1	14-3-3 σ is required for doxorubicin-mediated COP1 downregulation	32

3.2	14-3-3 σ -mediated COP1 downregulation is 26S proteasome-dependent	36
3.3	Identification of COP1 binding region on 14-3-3 σ and 14-3-3 σ binding region on COP1	40
3.4	14-3-3 σ promotes COP1 ubiquitination	45
3.5	14-3-3 σ affects COP1 subcellular localization	50
3.6	14-3-3 σ binding to COP1 is phosphorylation-dependent	60
3.7	COP1 S387 phosphorylation is required for 14-3-3 σ -mediated COP1 nuclear export	66
3.8	COP1 S387 phosphorylation is important for 14-3-3 σ -mediated COP1 degradation	69
3.9	14-3-3 blocks COP1-mediated p53 degradation and transcriptional repression	74
3.10	14-3-3 σ inhibits COP1-mediated cell proliferation and transformation	81
3.11	14-3-3 σ inhibits COP1-mediated tumor progression	88
3.12	COP1 and 14-3-3 σ has an inverse relationship	93
Chapter 4: Discussion		97
4.1	The functions of COP1 determined by binding of COP1-interacting proteins on regions of COP1	97
4.2	Regulation of COP1 stability in unstressed cells	98
4.3	COP1 is 14-3-3 σ phosphorylation binding protein	99
4.4	The stability of COP1 in response to DNA damage	100
4.5	14-3-3 σ is downregulating COP1 and inhibits COP1-mediated cell cycle	101

progression	
4.6 14-3-3 σ plays an important role in protection p53 from E3 ligase	102
4.7 Roles of COP1 in chromosome stability	103
4.8 14-3-3 σ impact on an oncoprotein COP1	104
4.9 Possible COP1 upstream positive regulators/kinases	104
4.10 Future directions	105
Chapter 5: References	111
Vita	126

LIST OF FIGURES

Figure 1-1	14-3-3 family cladogram	5
Figure 1-2	Domains and substrates of mammalian COP1	13
Figure 3-1	COP1 expression is downregulated in response to DNA damage	33
Figure 3-2	DNA damage-mediated COP1 downregulation is mitigated by the treatment with MG132	34
Figure 3-3	DNA damage-mediated COP1 downregulation is recovered in 14-3-3 σ null cells	35
Figure 3-4	14-3-3 σ downregulates steady-state levels of COP1	37
Figure 3-5	The half-life of COP1 is prolonged in 14-3-3 σ null cells	38
Figure 3-6	14-3-3 σ downregulates COP1 through 26S proteasome pathway	39
Figure 3-7	Endogenous 14-3-3 σ binds to endogenous COP1	41
Figure 3-8	14-3-3 σ directly binds to COP1	42
Figure 3-9	Map of the 14-3-3 σ binding region within COP1	43
Figure 3-10	Identification of 14-3-3 σ domains interacts with COP1	44
Figure 3-11	14-3-3 σ enhances polyubiquitination of COP1	46
Figure 3-12	COP1 ubiquitination is reduced in 14-3-3 σ -null cells	47
Figure 3-13	COP1 ubiquitination is reduced in 14-3-3 σ knockdown cells	48
Figure 3-14	14-3-3 σ promotes COP1 self-ubiquitination	49
Figure 3-15	COP1 nuclear accumulation is blocked in IR-induced cells using confocal microscopy	53
Figure 3-16	The portion of cytoplasmic COP1 is increased in response to	54

	doxorubicin and IR using cell fractionation	
Figure 3-17	COP1 shuttling is blocked by ectopic 14-3-3 σ expression	56
Figure 3-18	COP1 shuttling is blocked to the cytoplasm in 14-3-3 σ -null and knockdown cells	57
Figure 3-19	14-3-3 σ nuclear export signal is required for mediating cytoplasmic accumulation of COP1	59
Figure 3-20	COP1 contains 14-3-3 σ consensus binding motif	62
Figure 3-21	Binding between 14-3-3 σ and COP1 is phosphorylation-dependent	63
Figure 3-22	ATM facilitates the binding between 14-3-3 σ and COP1	64
Figure 3-23	COP1 (S387A) abolishes binding to 14-3-3 σ <i>in vivo</i>	65
Figure 3-24	14-3-3 σ -induced COP1 translocation to the cytoplasm is S387 phosphorylation-dependent	67
Figure 3-25	14-3-3 σ -induced COP1 translocation to the cytoplasm is S387 phosphorylation-dependent	68
Figure 3-26	14-3-3 σ downregulates COP1 (WT) but not COP1 (S387A) steady state	70
Figure 3-27	14-3-3 σ facilitates turnover rate of COP1 (WT) but not COP1 (S387A)	71
Figure 3-28	14-3-3 σ promotes COP1 (WT) but not COP1 (S387A) polyubiquitination	72
Figure 3-29	14-3-3 σ promotes cytoplasmic COP1 polyubiquitination in response to DNA damage	73

Figure 3-30	14-3-3 σ antagonizes COP1-mediated p53 degradation	76
Figure 3-31	14-3-3 σ inhibits COP1-mediated p53 polyubiquitination	77
Figure 3-32	14-3-3 σ reduces COP1-mediated poly-ubiquitination of p53 regardless of the deficiency of MDM2	78
Figure 3-33	14-3-3 σ impairs COP1-mediated p53 transcriptional repression determined by quantitative RT-PCR in cells	79
Figure 3-34	14-3-3 σ antagonizes COP1-suppressed p53 transcriptional activity	80
Figure 3-35	14-3-3 σ inhibits COP1-mediated cell proliferation	83
Figure 3-36	14-3-3 σ can sensitize COP1-expressing HCT116 cells to IR- mediated cell death	84
Figure 3-37	14-3-3 σ inhibits COP1-accumulated S phase population	85
Figure 3-38	14-3-3 σ antagonizes COP1-mediated foci formation	86
Figure 3-39	14-3-3 σ antagonizes COP1-promoted soft agar colony formation	87
Figure 3-40	Overexpression of COP1 promotes tumor progression	89
Figure 3-41	14-3-3 σ suppresses COP1-mediated tumor progression	90
Figure 3-42	Serial tumor sections stained with anti-cleaved Caspase 3 and anti- p53 from experiments in Figure 3-41	91
Figure 3-43	Serial tumor sections stained with anti-Ki67 from experiments in Figure 3-41	92
Figure 3-44	14-3-3 σ and COP1 expression levels are inversely correlated in malignant human breast cancer specimens	94
Figure 3-45	There is an inverse correlation between 14-3-3 σ and COP1 in	95

human primary pancreatic cancer specimens

Figure 4-1 Working model

110

LIST OF TABLES

Table 2-1	List of antibodies	20
Table 2-2	List of reagents	21
Table 2-3	List of plasmids	23
Table 2-4	PCR program for mutagenesis	24
Table 2-5	List of real time-PCR program for the amplification of p53 target genes	26
Table 3-1	An inverse correlation between 14-3-3 σ and COP1 in pancreatic cancer samples	95

LIST OF ABBREVIATION

ACC	Acetyl-CoA carboxylase
ATM	Ataxia telangiectasia, mutated
CDC2	Cell division control 2
CHK2	Checkpoint kinase 2
CSN3	COP9 signalosome complex subunit 3
CSN6	COP9 signalosome complex subunit 6
EFP	Estrogen-responsive finger protein
ERE	Estrogen response element
FOXO1	Forkhead box O1
HME1	Human mammary epithelium marker 1
MDM2	Mouse double minute-2
MLF1	Myeloid leukemia factor 1
NLS	Nuclear localization signal
NES	Nuclear export signal
RFWD2	Ring finger and WD repeat domain 2
SFN	Stratifin
TORC2	cAMP responsive coactivator
TRB3	pseudokinase Tribble 3

CHAPTER 1. INTRODUCTION

1.1 Introduction of 14-3-3 proteins

The 14-3-3 proteins (28 – 33 kDa) were originally isolated as acidic, abundant bovine brain proteins (Moore and McGregor, 1965). 14-3-3 proteins are found in all eukaryotic organisms, including humans, *Xenopus*, *Drosophila*, and yeast, (Boston and Jackson, 1980; Martens et al., 1992; Skoulakis and Davis, 1996; van Heusden et al., 1995) and in plant species (Aitken et al., 1992). The mammalian 14-3-3 proteins consist of seven isoforms (β , ϵ , γ , ζ , η , σ , and τ) and their isoforms have 75%-92% sequence identity (Broadie et al., 1997). According to alignments of 11 human, budding yeast, and fission yeast 14-3-3 proteins, a phylogenetic analysis of these sequences shows that 14-3-3 σ is the most divergent compared with the rest of 14-3-3 proteins in Figure 1-1. It has been known that 14-3-3 proteins can form homo- and heterodimers and bind to their targets through an amphipathic binding cleft (Jones et al., 1995; Tzivion et al., 1998). 14-3-3 proteins preferentially recognize the consensus phosphorylated binding motifs RSX (pS/T) XP and RXXX(pS/T)XP in their targets (Rittinger et al., 1999; Yaffe et al., 1997). These motifs are highly conserved among 14-3-3 proteins, which indicate that the 14-3-3 proteins are functionally redundant. Although the majority of 14-3-3 targets contain these consensus phosphorylated binding motifs, some of the more well-known 14-3-3 targets, such as IGF-1 receptor (Furlanetto et al., 1997) and Wee1 (Honda et al., 1997a; Wang et al., 2000), do not. Moreover, the 14-3-3 monomer has also been found to recognize targets, such as Raf (Tzivion et al., 1998), while Raf activity is different in 14-3-3 monomer binding compared to 14-3-3 dimer binding. In these cases, the binding is mediated by the conserved

amphipathic cleft which is present in all of 14-3-3 proteins (Henriksson et al., 2002; Zhang et al., 1997).

Due to the broad range of target proteins, 14-3-3 proteins are involved in many biological activities, including: apoptosis, cell cycle regulation, DNA damage, transcription, etc (Takahashi, 2003). There are five modes of action which explain how the 14-3-3 isoforms exert their functions on regulating their targets (Bridges and Moorhead, 2005). These modes of action include: (i) 14-3-3 proteins binding to their targets which subsequently change the ability of the targets to interact with other proteins. An example of such interaction involves nonphosphorylated BAD, a proapoptotic protein, and its association with Bcl-2/Bcl-xl, an anti-apoptotic protein. The Bcl-2 homology 3 (BH3) domain of BAD binds to Bcl-2/Bcl-xl to inhibit Bcl-2/Bcl-xl's the anti-apoptotic function. However, AKT phosphorylation of BAD at Ser-155 causes 14-3-3 to competitively bind against Bcl-2. This releases Bcl-2, which in turn allows it to utilize its anti-apoptotic effects (Datta et al., 2000; Hsu et al., 1997; Zha et al., 1996). (ii) 14-3-3 binding altering the subcellular localization of targets. For example, the phosphatase CDC25C dephosphorylates CDC2 at Thr-14 and Thr-15, which results in CDC2 activation for initiating mitotic entry (Gautier et al., 1991). When CHK1 phosphorylates CDC25C, 14-3-3 binds to phosphorylated form of CDC25C, thereby leading to cytoplasmic sequestration. This causes to increased CDC2 phosphorylation which inhibits the entry in mitosis (Graves et al., 2001; Sanchez et al., 1997). (iii) 14-3-3 binding preventing targets from receiving additional modification such as proteolysis and dephosphorylation (Chiang et al., 2001; Dent et al., 1995). This is observed during 14-3-3 binding to Arabidopsis cytosolic enzymes which have functions in protein synthesis and

carbon and nitrogen assimilation. When 14-3-3 binding is lost, the cytosolic proteins are cleaved into proteolytic fragments (Cotelle et al., 2000). (iv) 14-3-3 binding changing the transcriptional or catalytic activity of targets (Thorson et al., 1998; Tzivion et al., 1998). When phosphorylated p53 in Ser 378 binds to 14-3-3 after DNA damage, this leads to an increased binding affinity of p53 to its DNA sequence (Waterman et al., 1998). (v) 14-3-3 dimer binding two different proteins together. It has been demonstrated that 14-3-3 uses its N-terminus for dimerization. Whereas 14-3-3 uses its C-terminus for target binding. In these cases, one C-terminal arm can bind to one protein and the other one can bind to the other protein. Thus, both targets will be spatially constrained, and downstream effect of these complexes will be increased. This can be observed in Bcr-Raf and PKC ζ -Raf (Brasemann and McCormick, 1995; Bridges and Moorhead, 2005; Van Der Hoeven et al., 2000). Taken together, these five modes of action are responsible for 14-3-3 targets' specificity.

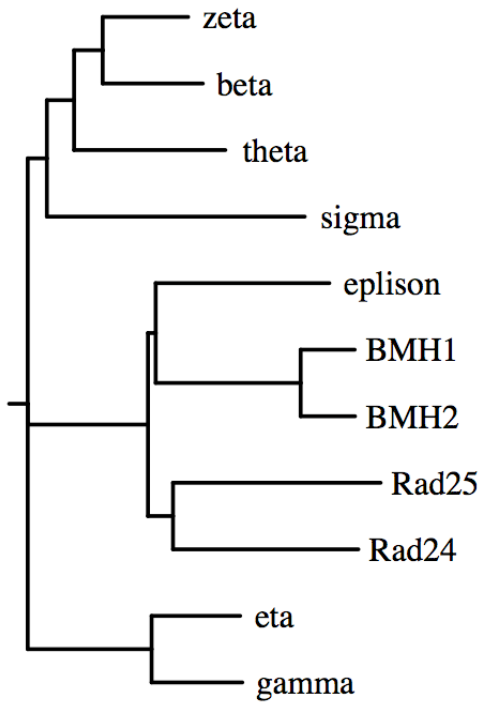


Figure 1-1. 14-3-3 family cladogram. A rooted phylogenetic tree of the sequences is generated among human 14-3-3 (YWHAZ, 14-3-3zeta; YWHAG, 14-3-3gamma; YWHAH, 14-3-3eta; YWHAQ, 14-3-3theta; SFN, 14-3-3sigma; YWHAB, 14-3-3beta; YWHAB, 14-3-3epsilon), budding yeast Rad25 and Rad24, fission yeast BMH1 and BMH2 using ClustalW2 program. This reveals that 14-3-3 σ is evolutionarily distinct from all other 14-3-3 isoforms.

1.2 Introduction of 14-3-3 σ

14-3-3 σ , also called HME1, was originally isolated in human mammary epithelial cells, and was downregulated during neoplastic transformation (Prasad et al., 1992). 14-3-3 σ is also known as SFN (stratifin) due to its expression in epithelial cells, especially within stratified epithelia. There are several evidence that show that 14-3-3 σ has unique functions in comparison to other isoforms (Leffers et al., 1993). The evidence includes: (i) 14-3-3 σ has two unique residues, Ser 5 and Glu 80, that lie opposite to each other at the interface, whereas, other 14-3-3 isoforms have Asp 5 or Glu 5 residues. When the σ isoform forms the heterodimer with other isoforms, the structure is highly unstable between positions 5 and 80, supporting that 14-3-3 σ preferentially forms homodimers (Wilker et al., 2005). (ii) 14-3-3 σ has three unique residues (Met 202, Asp 204, and His 206) that allow the σ isoform to bind to particular targets that are not recognized by other 14-3-3 proteins (Wilker et al., 2005). (iii) 14-3-3 σ located in chromosome 1p35 is a direct target of the transcriptional factor p53 and is induced by tumor suppressor p53 upon DNA damage (Hermeking et al., 1997). It also binds to and activates p53 in a positive feedback loop (Yang et al., 2007). (iv) 14-3-3 σ can sequester CDC2-cyclin B to the cytoplasm which results in G2 arrest following DNA damage (Chan et al., 1999; Laronga et al., 2000). (v) 14-3-3 σ is the only isoform directly linked to tumorigenesis, in that 14-3-3 σ expression is hypermethylated at high frequency in carcinomas of the breast, prostate, liver, lung, skin, and ovaries (Benzinger et al., 2005; Ferguson et al., 2000; Iwata et al., 2000; Lodygin et al., 2004; Lodygin et al., 2003; Mhawech et al., 2005; Osada et al., 2002). (vi) 14-3-3 σ silencing in cells causes chromosome aberrations such as DNA double strand breaks, aneuploidy, nonreciprocal

translocations and end-to-end fusion. This increases to genomic instability, suggesting that 14-3-3 σ plays an important role in maintaining genomic integrity (Dhar et al., 2000). In summary, 14-3-3 σ has critical residues that are not found in other isoforms. These lead to a unique structure and function of 14-3-3 σ . 14-3-3 σ is the only isoform that functions as a tumor suppressor and is silenced in cancer. Therefore, it is interesting to identify the possible regulators in silencing 14-3-3 σ during tumorigenesis.

1.3 The E3 ligase EFP for 14-3-3 σ

In addition to epigenetic silencing of 14-3-3 σ , it has been shown that 14-3-3 σ is ubiquitinated by estrogen-response finger protein (EFP). EFP has been isolated as an estrogen-response gene by the genomic binding site cloning method (Inoue et al., 1993). EFP contains RING-finger, B-box, and SPRY domains (Inoue et al., 1993). The RING-finger has E3 ligase activity, while B-box allows for zinc binding. SPRY domain mediates protein-protein interactions. The *efp* gene contains an estrogen-responsive element (ERE) at the 3'-untranslated region (Orimo et al., 1995; Thomson et al., 2001). In addition to ERE, the levels of EFP is regulated by upstream stimulatory factor-1 (USF-1), which can bind to the E-box in the promoter region of EFP (Ikeda et al., 1997; Ikeda et al., 1998). Previous findings show that estrogen responses are markedly reduced in the uterus of EFP-deficient mice, supporting that EFP is essential for estrogen-induced cell growth (Orimo et al., 1999). In contrast, EFP-overexpressing MCF7 cells generate tumors independent of estrogen levels. EFP is thought to promote breast cancer by functioning as E3 ligase on 14-3-3 σ . Conversely, the loss of EFP has shown to cause the accumulation of 14-3-3 σ in EFP

knockout MEF cells (Urano et al., 2002). Given that EFP is expressed in the uterus, ovary, brain, placenta, and mammary glands, and that 14-3-3 σ is deregulated in cancers (Orimo et al., 1995), it remains to be seen if EFP may be required for the deregulation of 14-3-3 σ in these tissues during tumorigenesis.

1.4 14-3-3 σ regulations on p53 in a positive feedback loop in response to DNA damage

As mentioned in section 1.2, 14-3-3 σ , a p53 target gene, is induced by p53 in response to DNA damage (Hermeking et al., 1997). 14-3-3 σ functions as a negative regulator of cyclin-dependent kinase (CDK). For example, cdc2-cyclinB, responsible for G2-M transition, is accumulated in the nucleus. However, 14-3-3 σ sequesters this complex to the cytoplasm, which causes G2 arrest (Chan et al., 1999; Samuel et al., 2001). Moreover, it has been shown that 14-3-3 σ is associated with cyclin-CDK2. Ectopic expression of 14-3-3 σ inhibits cyclin-Cdk2 activity and inhibits cell proliferation in breast cancer cell lines (Laronga et al., 2000). Thus it is shown that 14-3-3 σ , like p53, has a role in negatively regulating cell cycle progression, which further suggests that 14-3-3 σ functions as a tumor suppressor and has a possible linkage on p53. An example of 14-3-3 σ 's tumor suppressor function involves its role in p53 tetramerization which is critical for both p53 binding to DNA sequence and facilitating p53 transcriptional activity (Waterman et al., 1998). It has been shown that 14-3-3 σ facilitates p53 dimer-dimer interactions, which stabilizes p53 binding to DNA, and enhances p53 transcriptional activity. In addition to tetramer formation, 14-3-3 σ has been shown to negatively regulate the p53-interacting protein: MDM2 (Yang et al., 2003; Yang et

al., 2007). Thus it is observed that 14-3-3 σ positively regulates p53 proteins through stabilizing p53 and increasing p53 transcriptional activity.

1.5 14-3-3 σ negative regulation on a p53 E3 ligase MDM2

MDM2 (murine double minute 2) is an ubiquitin ligase and located at position 12q13. *mdm2* gene is amplified in many cancers and MDM2 is overexpressed in many types of cancers in which gene is not amplified (Freedman et al., 1999; Momand et al., 1998; Oliner et al., 1992). MDM2 contains a RING-finger domain at the C-terminus and a p53-binding domain at the N-terminus, suggesting that MDM2 functions as E3 ligases. It has been known that MDM2 is a major E3 ubiquitin ligase for p53 (Haupt et al., 1997; Honda et al., 1997b; Kubbutat et al., 1997). It binds to and ubiquitinates p53. Studies have shown that the expression level of p53 is increased in the presence of 14-3-3 σ . Mechanistically, ectopic 14-3-3 σ expression increases the steady state and half-life of p53. In this case, an increasing level of 14-3-3 σ results in shortening the half-life of MDM2. These observations indicate 14-3-3 σ stabilizes p53 by downregulating MDM2. At the same time, 14-3-3 σ blocks MDM2-mediated p53 ubiquitination (Yang et al., 2003).

MDM2 contains both nuclear localization signal (NLS) and nuclear export signal (NES), supporting that MDM2 is moved between the cytoplasm and nucleus (Deb, 2002). It is known that MDM2 binds to p53 and promotes p53 nuclear export, which can be inhibited by 14-3-3 σ (Boyd et al., 2000; Chen et al., 1993; Geyer et al., 2000). 14-3-3 σ blocks MDM2-mediated nuclear export, thereby stabilizing and retaining p53 in the nucleus (Yang et al., 2007).

In summary, 14-3-3 σ positively regulates p53 by: (i) 14-3-3 σ binds to and promotes p53 oligomerization, thereby enhancing p53 transcriptional activity. (ii) 14-3-3 σ blocks MDM2-mediated p53 nuclear export and degradation. However, it is interesting to explore further how 14-3-3 σ regulates other p53-interacting proteins and protect p53 from degradation. This regulation eventually leads to proper cell cycle and genomic integrity.

1.6 The discovery of COP1 and its role in Arabidopsis

COP1 (constitutive photomorphogenic 1) is first identified in Arabidopsis photomorphogenesis using a genetic screen. Dr. Deng shows that *cop1* mutant seedlings have light-grown morphology even when it is grown in the dark, suggesting that COP1 functions as a repressor of light-induced genes and negatively regulates photomorphogenesis in the dark (Deng et al., 1991). Later on a genetic analysis has identified a set of genes that suppress photomorphogenesis, consisting of 11 pleiotropic de-etiolated (*DET*), constitutively photomorphogenic (*COP*), or fusca (*FUS*) loci in Arabidopsis (Wei et al., 1994). Among them, *det1*, *cop1*, *cop8*, *cop9*, *cop10*, and *cop11* mutant display light-grown phenotypes in the dark (Castle and Meinke, 1994; McNellis et al., 1994; Misera et al., 1994). However, the rest of genes, including *cop2*, *cop3*, *cop4*, *det2*, and *det3*, only play a minor effect in seedling development. During this early period, they show that Arabidopsis COP9 is a component of the huge (550 kDa – 600 kDa) complex and COP8 and COP11 are involved in the formation or stability of COP9 complexes (Wei et al., 1994). Arabidopsis COP8, COP9, COP11 are known as CSN4, CSN8, and CSN1, respectively in mammals (Serino et al., 1999; Wei and Deng, 1998, 1999; Wei et al., 1998).

Arabidopsis COP1 has 51 % identity in the RING-finger and the WD40 repeat domains compared to mouse COP1 (Wang et al., 1999) and mouse COP1 and mammalian COP1 protein share around 97% identity (Yi et al., 2002). This indicates that functions and regulations of COP1 may be conserved in animals and plants. Arabidopsis COP1 contains three highly conserved domains: RING-finger, coiled-coil domain, and seven WD40 repeats, suggesting that COP1 has E3 ligase activity. The Arabidopsis COP1 nuclear localization signal (NLS) is located immediately upstream of the WD40 repeats. Two of Arabidopsis COP1 nuclear export signals (NES) are located in RING-finger and coiled-coil domain (Holm and Deng, 1999). Arabidopsis COP1 displays light-mediated shuttling between the cytoplasm and nucleus, supporting the notion that localization of COP1 is critical for COP1 activity and functions. For example, COP1 is located in the cytoplasm in the light but translocates to the nucleus in the dark where it degrades HY5, a light-induced transcription factor (Hardtke et al., 2000; Osterlund et al., 2000). Thus the light in plant triggers COP1 nuclear–cytoplasmic repartitioning.

1.7 Introduction of mammalian COP1

COP1 is also known as RFWD2, ring finger and WD repeat domain 2. COP1 has three isoforms generated by alternative splicing of COP1 pre-mRNA. In addition to full length of COP1 (731 kDa, around 90 kDa), COP Δ 24 lacks the four terminal amino acids in exon 4 and all 20 amino acids in exon 7 (707 kDa, less than 90 kDa). The other is COP1 Δ RING + cc, which lack all the RING-finger and part of coiled-coil domain (506 AA, 50-60 kDa)

(Wertz et al., 2004). The physiological roles of COP1 isoforms would certainly be of interest to study in the future.

COP1 is an E3 ligase and degrades tumor suppressor p53, hinting that COP1 plays a negative role in cell cycle arrest and apoptosis (Dornan et al., 2004a). However, roles of COP1 are poorly understood in cancer although previous studies have shown that COP1 is widely expressed in normal human tissues, including human testes, thymus, tonsil, pancreas, colon, heart, prostate, spleen, intestine, and liver (Bianchi et al., 2003; Dornan et al., 2004a). Thus it would be of interest to examine further what role COP1 deregulation and COP1 regulatory pathways play in these types of tumors. In concordance of COP1 localization in 1q25.1-1q25.2, it could be further addressed whether *cop1* gene is amplified in these types of cancer.

1.8 Substrates of COP1 E3 ligase

Mammalian COP1 ring-finger and WD40 repeats share 51 % identity in these domains of Arabidopsis COP1. It indicates that COP1's E3 ligase function is conserved and that target similarity is high between organisms. For example, Arabidopsis COP1 degrades HY5 and HYH, which are basic-leucine zipper (bZIP) transcription factors, and mammalian COP1, functions as an adaptor, directly binds to the bZIP transcription factor c-Jun. c-Jun is ubiquitinated by CUL4-associated complex, including DDB1, DET1, and COP1 (Wertz et al., 2004). While attempting to identify the physiological roles of mammalian COP1, an ever-increasing number of mammalian COP1 E3 ligase substrates are being identified. Some examples include COP1 reportedly binding and ubiquitinating apoptosis-inducing

transcriptional factor FOXO1 and stress-response transcriptional factor p53 (Dornan et al., 2004a; Kato et al., 2008). This reveals that COP1 has negative impact on cell cycle arrest. COP1 is also shown to play a role in lipid metabolism by regulating the stability of acetyl-coenzyme A carboxylase (ACC) through interaction with pseudokinase Tribble 3 (TRB3). Moreover, COP1 plays a role in insulin-modulated gluconeogenesis by regulating the stability of cAMP-response CREB coactivator TORC2 (Dentin et al., 2007; Qi et al., 2006). Moreover, COP1 also plays a role in metastasis by regulating the stability of the transcriptional factor ERM in the presence of DET1 (Baert et al., 2010). Domains and substrates of COP1 are shown in Figure 1-2. The COP1 binding motif has been recently reported as DD (EE)-XX-VP (Dentin et al., 2007). Analysis of amino acid sequences of COP1 E3 ligase substrates reveals that c-JUN, DDB1, TRB3, TORC2, and ERM all contains the COP1 consensus binding motif. This is suggestive that substrates of COP1 can be identified through the COP1 binding motif in the future.

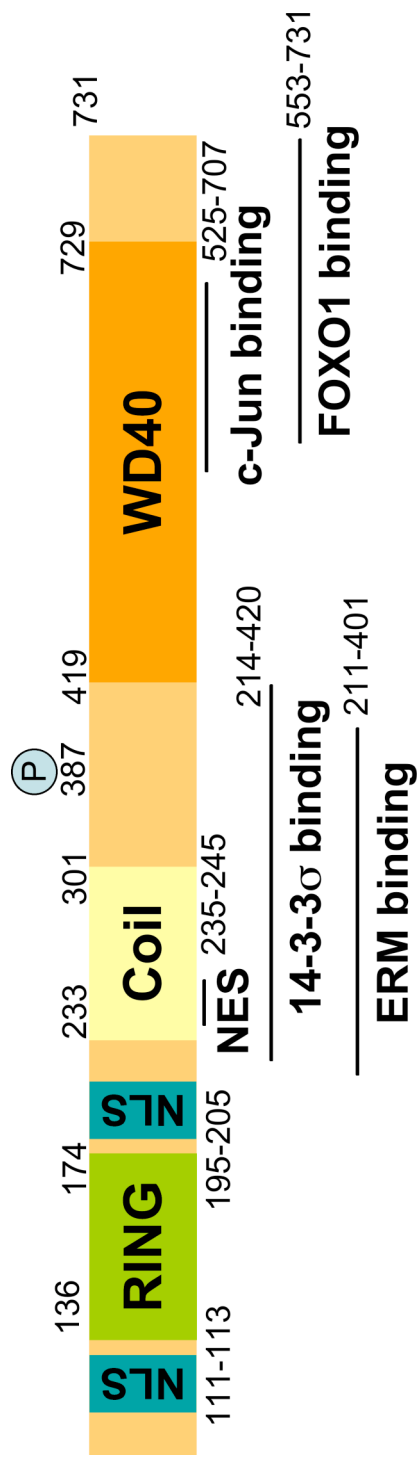


Figure 2-1. Domains and substrates of mammalian COP1. COP1 has RING-finger, coiled coil, and seven WD40 repeats (WD1, 419-458 residues; WD2, 468-508 residues; WD3, 511-551 residues; WD4, 553-593 residues; WD5, 597-635 residues; WD6, 638-677 residues; WD7, 691-729 residues). COP1 also contains nuclear localization signal and nuclear export signal. FOXO1 and c-Jun binds to WD40 repeats of COP1. 14-3-3 σ and ERM binds to coiled-coil region of COP1.

1.9 COP1 upstream regulators: COP9 signalosome

COP9 signalosome is a conserved protein complex in plants and animals. It consists of eight distinct subunits spanning molecular weights from 57 kDa to 22 kDa (Wei and Deng, 1998; Wei et al., 1998). Like COP1, it plays a negative role in Arabidopsis seedling development. It has been shown that COP9 is required for nuclear accumulation of COP1 in the dark; COP1 normally locates in the cytoplasm in the light but translocates to the nucleus in the dark (von Arnim and Deng, 1994). However, in *cop9* and other *cop/det/fus* mutant, COP1 can not be found in the nucleus in the dark (Chamovitz et al., 1996; Schwechheimer and Deng, 2000). There are two potential mechanisms to explain this phenomenon. First is that the COP9 signalosome may be directly involved in nuclear import of COP1. In addition, the COP9 signalosome may be indirectly involved in nuclear import of COP1 through removal of COP1 binding partners that drives COP1 into the cytoplasm. The second mechanism could be that the COP9 signalosome may be protecting COP1 from degradation in the nucleus. In any event, these mechanisms indicate that the COP9 signalosome is a COP1 upstream effector, which in turn regulates COP1's functions. In mammals, it has been shown that MLF1, myeloid leukemia factor 1, collaborates with CSN3 to induce G1 arrest in a p53-dependent manner through inhibition of COP1-mediated p53 instability (Yoneda-Kato et al., 2005). This is the first time to show CSN3-COP1 regulations in mammalian cells. In DNA damage pathway, it has been observed that CSN3 is phosphorylated and recognized by ATM (Ataxia telangiectasia, mutated) in response to DNA damage through the use of large-scale screens. More specifically this phosphorylated CSN3 is located on DNA double strand

breaks (Matsuoka et al., 2007; Shiloh, 2006). It is also observed that the ubiquitination processes of repair proteins, such as DDB1 and DDB2, and Cdt1, are regulated by COP9 signalosome. COP1 is also phosphorylated by ATM following DNA damage (Groisman et al., 2003; Higa et al., 2003). These suggest that roles of COP1 in DNA damage and DNA repair may be regulated by its upstream effector, COP9 signalosome.

1.10 The role of COP1 in response to DNA damage

As mention above, COP1 is a p53 E3 ligase and promotes p53 degradation through ubiquitination. It is conceivable that the inhibition of p53 E3 ligases is an important step for p53 stabilization after DNA damage. The steady-state levels of COP1 are reduced which is dependent on ATM in response to ionizing radiation (Dornan et al., 2006). ATM is the key regulators in DNA damage checkpoint pathways (Ljungman and Lane, 2004; Yang et al., 2004). For example, ATM directly phosphorylates p53 on Ser 15, leading to the stabilization of p53 and to the increase in transcriptional activity of apoptosis and cell cycle checkpoint genes (Banin et al., 1998; Canman et al., 1998; Nakagawa et al., 1999). ATM-activated CHK2 phosphorylates p53 on Ser 20, thereby preventing binding between MDM2 and p53, thus p53 levels are accumulated after DNA damage (Chehab et al., 2000; Chehab et al., 1999; Hirao et al., 2000). Because of this, it is thought that ubiquitination of p53 is blocked in a ATM-dependent manner in response to DNA damage. Another example of indirect ATM regulations of p53 is COP1. Ectopic COP1 levels are reduced in the presence of ATM but not ATM-kinase dead mutant. ATM phosphorylates COP1 at Ser 387 and phosphorylated COP1 at Ser 387 reduces the binding between COP1 and p53, which in turn causes p53 stabilization after DNA damage. This also results in the phosphorylated COP1

being autoubiquitination (Dornan et al., 2006). In summary, COP1 loses its binding affinity for p53 once it is phosphorylated by ATM in response to DNA damage

The turnover of endogenous COP1 was decreased in CSN3-knockdown cells compared to when NIH3T3 cells are treated with ultraviolet light (UV, 25 J/m²). Indicating that CSN3 is involved in the instability of COP1 although currently the details of this are unknown. Furthermore, UV-induced COP1 degradation occurs in human keratinocytes. These observations indicate that levels of COP1 are regulated in normal and cancer cells by DNA damage agents. Altogether the evidence indicates that the functions of COP1 are important in cell signaling.

1.11 The role of COP1 in cancer

On the basis that COP1 is a p53 E3 ligase it can be assumed that COP1 negatively regulates cell cycle progression and may play a role in tumor progression. It has been reported that COP1 is overexpressed in ovarian adenocarcinoma using a tissue microarray (Dornan et al., 2004a). COP1 overexpressed samples show decreased *p21* mRNA levels, which are *p53* wild-type. This could indicate that COP1 overexpression in ovarian cancer is in p53-dependent manner through degrading tumor suppressor p53 and further reducing p53 transcriptional activity. In breast adenocarcinomas, COP1 is overexpressed in 67% of cases. When the levels of wild-type p53 are reduced, COP1 is found overexpressed. Recent studies show that COP1 is overexpressed in hepatocellular carcinoma (HCC), the third most lethal neoplasm in the world (Lee et al. 2010). Taken together, COP1 is overexpressed in breast cancer, ovarian cancer and hepatocellular carcinoma. It suggests that COP1 play a role in

tumor progression through inhibiting the functions of wild-type p53. Due to its roles in tumorigenesis, COP1 deregulation and signaling in many other types of cancer will be further addressed.

1.12 Rationale and hypothesis

In this study we investigate whether the tumor suppressor 14-3-3 σ negatively regulates COP1 through the use of COP1 nuclear export and manipulation of COP1 stability. It has been reported that COP1 is an E3 ligase of the tumor suppressor p53. Moreover, COP1 knockdown by siRNA sensitizes U2OS cells, a p53 wild-type cell line, to p53-induced cell death in response to ionizing radiation. It indicates that COP1 may promote cell growth and tumor formation through inhibiting the functions of p53. 14-3-3 σ , a p53 target gene, is induced in response to DNA damage. 14-3-3 σ induction causes G2 arrest because it inhibits the activities of cyclin-dependent kinases (CDK), suggesting that 14-3-3 σ tightly controls the activity of cell cycle checkpoints. However 14-3-3 σ silencing cells causes mitotic catastrophe following DNA damage. This indicates that 14-3-3 σ plays a positive role in the levels of p53 and functions as a tumor suppressor gene. According to the above observations, we hypothesize that 14-3-3 σ negatively regulates COP1, and this interplay between 14-3-3 σ and COP1 prevents COP1-mediated p53 instability. Moreover the negative impact of COP1 on p53 may translate to COP1-mediated cell cycle progression and tumor formation, which may be abolished by 14-3-3 σ . First, we detect whether or not 14-3-3 σ affects COP1 localization in response to DNA damage. Second, COP1 stability is addressed in the presence of 14-3-3 σ compared to the absence of 14-3-3 σ . Third, we examine whether COP1 promotes cell proliferation, cell transformation and tumor progression. Lastly, to

address the biological significance of this study, we measure whether 14-3-3 σ blocks the biological functions of COP1 and 14-3-3 σ prevents COP1-mediated p53 ubiquitination and degradation and COP1-mediated cell proliferation and tumor progression.

CHAPTER 2. MATERIALS AND METHODS

2.1 Cell culture and reagents

Human 293T, A549, and H1299 are obtained from American Type Culture Collection (ATCC). MEF (p53^{-/-}, MDM2^{-/-}) are generously provided by Guillermina Lozano's laboratory, AT22IJE-T/pEBS7 (ATM^{-/-}), AT22IJE-T/YZ5 (ATM^{+/+}) cells were maintained in DMEM/F12 medium supplemented with 10% fetal bovine serum, 100 U/ml Penicillin, and 100 µg/ml streptomycin at 37 °C in 5% CO₂. AT22IJE-T cells (ATM^{-/-} fibroblasts) and AT22IJE-TpEBS7-YZ5 cells (ATM^{-/-} fibroblasts complemented with ATM cDNA) were generously provided by Dr. Y. Shiloh's laboratory (Tel Aviv University, Tel Aviv, Israel). HCT116 14-3-3σ^{-/-}, HCT116 14-3-3σ^{+/+} cells and U2OS cells were cultured in McCoy's 5A medium supplemented with 10% FBS and antibiotics. HCT116 14-3-3σ^{-/-}, HCT116 14-3-3σ^{+/+} cells were provided by Dr. Bert Vogelstein. For transient transfection, cells were transfected with DNA by either FuGENE® HD, or Lipofectamine™ 2000 reagents according to protocols by the manufacturers.

2.2 Antibodies and reagents

Table 1 shows the list of antibodies and Table 2 shows the list of reagents.

Table 2-1. List of antibodies.

Antibody	Clone #	Manufacturer	Description	S	Catalog #
14-3-3 σ	1433S01	RDI (MA, USA)		M	1433Sabm
p53	FL-393	Santa Cruz (CA, USA)	amino acids 1-393	R	sc-6243
p53	DO-1	Santa Cruz (CA, USA)	amino acids 11-25	M	sc-126
COP1		Bethyl Lab. (TX, USA)	amino acids 1-50	R	A300-894A
Flag		Sigma (MI, USA)	Flag peptide	M	F1804
GST	B-14	Santa Cruz (CA, USA)	GST specific domain	M	sc-138
HA	12CA5	Roche (IN, USA)		M	583816001
His		Cell Signaling (CA, USA)	6xHis epitope	R	2365
γ -H2AX	JBW301	Millipore (MA, USA)		R	05-636
Lamin B1		Abcam (MA, USA)	400-500 of Lamin B1	R	ab16048
Myc		Sigma (MI, USA)		R	C3956
Myc	9E-10	Santa Cruz (CA, USA)	amino acids 408-439	M	sc-40
α -Tubulin	B-5-1-2	Sigma (MI, USA)		M	T5168
Ubiquitin	P4D1	Santa Cruz (CA, USA)	amino acids 1-76	M	sc-8017
Alexa Fluor					
488		Molecular Probes (CA)	Goat α Rabbit IgG (H+L)	R	A11034
568		Molecular Probes (CA)	Goat α Mouse IgG (H+L)	M	A11031
ImmunoPure Antibody					
α Mouse IgG		Thermo scientific (CA)	Goat α Mouse IgG (Fc)	M	31437
α Rabbit IgG		Thermo scientific (CA)	Goat α Rabbit IgG (Fc)	R	31463
TrueBlot Antibody					
α Mouse IgG		eBioscience (CA, USA)	α Rabbit IgG HRP	M	18-8817-33
α Rabbit IgG		eBioscience (CA, USA)	α Mouse IgG HRP	R	18-8816-33

Table 2-2. List of reagents.

Reagent	Manufacturer	Catalog #
M2 beads	Santa Cruz (CA, USA)	A2220
G-418 disulfate salt	Sigma (MI, USA)	A1720
Puromycin	Invivogen (CA, USA)	ant-pr-5
Blasticidin	Invivogen (CA, USA)	ant-bl-1
MTT	Sigma (MI, USA)	M5655
L-Glutathione reduced	Sigma (MI, USA)	G4251
SYBR Green Supermix	Bio-Rad (CA, USA)	170-8882
cDNA synthesis Kit	Bio-Rad (CA, USA)	170-8891
DAPI	Sigma (MI, USA)	D9542
Flag-peptide	Sigma (MI, USA)	F3290
E1	Boston Biochem (MA)	E-305
E2	Boston Biochem (MA)	E2-622
Ubiquitin	Boston Biochem (MA)	U530
Doxorubicin	Sigma (MI, USA)	44583
FuGENE® HD	Roche (IN, USA)	4709691001
Lipofectamine™ 2000	Invitrogen (CA, USA)	11668019
MG132	Sigma (MI, USA)	C2211
ECL	Milipore (MA, USA)	WBLUR0100
N-Ethylmaleimide	Sigma (MI, USA)	E1271
Dual luciferase assay system	Promega (WI, USA)	E1960
Propidium Iodide	Sigma (MI, USA)	P4864
Protein A	Santa Cruz (CA, USA)	sc-2001
Protein G	Santa Cruz (CA, USA)	sc-2002
Trizol reagent	Invitrogen (CA, USA)	15596-018
Cycloheximide	Sigma (MI, USA)	C4859
PfuTurbo DNA Polymerase	Stratagene (CA, USA)	600255
RNase OUT	Invitrogen (CA, USA)	10777019

2.3 Construction of expression plasmid

Proper primers were designed and used to amplify target genes using PCR, which were followed by enzyme digestion. COP1-C136S/C139S and COP1-S387A mutants were generated using PCR-directed mutagenesis and verified by DNA sequencing. The pET15b plasmids (Flag and His tag) expressing Flag-COP1 (1-226 aa), COP1 (216-420 aa), and COP1 (392-731 aa) were generated using PCR. The ligation reactions were transformed into DH5 α competent cells and colonies were verified by DNA sequences. More information of plasmids is listed in Table 2-3. Table 2-4 shows that the PCR conditions are used for the generation of COP1 RING and S387A mutant.

2.4 Immunoprecipitation and immunoblotting

Cells were lysated in lysis buffer (50 mM Tris, pH 7.5, 150 mM NaCl, 1 mM EDTA, 0.5% NP-40, 0.5% Triton X-100, 1 mM phenylmethylsulfonyl fluoride, 1 mM sodium fluoride, 5 mM sodium orthovanadate, 1 μ g each of aprotinin, leupeptin, and pepstatin per ml) (Laronga et al., 2000). Lysates were processed either by immunoprecipitation assay or by immunoblotting assay. Samples used for detection of COP1, 14-3-3 σ , and p53 were resolved by 10% SDS-PAGE gels. Samples used for ubiquitination assay were resolved using 6% gel. Proteins were transferred (Bio-Rad) to polyvinylidene difluoride membranes (Millipore). The membranes were blocked with 5% nonfat milk for 1 h at room temperature prior to incubation with indicated primary antibodies. Subsequently membranes were washed three times with TBST or PBST buffer and incubated for 1 h at room temperature with peroxidase-conjugated secondary antibodies. Following three-time washes, chemiluminescent images of immunodetected bands on the membranes were recorded on X-

ray films using the enhanced chemiluminescence (ECL) system according to the manufacturer's instructions. For immunoprecipitation, cell lysates were pre-cleaned by either protein A or protein G beads at 4 °C for 30 minutes and immunoprecipitated by indicated antibodies overnight. On the 2nd day, either protein A or protein G was incubated with the IP complex for 4 hours. This was then followed by Western blot analysis.

Table 2-3. List of plasmids

Plasmid	Primer Sequence	Vector
Flag-COP1	Provided by Dr. Elisabetta Bianchi	pCMV5
RFP-COP1	COP1-Bgl II was ligated in pDsRed1-C1-Bgl II and CIP)	pDsRed1-C1
GFP-COP1	COP1-Bgl II- 3' filled was ligated in pEGFPC-3-Sma I cut and CIP)	pEGFPC-3
Flag-COP1(1-334 aa)	Provided by Dr. Elisabetta Bianchi	pCMV5
Flag-COP1(401-731 aa)	Provided by Dr. Elisabetta Bianchi	pCMV5
Myc-COP1	COP1-Bgl II was ligated in pDsRed1-C1-EcoRI and CIP)	pCDNA6
Bacterial expressed-Flag COP1		
1-226	5'-CTGCCGCTCGAGTCTGGTAGCCGCCAGGCC	pET15b
	5'-CCAGCCCTCGAGTCACAACCAATCTTGAAATATCTGCC	pET15b
216-420	5'-CTGCCGCTCGAGGGCCACAGGTGGCAGATATTT	pET15b
	5'-CCAGCCCTCGAGTCAACCATATAGAGATCACTAGC	pET15b
392-731	5'-CTGCCGCTCGAGTTTCAGGAATGCTTGTCCAAG	pET15b
	5'-CCAGCCCTCGAGTCATACCAATTCTAGCACCTTAA	pET15b
COP1 (RING mutant)	5'-AGCAACGACTTCGTATCCCCATCTCCTTTGATATGATTGAA	pCMV5
shCOP1	5'-CTGACCAAGATAACCTTGATTCAAGAGATCAAGGTTATCTTG	pSilencer 1.0-U6
	5'-GTCAGTTTTTTT	pSilencer 1.0-U6
	5'-AATTAAAAAACTGACCAAGATAACCTTGATCTCTTGAATCAA	pSilencer 1.0-U6
	5'-GGTTATCTTGGTCAGGGCC	pSilencer 1.0-U6
Flag-COP1 (S387A)	5'-GACAGTCGAACTGCAGCCCAGTTGGATGAATTT	pCMV5
	5'-AAATTCATCCAACCTGGGCTGCAGTTCGACTGTC	pCMV5

Table 2-4. PCR conditions for mutagenesis

Steps	Temperature	Duration	Cycles
Initiation	94°C	5 minutes	1
Denaturation	94°C	60 seconds	30
Annealing	55°C	60 seconds	
Extension	68°C	60 seconds	
	68°C		1

2.5 *In vitro* binding Assay

For full-length COP1 binding assay, ³⁵S labeled COP1 was produced by TNT quick coupled Transcription/Translation system in vitro (Promega). TNT products of COP1 were incubated with GST or GST-14-3-3σ.

To determine which domains of Flag-COP1 bind to 14-3-3σ *in vitro*, Flag-COP1 fragments (a.a. 1-226, 216-420, 392-731) were inserted into pET15b vector and transformed into BL21 (DE3). *E.coli* cells were lysed in the NETN buffer (0.5% NP-40, 20mM Tris, pH 8.0, 100mM NaCl, 1mM EDTA). Lysates were incubated with M2-conjugated agarose beads for overnight. The immobilized Flag-COP1 was eluted from Flag peptide and then eluents were incubated with GST-14-3-3σ for the binding. The binding proteins were resolved by SDS-PAGE and immunoblottings were detected with anti-M2.

2.6 *In vivo* ubiquitination Assay

HCT116 14-3-3σ^{-/-} and 14-3-3σ^{+/+} cells were used to detect endogenous COP1 ubiquitination. 293T cells were cotransfected with indicated plasmids to detect exogenous

COP1 and p53 ubiquitination. Twenty-four hours later, cells were treated with 5 µg/ml MG132 for 6 h. Cells were harvested and lysed with regular lysis buffer, containing 5 mM NEM. The ubiquitinated p53 was immunoprecipitated with anti-p53 and immunoblotted with anti-ubiquitin or anti-HA. The ubiquitinated COP1 were immunoprecipitated by anti-Myc, or anti-COP1, and immunoblotted by anti-HA or anti-ubiquitin. The protein complexes were then resolved by 6% SDS-polyacrylamide gel to observe the polyubiquitinated p53 or COP1.

2.7 *In vitro* ubiquitination Assay

COP1 and COP1 RING mutant (C136S, C139S) cDNAs were transcribed and translated *in vitro* using TNT kit (Promega). COP1 and COP1 RING mutant were incubated with either GST- or GST-14-3-3 σ and the complex were incubated with different combination of ubiquitin (200 pmol), E1 (2 pmol), E2-UbcH5a/5b (10 pmol), and ATP (2 mM) in a total volume of 50 µl for 1 h at 37°C. Reaction products were immunoprecipitated with M2 beads, immunoblotted with anti-ubiquitin, and resolved by 6% SDS-polyacrylamide gel.

2.8 Quantitative-PCR

Primers for real-time quantitative PCR of *COP1* (5'- CTGCAACGGGCTCATCAACT; 5'- GGCCACATTTTGTTCATGTATGCT). p53 target genes, including *CDKN1A* (5'- CCTGTCACTGTCTTGTACCCT; 5'-GCGTTTGGAGTGGTAGAAATCT), *SFN* (5'- CTCTCCTGCGAAGAGCGAAAC; 5'- CCTCGTTGCTTTTCTGCTCAA), *BAX* (5'- CCCCAGAGAGGTCTTTTCCG; 5'- GGCGTCCCAAAGTAGGAGA), *PUMA* (5'- GACCTCAACGCACAGTACGAG; 5'-AGGAGTCCCATGATGAGATTGT) and p53

primer (5' - CCGCAGTCAGATCCTAGCG; 5' - AATCATCCATTGCTTGGGACG) were as referred by Primer Bank (<http://pga.mgh.harvard.edu/primerbank/>). *GAPDH* amplification was used for normalization. Total RNAs were extracted from cells using TRIZOL (Invitrogen). 1µg RNA was used for producing cDNA by iScript cDNA Synthesis Kit. Real-time PCR analysis was performed using iQ SYBR Green Super mix, and iCycler iQ Real-time PCR detection system. The amplification folds of genes were analyzed and visualized by Cluster and TreeView software (Eisen, MB), and presented in the form of heat maps. Table 2-5 shows the real time-PCR program for amplification of p53 target gene.

Table 2-5. List of real time-PCR program for the amplification of p53 target genes.

Steps	Temperature	Duration	Cycles
Initiation	94°C	10 minuts	1
Denaturation	94°C	30 seconds	40
Annealing	58°C	30 seconds	
Extension	72°C	30 seconds	
	72°C		1

2.9 Luciferase reporter gene assay

The BDS2-3X-luc reporter containing a p53-responsive element, p53, Flag-COP1 or Flag-14-3-3σ expressing vectors were transfected into H1299 cells. Luciferase activity was assayed using the dual luciferase assay system (TD-20/20 Luminometer) according to the manufacturer's instructions.

2.10 Generation of stable transfectants

For the generation of 14-3-3 σ knock-down stable cells, HCT116 cells were infected by lentiviral shRNA transduction particles (Sigma, MISSION shRNA lentiviral transduction particles) containing either control luciferase shRNA or two specific 14-3-3 σ shRNA (1) (5'-CCGGC CGGGT CTTCT ACCTG AAGAT CTCGA GATCT TCAGG TAGAA GACCC GGTTT TTG) or 14-3-3 σ shRNA (2) (5'-CCGGG ACGAC AAGAA GCGCA TCATT CTCGA GAATG ATGCG CTTCTT GTCGT CTTTT TG). After infection, cells were selected with 2 μ g/ml puromycin for two weeks according to protocols by the manufacturer.

For the generation of RFP-COP1 overexpression stable transfectants, U2OS cells were transfected with RFP vector or RFP-COP1 plasmids using electroporation (Amaxa). After 2 days, cells were selected in medium containing 500 μ g/ml G418 for 4 weeks.

For the generation of Myc-COP1 overexpression stable transfectants, HCT116 cells were transfected with either pCDNA6 or pCDNA6-Myc-COP1 plasmids by electroporation (Amaxa). After 2 days, cells were selected in medium containing 8 μ g/ml blasticidin for 2 weeks.

2.11 Live-cell imaging

RFP-COP1 expressing cells were treated with DNA damage agent, including 1 μ g/ml doxorubicin, IR (10 Gy) or infected with Ad- β -gal (MOI = 100) or Ad-14-3-3 σ (MOI =100). Live-cell images of stably expressing RFP-COP1 cells were observed with Olympus

FV300 and ZEISS LSM 710 confocal microscopes. Both of them are fully motorized incubator chambers that maintain cells at 37 °C in 5% CO₂.

2.12 Cell fractionation

Cells were lysed in 500 – 1000 µl cold lysis buffer (10 mM MgCl₂, 10 mM Tris, pH 7.6, 0.5% NP-40, 1 µM DTT, phosphatase inhibitors and proteasome inhibitors), and keep on ice less than 30 min. Cells were broken using a glass homogenizer (20 strokes). The dounced lysates were centrifuged (4,000 rpm for 5 min at 4°C) to sediment the nuclei portion and other fragments. The supernatant was then prepared (13,200 rpm for 10 – 20 minutes) and the supernatant was saved for the cytoplasmic fraction. The nuclear pellet was washed for three times. Nuclear pellet were resuspended in 150 µl regular lysis buffer and sonicated to extract nuclear proteins on ice. The nuclear lysates were centrifuged (13,200 rpm for 30 minutes), and the supernatant was the nuclear fraction.

2.13 Soft agar colony formation

For soft agar colony assays, 3×10^3 cells mixed in 0.35% agarose/complete media were plated on 0.7% agarose/complete media bottom layer (Invitrogen) in appropriate culture medium and grown for 4 weeks. Colonies were stained with 0.5 mg/ml p-iodonitrotetrazolium violet (Sigma) and were counted under a light microscope (Olympus IX70 and IX71). Each experiment was done at least two times in triplicate wells.

2.14 Foci formation assay

One, two, or three thousand cells were plated in 6-multiwell plates and then incubated for 7 – 10 days. Cells were stained with 0.005% crystal violet to visualize the colonies growing in each well. The 6-multiwell plates containing colonies were scanned by the scanner and the number of colonies were determined by counting in images.

2.15 MTT Assay

Vector control or COP1 expressing cells or COP1 expressing cells were infected with Ad- β -gal (MOI = 10) or Ad-HA-14-3-3 σ (MOI =100). Cells were plated at 3×10^3 cells/well in 96-multiwell plates in triplicate and grown in the continued presence of selective antibiotics. Cells viability was determined every day from day 1 to 7 by incubation with 5 mg/ml MTT (3-(4,5-dimethylthiazol-2-yl)-2,5-diphenyltetrazolium bromide) for 3 h. Following MTT incubation, cells were lysed in 200 μ l of 100% DMSO (Fisher). The samples were then analyzed using a microplate reader to measure the optical density at 570 nm.

2.16 Cell cycle analysis

2×10^6 cells were collected by centrifugation, washed with PBS (pH 7.4), fixed with ethanol and incubated with Propidium Iodide (50 μ g/ml). Fluorescence signal resulting from PI was measured at 630 nm. 10,000 events per sample were acquired. Samples were analyzed by BD FACSCANTO II flow cytometer (BD Biosciences).

2.17 Nude mice experiment

Four to 6-week-old *nu/nu* mice (Charles River Laboratories) were maintained in the animal facility at the University of Texas M. D. Anderson Cancer Center. Mice were divided into

four experimental groups, five for each. Groups included vector control stable cell lines, COP1 expressing cells left uninfected, COP1 expressing cells infected with Ad- β -gal (MOI = 100) or Ad-14-3-3 σ (MOI =100) for forth to eight hours. Cells were harvested and injected into the flanks of each mouse. Tumor volumes were measured and recorded three times a week from day 10 after cell inoculation. At the end of experiment, the mice were sacrificed, and the tumors were removed and weighed.

2.18 Immunohistochemistry

A pancreatic tissue microarray consisting of 121 cases of primary pancreatic carcinoma specimens from patients who underwent initial pancreaticoduodenectomy was used for immunohistochemistry of 14-3-3 σ and COP1. These microarray patience resources were from The University of Texas M. D. Anderson Cancer Center (MDACC) between 1990 and 2004. None of these patients received pre-operative chemotherapy or radiation therapy before surgery. The use of archival paraffin-embedded tissue blocks was in accordance with a protocol approved by the Institutional Review Board of MDACC. 5- μ m unstained sections in the tissue microarray blocks were performed for immunohistochemistry of 14-3-3 σ and COP1. To retrieve the antigenicity, deparaffinized sections were treated at 100 °C in a steamer containing 10 mM citrate buffer (pH, 6.0) for 60 min. The sections were then immersed in methanol containing 0.3% hydrogen peroxidase for 20 min to inhibit endogenous peroxidase activity and then incubated in 2.5% blocking serum to block nonspecific binding. Sections were incubated with primary antibodies against 14-3-3 σ and COP1 at a 1:100 dilution (90 min at 37°C). Standard avidin-biotin immunohistochemical analysis of the sections was performed according to the instructions by the manufacturer

(Vector Laboratories, Burlingame, CA). Diaminobenzidine was used as a chromogen, and hematoxylin was used for counterstaining. The staining results were analyzed by a board-certified pathologist (H.Wang). The scores, 0 (no nuclear staining); 1(<10% nuclear staining); 2 (10-50% nuclear staining) and 3 (>50% nuclear staining), were used for analyzing for standard of COP1 levels.

CHAPTER 3. RESULTS

3.1 14-3-3 σ is required for doxorubicin-mediated COP1 downregulation

It is known that 14-3-3 σ is a p53 target (Hermeking et al., 1997). DNA damage leads to p53 activation and stabilization, which in turn induces 14-3-3 σ to execute G2/M arrest (Hermeking et al., 1997). COP1, a p53 E3 ligase, ubiquitinates and degrades p53 (Dornan et al., 2004b). Given that COP1 has a shorter half-life following DNA damage, we address whether 14-3-3 σ is involved in DNA damage-mediated COP1 downregulation. To test our hypothesis, we treated A549 cells (Human lung adenocarcinoma epithelial cell line) with doxorubicin for the indicated time points, followed by immunoblotting assays. Indeed, as doxorubicin-induced DNA damage increased the levels of 14-3-3 σ , COP1 expression was downregulated (Figure 3-1). This suggests that 14-3-3 σ and COP1 may have a negative relationship following DNA damage. Furthermore, we found that DNA damage-mediated COP1 downregulation was rescued when A549 cells were treated with MG132, a proteasome inhibitor (Figure 3-2). This result indicates that doxorubicin-mediated COP1 downregulation is through 26S proteasome pathway. Figure 3-1 shows that 14-3-3 σ is involved in COP1 downregulation following genotoxic challenges. We further clarify whether disruption of 14-3-3 σ compromises doxorubicin-mediated COP1 downregulation. Interestingly, downregulation of COP1 upon doxorubicin-induced DNA damage was observed in HCT116 14-3-3 $\sigma^{+/+}$ cells, but was absent in HCT116 14-3-3 $\sigma^{-/-}$ cells (Figure 3-3). This result implies that 14-3-3 σ is required for DNA damage-mediated COP1 downregulation.

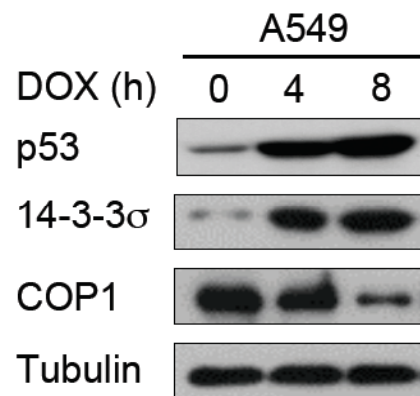


Figure 3-1. COP1 expression is downregulated in response to DNA damage. A549 cells were treated with 1 μ g/ml of doxorubicin (DOX) for the indicated times. Lysates were analyzed by immunoblotting for the expression of 14-3-3 σ , COP1 and p53.

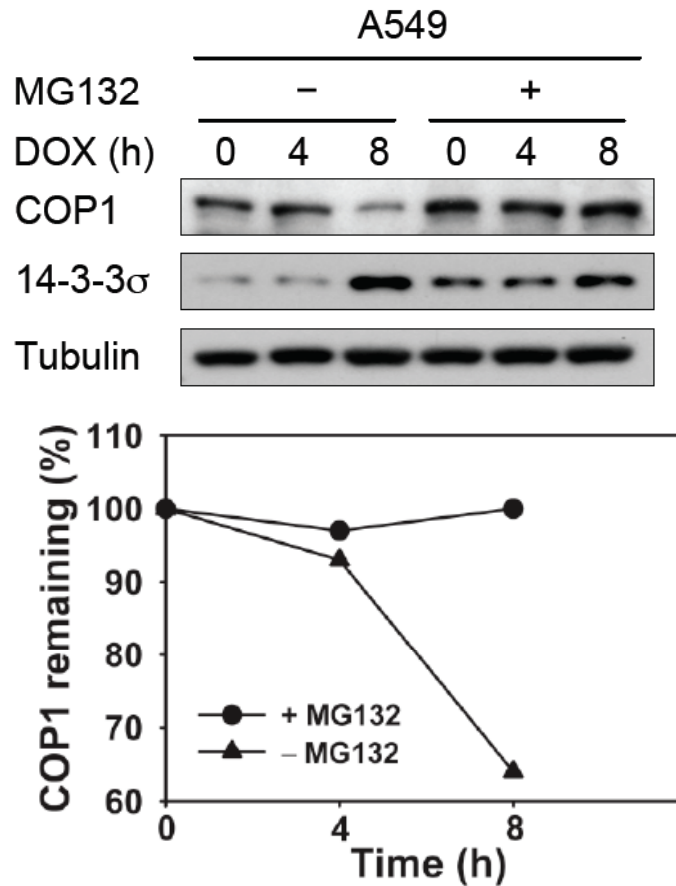


Figure 3-2. DNA damage-mediated COP1 downregulation is mitigated by the treatment with MG132. A549 cells were treated with 1 μ g/ml of doxorubicin (DOX) for the indicated times and treated with or without proteasome inhibitor MG132 for 3 hours before harvesting. Lysates were collected at the indicated times and analyzed by immunoblotting with indicated antibodies. The protein levels of COP1 in response to DNA damage at the different time points were determined by measuring the integrated optical intensity of the bands in the immunoblots (bottom).

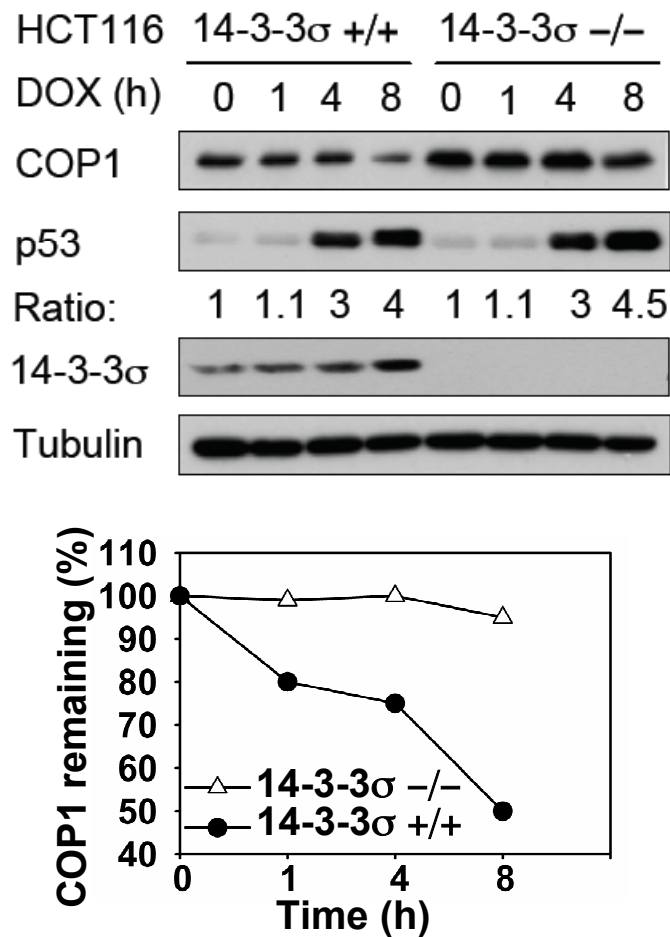


Figure 3-3. DNA damage-mediated COP1 downregulation is recovered in 14-3-3 σ null cells. HCT116 14-3-3 σ ^{+/+} and HCT116 14-3-3 σ ^{-/-} cells were treated with doxorubicin (DOX) for the indicated times. Cell lysates were immunoblotted with anti-14-3-3 σ , anti-COP1, and anti-tubulin (top). The protein levels of COP1 in response to DNA damage at the different time points were determined by measuring the integrated optical intensity of the bands in the immunoblots (bottom). The level of COP1 at time 0 is set at 100%.

3.2 14-3-3 σ -mediated COP1 downregulation is 26S proteasome-dependent

Given that 14-3-3 σ is required for DNA damage-mediated COP1 downregulation and 14-3-3 σ is a positive regulator of p53 (Yang et al., 2003), we further examine whether 14-3-3 σ negatively regulates the stability of COP1. We generated lentiviral shRNA-mediated knockdown of 14-3-3 σ in HCT116 cells. We found that endogenous COP1 steady-state levels were accumulated in 14-3-3 σ knockdown cells (Figure 3-4 A). To confirm the role of 14-3-3 σ in the stability of COP1, we used 293T cells, a 14-3-3 σ null cell line, and transfected COP1 and increasing amount of 14-3-3 σ in 293T cells. The results showed that an increasing amount of 14-3-3 σ led to COP1 downregulation (Figure 3-4 B). We found that 14-3-3 σ does not reduce mRNA levels of COP1 (data not shown). Given that 14-3-3 σ decreases the steady-state levels of COP1 (Figure 3-4), we further measure whether 14-3-3 σ shortens the half-life of COP1. HCT116 14-3-3 $\sigma^{+/+}$ and HCT116 14-3-3 $\sigma^{-/-}$ cells were treated with cycloheximide (CHX), a protein synthesis inhibitor. We found that the half-life of endogenous COP1 was reduced in the presence of 14-3-3 σ compared to COP1 levels in the absence of 14-3-3 σ cells (Figure 3-5). This suggests that 14-3-3 σ plays a role in COP1 degradation. It is interesting to further investigate whether 14-3-3 σ -mediated COP1 degradation is dependent on 26S proteasome. Consistent with doxorubicin-mediated COP1 downregulation (Figure 3-2), we found that 14-3-3 σ -mediated COP1 degradation was recovered by MG132 treatment (Figure 3-6).

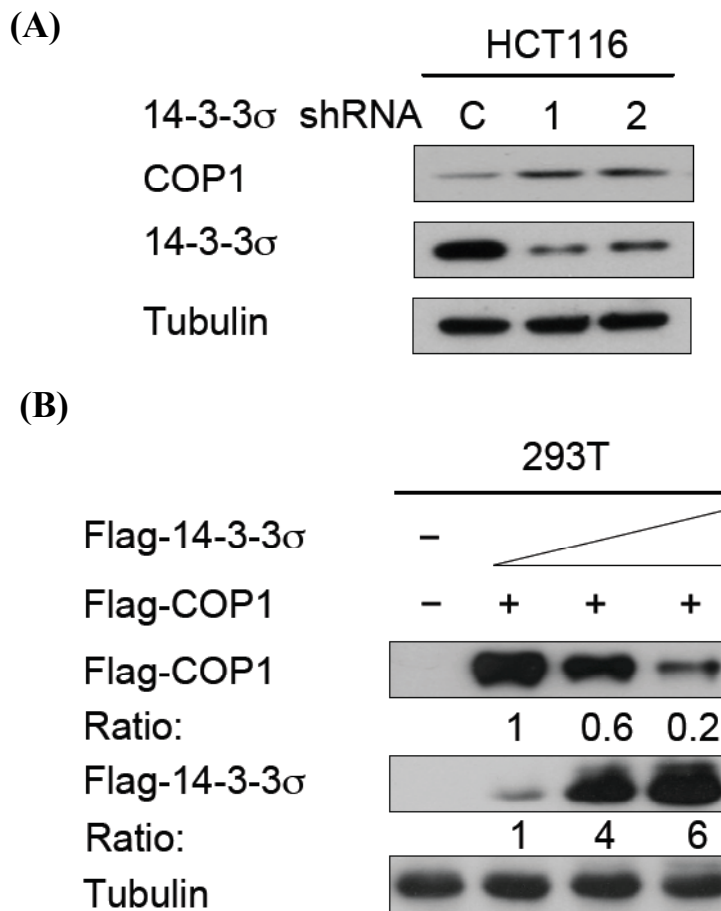


Figure 3-4. 14-3-3 σ downregulates steady-state levels of COP1. (A) 14-3-3 σ decreases COP1 steady state. 14-3-3 σ was stably knocked down with shRNA 1 (1) and shRNA 2 (2) in HCT116 cells. Luciferase shRNA was used as control (C). Lysates were immunoblotted with anti-COP1, and 14-3-3 σ . (B) Ectopic 14-3-3 σ expression leads to COP1 downregulation. The indicated plasmids were transfected in 293T cells. Equal amounts of cell lysates were immunoblotted with the indicated antibodies.

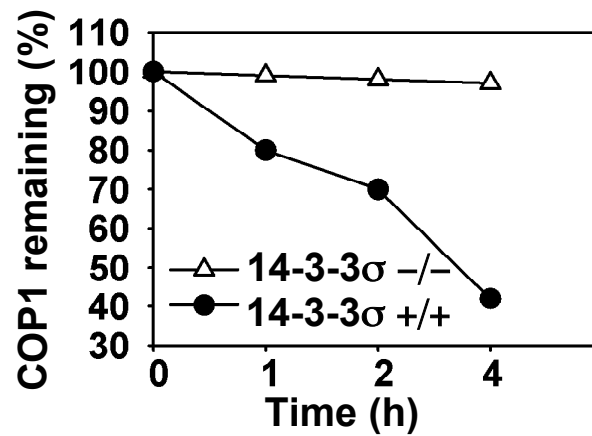
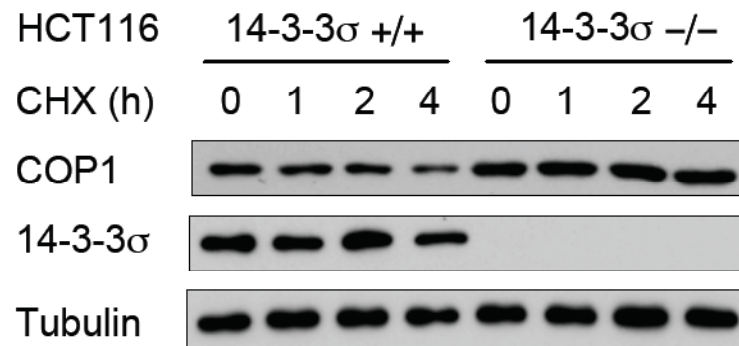


Figure 3-5. The half-life of COP1 is prolonged in 14-3-3 σ null cells. HCT116 14-3-3 σ ^{+/+} and HCT116 14-3-3 σ ^{-/-} cells were treated with cycloheximide (CHX) for the indicated times. Cell lysates were immunoblotted with anti-14-3-3 σ , anti-COP1, and anti-tubulin (top). The protein levels of COP1 over time are shown (bottom).

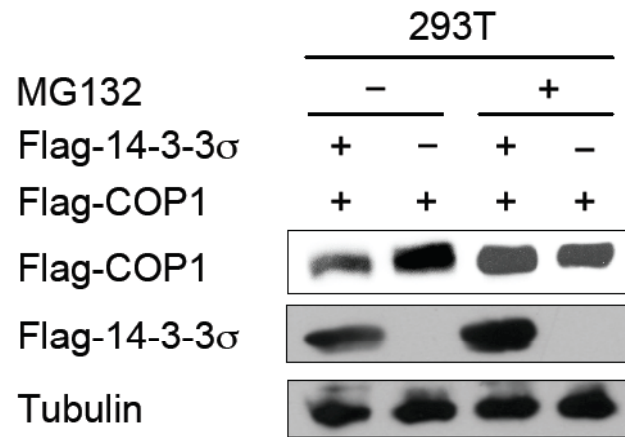


Figure 3-6. 14-3-3 σ downregulates COP1 through 26S proteasome pathway. 293T cells were transfected with the indicated plasmids. Cells were treated with or without proteasome inhibitor MG132 for 6 hours before lysates were collected. Lysates were immunoblotted with anti-Flag or anti-tubulin.

3.3 Identification of COP1 binding region on 14-3-3 σ and 14-3-3 σ binding region on COP1

In order to explore the molecular mechanism of 14-3-3 σ -mediated downregulation of COP1 following DNA damage, we first address whether 14-3-3 σ interacts with COP1. A549 cells were treated with doxorubicin overnight in order to induce 14-3-3 σ levels. Using reciprocal co-immunoprecipitation, we found that COP1 bound to 14-3-3 σ under physiological conditions (Figure 3-7). We further detected a direct binding between 14-3-3 σ and COP1. COP1 was produced in an *in vitro* transcription coupled with translation reaction, and then we performed GST pull-down assays. Interestingly, COP1 directly bound to 14-3-3 σ (Figure 3-8). To further identify the binding domains on each protein, we first define the region of COP1 that is required for binding to 14-3-3 σ . We generated different bacterial expressed COP1 fragments (1 aa-226 aa, 216 aa-420 aa, and 392 aa-731 aa containing RING, coiled-coil, and WD40 repeat domains, respectively). Different COP1 fragments were incubated with GST or GST-14-3-3 σ . We found that 14-3-3 σ directly bound to RING finger and coiled-coil region of COP1 (Figure 3-9). On the other hand, to define the region of 14-3-3 σ , which is required for binding to COP1, 293T cells were transfected with Myc-COP1 and different 14-3-3 σ fragments (full-length, 1 aa-161 aa, and 153 aa-248 aa). We found that COP1 bound to N-terminus of 14-3-3 σ . This indicates that the N-terminus of 14-3-3 σ binds to RING-finger and coiled-coil domain of COP1 (Figure 3-10).

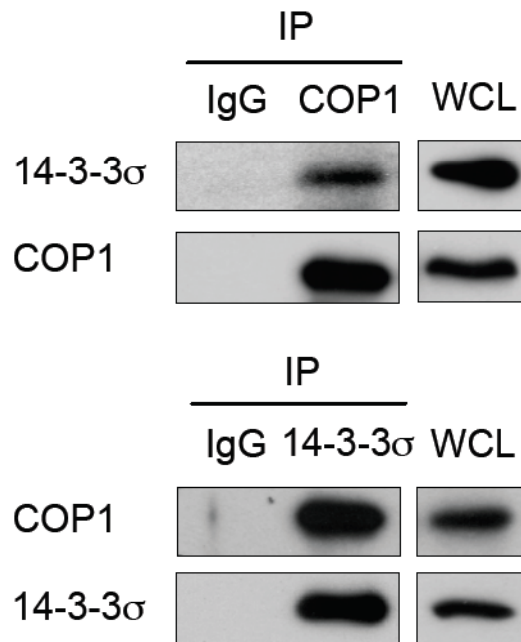


Figure 3-7. Endogenous 14-3-3 σ binds to endogenous COP1. Endogenous 14-3-3 σ interacts with endogenous COP1. A549 cells were treated with 1 μ g/mL doxorubicin overnight. Before harvesting, cells were treated with a proteasome inhibitor, MG132 for six hours. Equal amounts of cell lysates were immunoprecipitated with either rabbit IgG (as control) or anti-COP1, and immunoblotted with anti-14-3-3 σ (top panel). Lysates were also immunoprecipitated with either mouse IgG (as control) or anti-14-3-3 σ and immunoblotted with anti-COP1 (bottom panel). WCL: whole cell lysate.

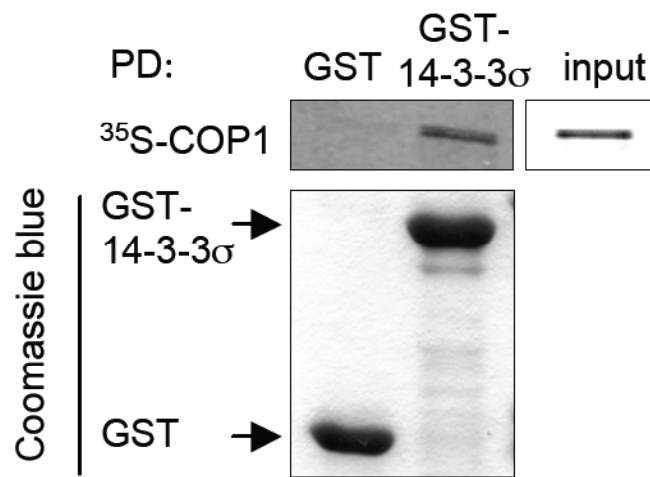


Figure 3-8. 14-3-3 σ directly binds to COP1. 14-3-3 σ specifically interacts with COP1 *in vitro*. COP1 cDNAs were transcribed and translated *in vitro*. ^{35}S -labeled COP1 proteins were incubated with either GST- or GST-14-3-3 σ and analyzed by SDS-PAGE and autoradiography. The bottom panel shows the input of GST and GST-14-3-3 σ analyzed by Coomassie Blue staining. PD: pull down.

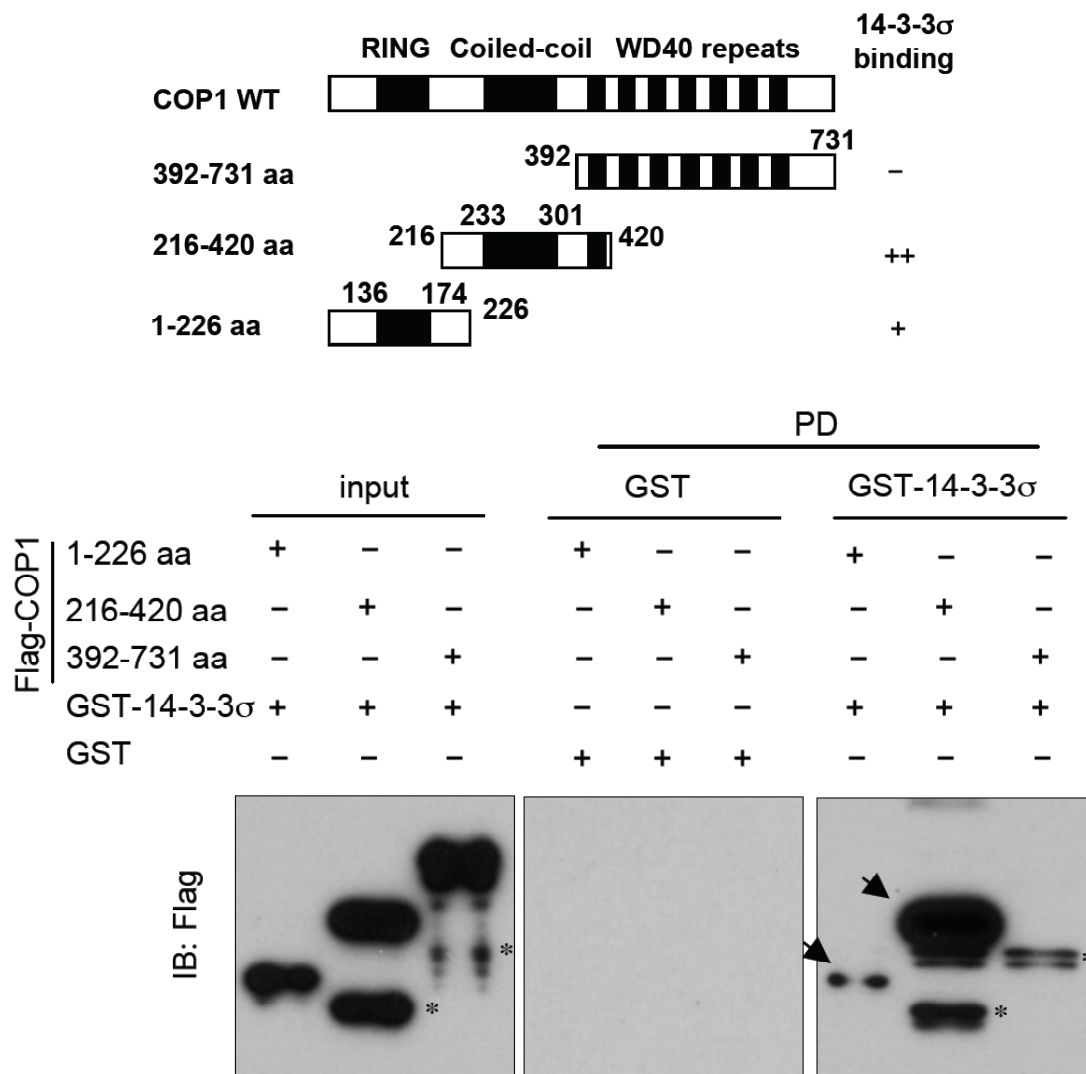


Figure 3-9. Map of the 14-3-3 σ binding region within COP1. Bacterially expressed Flag-COP1 domains were eluted with Flag-peptide. GST-14-3-3 σ was incubated with eluents of bacterially expressed Flag-COP1 domains, and then the mixture was subjected to GST pull-down (PD) followed by immunoblotting using anti-Flag. Specific interaction of COP1 domains with 14-3-3 σ is indicated by arrows. The asterisks indicate non-specific bands.

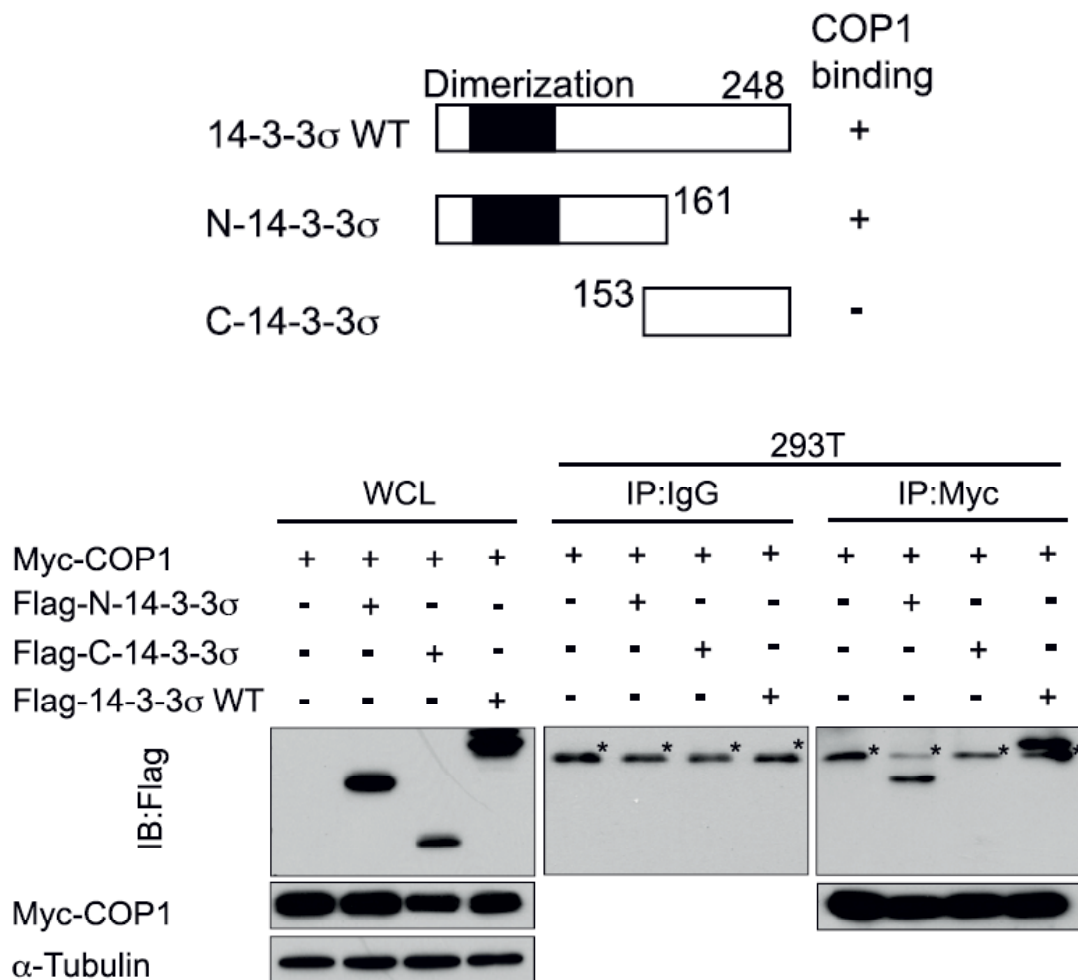


Figure 3-10. Identification of 14-3-3 σ domains interacts with COP1. 293T cells were cotransfected with Myc-COP1 and wild-type (aa 1-248), N-terminus (aa 1-161), or C-terminus (aa 153-248) of Flag-14-3-3 σ . Before harvesting, cells were treated with proteasome inhibitors. Lysates were immunoprecipitated with anti-Myc and immunoblotted with anti-Flag. Specific interactions of 14-3-3 σ domains with COP1 are indicated. The asterisk marks the IgG light chain.

3.4 14-3-3 σ promotes COP1 ubiquitination

Given that 14-3-3 σ affects the instability of COP1 (Figure 3-5), 14-3-3 σ -mediated COP1 downregulation is 26S proteasome-dependent (Figure 3-6), we address that 14-3-3 σ may participate in COP1 ubiquitinated proteolysis. 293T cells were transfected with Myc-COP1, HA-ubi, and increasing amount of Flag-14-3-3 σ . We found that increasing 14-3-3 σ expression facilitated COP1 polyubiquitination (Figure 3-11). To determine whether 14-3-3 σ -promoted COP1 ubiquitination occurs under physiological conditions, we performed ubiquitination assay in HCT116 14-3-3 $\sigma^{+/+}$ and HCT116 14-3-3 $\sigma^{-/-}$ cells. More COP1 ubiquitination was detected in HCT116 14-3-3 $\sigma^{+/+}$ cells than in HCT116 14-3-3 $\sigma^{-/-}$ cells (Figure 3-12). Consistently, less COP1 ubiquitination was detected in 14-3-3 σ knockdown HCT116 cells compared to those in HCT116 14-3-3 $\sigma^{+/+}$ cells (Figure 3-13). We were further interested in exploring COP1 self-ubiquitination using *in vitro* ubiquitination assay. Bacterial expressed COP1 was incubated with GST or GST-14-3-3 σ . Interestingly COP1 polyubiquitination was enhanced by GST-14-3-3 σ . Additionally COP1 lost its self-ubiquitination activity when cysteines at positions 136 and 139 within the RING finger were mutated (Figure 3-14). It indicates that 14-3-3 σ facilitates COP1 self-ubiquitination and RING domain is necessary for 14-3-3 σ -mediated COP1 self-ubiquitination. It will be interesting to address whether 14-3-3 σ has a negative impact on the turnover rate of COP1 RING mutant (C136S/C139S) determine whether 14-3-3 σ facilitates either Lys-48 or Lys-63 ubiquitin chain of COP1.

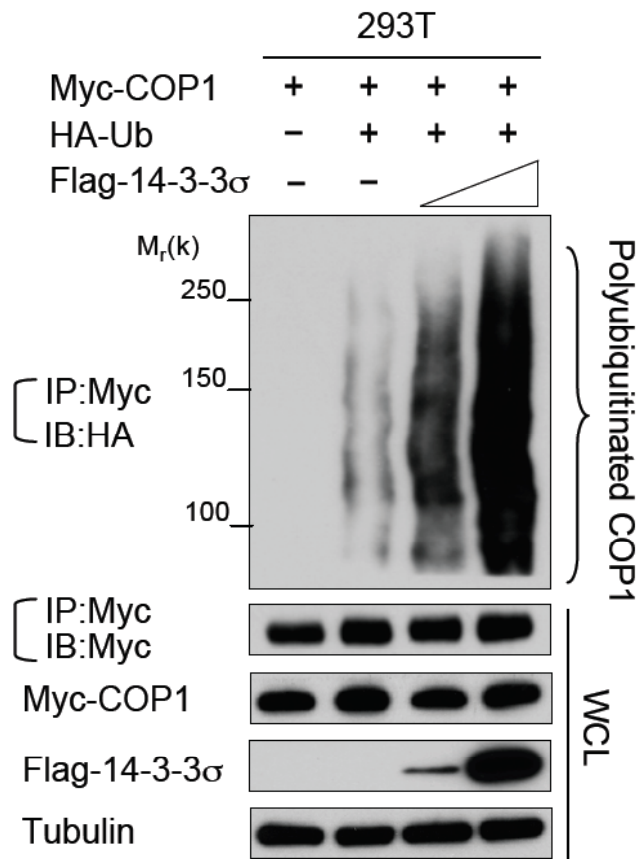


Figure 3-11. 14-3-3 σ enhances polyubiquitination of COP1. 293T cells were cotransfected with the indicated plasmids and increasing amounts of Flag-14-3-3 σ . The cells were treated with MG132 for 6 hr before harvesting, and the ubiquitinated COP1 was immunoprecipitated with anti-Myc and immunoblotted with anti-HA. Equal amounts of whole cell lysate (WCL) were immunoblotted with anti-Myc, anti-Flag, or anti-tubulin.

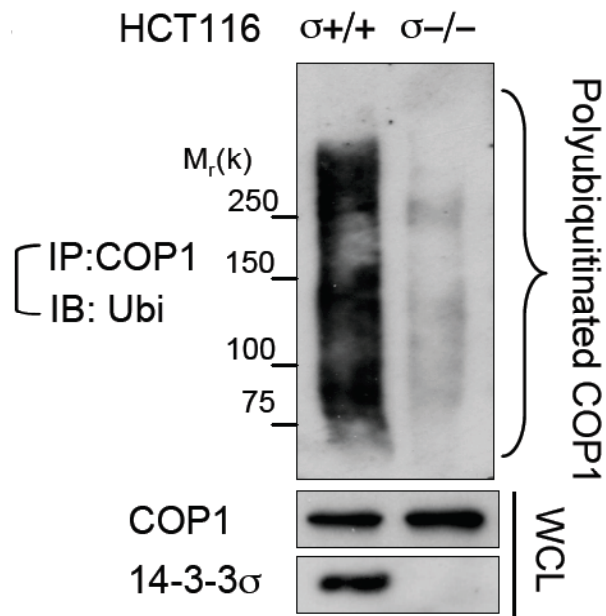


Figure 3-12. COP1 ubiquitination is reduced in 14-3-3 σ -null cells. HCT116 14-3-3 $\sigma^{-/-}$ and HCT116 14-3-3 $\sigma^{+/+}$ cells were treated with MG132 for 6 hr before harvesting. Polyubiquitinated COP1 was detected by immunoprecipitation with anti-COP1 and immunoblotting with anti-ubiquitin in indicated cells.

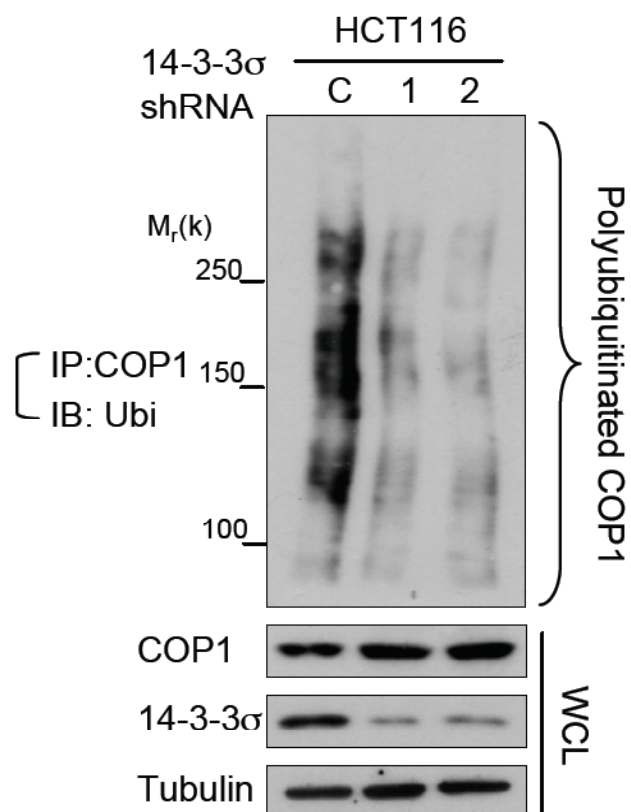


Figure 3-13. COP1 ubiquitination is reduced in 14-3-3 σ knockdown cells. 14-3-3 σ knockdown cells were created by stably infecting HCT116 cells with two specific 14-3-3 σ shRNA (1 & 2). Luciferase shRNA was used as a control (C). Lysates were immunoprecipitated with anti-COP1 and immunoblotted with anti-ubiquitin.

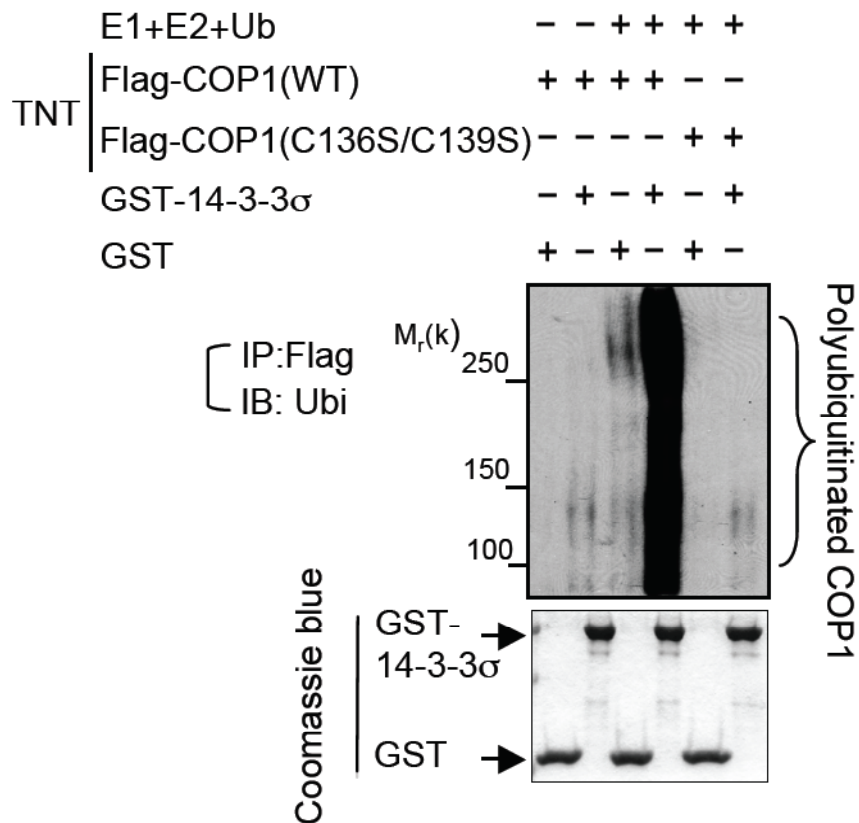


Figure 3-14. 14-3-3 σ promotes COP1 self-ubiquitination. Flag-COP1 and Flag-COP1 RING (C136S, C139S) mutant proteins were made using an *in vitro* Transcription/Translation system (TNT) and then incubated with the indicated purified GST proteins. Polyubiquitinated COP1 was examined by immunoprecipitating with anti-Flag, followed by immunoblotting with anti-ubiquitin (top panel). The bottom panel shows the input of GST proteins (Coomassie Blue staining).

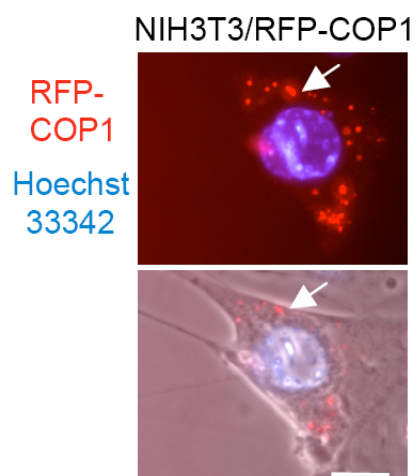
3.5 14-3-3 σ affects COP1 subcellular localization

Given that COP1 contains NES and NLS (Yi et al., 2002), COP1 is nuclear-cytoplasmic repartitioning. Arabidopsis COP1 localization is shuttling between the nucleus and cytoplasm and is regulated by light (Osterlund et al., 2000). In mammal, it has been demonstrated that endogenous COP1 localization is regulated by DNA damage using the fractionation assay (Dornan et al., 2006). To confirm this observation, we observed COP1 localization in NIH3T3 cells expressing RFP-COP1 in live cells. Time-lapse confocal microscopy showed that COP1 formed punctate foci (Figure 3-15 A) and COP1 shuttled between the nucleus and cytoplasm in unstressed cells (Figure 3-15 B, top panel); however, COP1 shuttling to the nucleus was blocked in ionizing radiation-treated cells (Figure 3-15 B, bottom panel). It indicates that IR blocks COP1 shuttling from the cytoplasm to the nucleus. In Figure 3-16, cell fractionation assay showed that cytoplasmic portions of COP1 were increased in cells treated with doxorubicin or IR compared to those in unstressed cells. It suggests DNA damage-induced COP1 nuclear exclusion. Given that 14-3-3 σ is induced by DNA damage and have an effect on regulating the subcellular localization of its targets (Rittinger et al., 1999), U2OS cells stably expressing RFP-COP1 were infected with Ad- β -gal or Ad-14-3-3 σ . COP1 was shuttled between the cytoplasm and nucleus when cells were infected with Ad- β -gal as observed by confocal microscopy. However, COP1 shuttling was blocked when cells were infected with Ad-14-3-3 σ . Cell fractionation also confirmed that cytoplasmic COP1 levels increased in 14-3-3 σ -infected cells compared to Ad- β -gal-infected cells (Figure 3-17). Together, COP1 localization is accumulated to the cytoplasm in response to DNA damage and in 14-3-3 σ -infected cells.

Next we address the specific role of 14-3-3 σ in IR-induced COP1 translocation to the cytoplasm. We further detected cytoplasmic and nuclear COP1 portion by irradiating HCT116 14-3-3 $\sigma^{+/+}$ and HCT116 14-3-3 $\sigma^{-/-}$ cells. We found that IR-induced COP1 translocation from the nucleus to the cytoplasm was impaired in HCT116 14-3-3 $\sigma^{-/-}$ cells compared to HCT116 14-3-3 $\sigma^{+/+}$ cells (Figure 3-18A). Consistently, COP1 translocation from the nucleus to the cytoplasm was compromised in 14-3-3 σ knockdown cells (Figure 3-18B). Taken together, 14-3-3 σ plays a critical role in the nuclear export of COP1.

It is known that 14-3-3 σ 's NES is required for its target's translocation to the cytoplasm (Rittinger et al., 1999). To examine whether 14-3-3 σ 's NES is required for mediating COP1 nuclear export, RFP-14-3-3 σ NES (I205A, L208A) mutant or 14-3-3 σ (WT) were constructed and cotransfected with GFP-COP1 in U2OS cells. Using immunofluorescence microscopy, we found that localization of COP1 was more in the nucleus when cells were transfected with RFP-14-3-3 σ NES (I205A, L208A) mutant (Figure 3-19). It suggests that COP1 nuclear export is required for 14-3-3 σ NES signal.

A



B

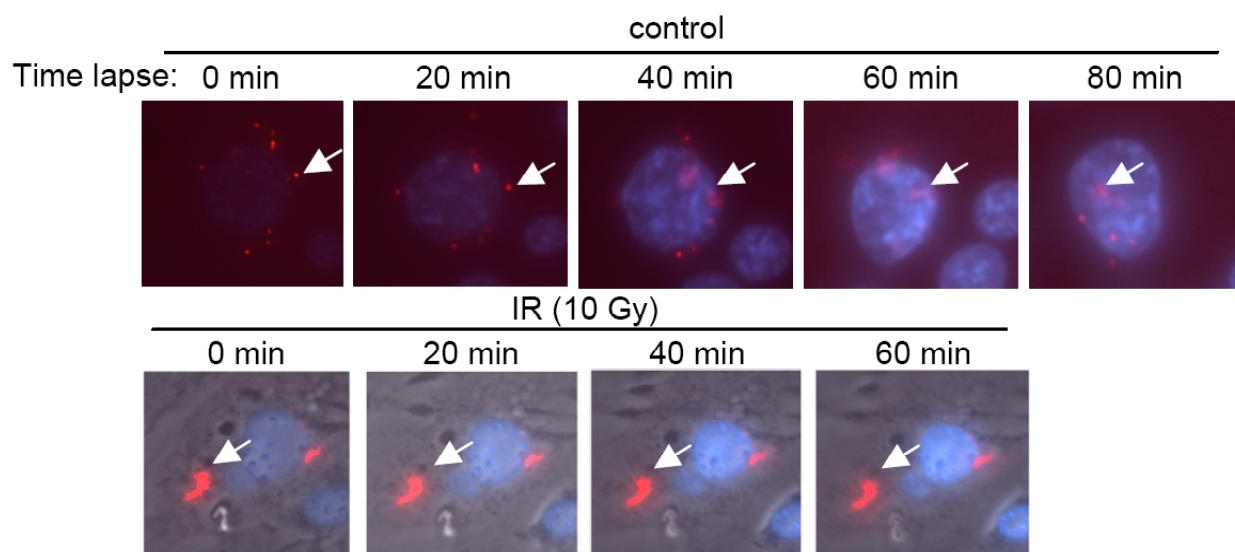


Figure 3-15. COP1 nuclear accumulation is blocked in IR-induced cells using confocal microscopy. (A) COP1 is shuttling between the cytoplasm and nucleus. Live-cell imaging is captured in NIH3T3 cells expressing RFP-COP1. Typical subcellular localization of RFP-COP1 (red, indicated by arrow) is shown. Hoechst 33342 (0.04 $\mu\text{g/mL}$) was added for DNA staining (blue). Merged image containing phase-contrast image is also indicated. Scale bar, 10 μm . (B) Dynamic shuttling of RFP-COP1 in NIH3T3 cells was abolished when cells were treated with ionizing radiation (IR, 10Gy). Images were captured at 20-min intervals. The minutes indicate the elapsed time since the first picture was taken (30 min after treatment).

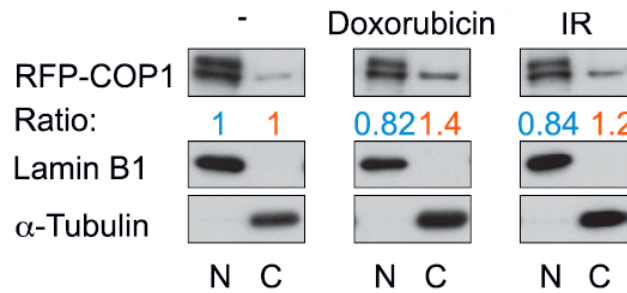


Figure 3-16. The portion of cytoplasmic COP1 is increased in response to doxorubicin and IR using cell fractionation. In U2OS cells, stably expressing RFP-COP1 was treated with 1 μ g/mL doxorubicin (DOX) or 10 Gy ionizing radiation (IR). Subcellular localization of RFP-COP1 was shown by immunoblotting. Lamin B1 was used as the marker of nuclear (N) fraction, while α -tubulin was used as the marker for cytoplasmic (C) fraction.

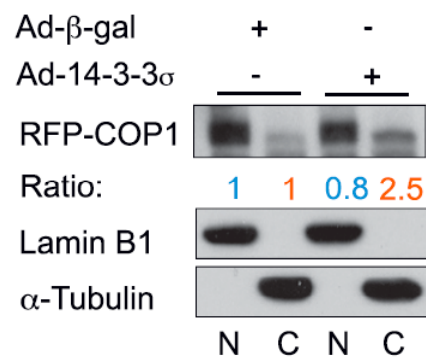
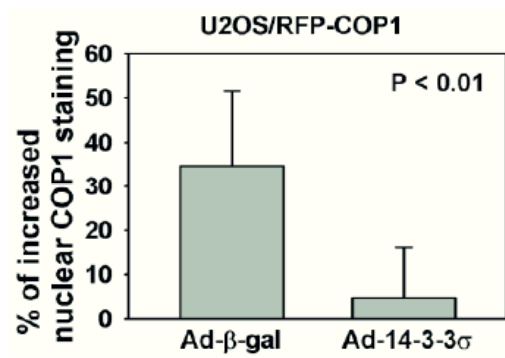
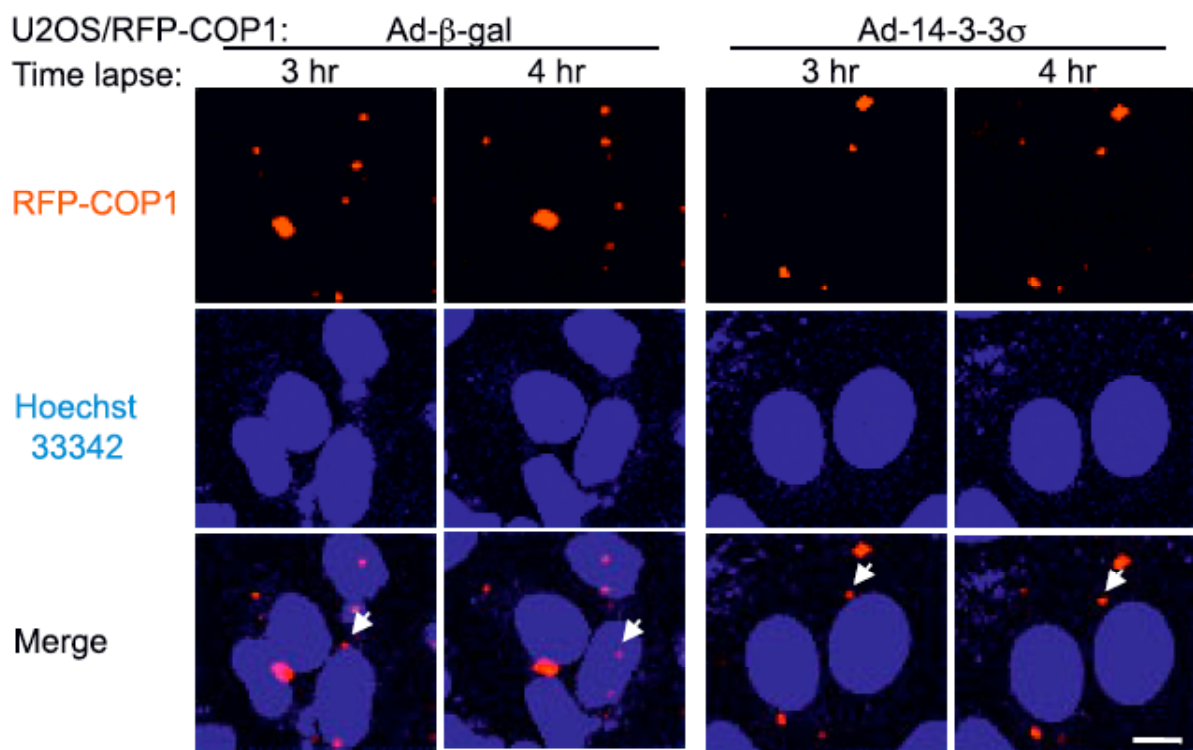


Figure 3-17. COP1 shuttling is blocked by ectopic 14-3-3 σ expression. 14-3-3 σ inhibits COP1 nuclear shuttling. RFP-COP1-expressing cells were infected with Ad- β -gal or Ad-14-3-3 σ . Live-cell images were collected using a confocal microscope at the indicated time points (top). Arrows indicate the representative COP1 translocation from the cytoplasm to the nucleus in the Ad- β -gal treatment group and the lack of nuclear migration in the Ad-14-3-3 σ group. Bar graph shows the percentage of COP1 staining increase in the nucleus in each group (bottom, left panel). Scale bar= 10 μ m. Error bars represent 95% confidence intervals. Cell fractionation of RFP-COP1 in each group is shown by immunoblotting. (N), nuclear fraction. (C), cytoplasmic fraction (bottom, right panel).

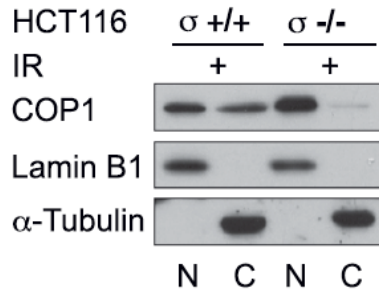
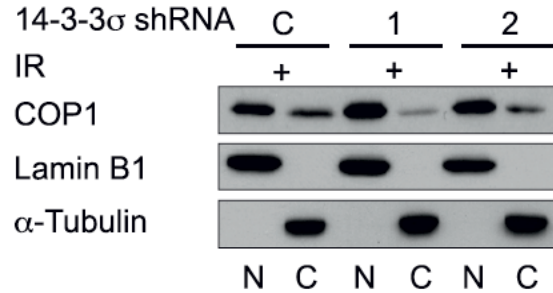
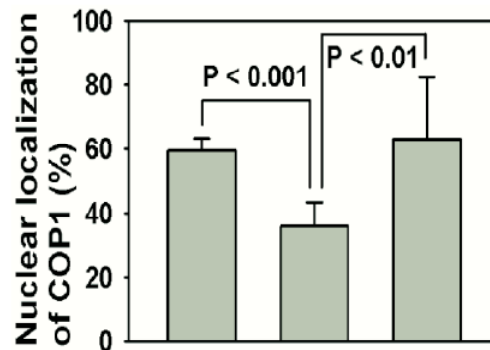
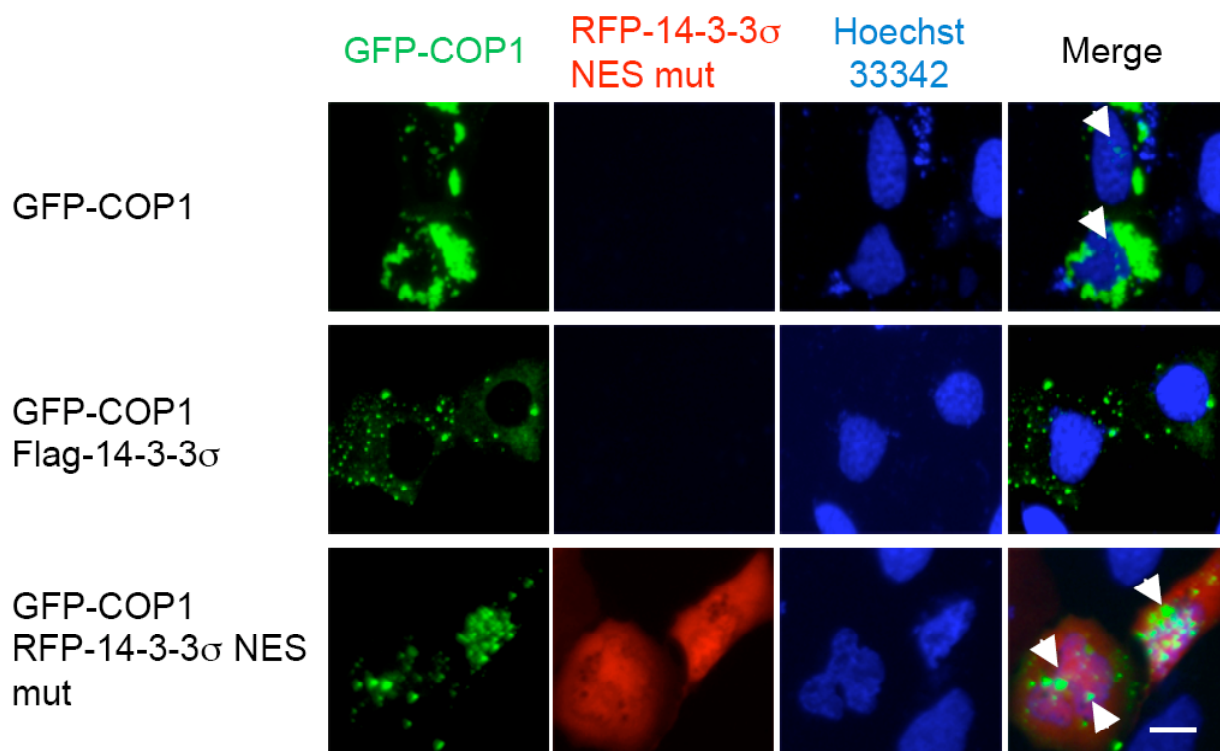
A**B**

Figure 3-18. COP1 shuttling is blocked to the cytoplasm in 14-3-3 σ -null and knockdown cells. (A) Cytoplasmic COP1 localization is compromised after DNA damage in 14-3-3 σ -null cells. HCT116 14-3-3 $\sigma^{+/+}$ and HCT116 14-3-3 $\sigma^{-/-}$ cells were treated with 10 Gy IR. Cytoplasmic and nuclear extracts were prepared 2 hr after irradiation. N, nuclear fraction. C, cytoplasmic fraction. (B) Cytoplasmic COP1 localization is reduced in 14-3-3 σ knockdown cells after IR. HCT116 cells were stably transfected with two specific 14-3-3 σ shRNA (1 & 2). Luciferase shRNA was used as a control (C). Cytoplasmic and nuclear extracts were prepared 2 hours after cells were treated with 10 Gy IR.



GFP-COP1	+	+	+
Flag-14-3-3 σ	-	+	-
RFP-14-3-3 σ NES mut	-	-	+

Figure 3-19. 14-3-3 σ nuclear export signal is required for mediating cytoplasmic accumulation of COP1. Flag-14-3-3 σ wild type (WT), RFP-14-3-3 σ NES (I205A, L208A) or GFP-COP1 mutant plasmids were cotransfected into U2OS cells. Live-cell images of GFP-COP1 localization were observed using a fluorescence microscope (top). Quantification of the nuclear localization of COP1 are shown as a bar graph (bottom). Error bars represent 95% confidence intervals. Scale bar, 10 μ m.

3.6 14-3-3 σ binding to COP1 is phosphorylation-dependent

It is known that 14-3-3 preferentially binds to target proteins at the sequences matching the consensus motif RSXpS/pTXP and RXXXpS/pTXP, where pS/pT represents phosphoserine and phosphothreonine (Hermeking et al., 1997). We analyzed the COP1 sequence and found that COP1 has a putative 14-3-3 σ binding motif, located at Ser 387. This motif (RTAS387QL) is evolutionarily conserved in mammals (Figure 3-20). We hypothesized that interaction between 14-3-3 σ and COP1 is phosphorylation-dependent since other known targets of 14-3-3 σ are phosphorylated prior to 14-3-3 σ binding. To test this hypothesis, lysates from cells stably expressing Flag-COP1 were treated with or without phosphatase inhibitors (sodium fluoride and sodium orthovanadate). We found that the levels of binding between 14-3-3 σ and COP1 were accumulated when cells were treated with phosphatase inhibitors (Figure 3-21). We will further confirm the binding between COP1 and 14-3-3 σ in CIP-treated cells. It indicates that binding is dependent on phosphorylation of COP1. To further confirm whether ATM-mediated COP1 phosphorylation is required for 14-3-3 σ binding, we detected COP1 and 14-3-3 σ in ataxia-telangiectasia mutated protein (ATM^{-/-}) fibroblasts without and with full-length cDNA (AT22IJE-T and AT22IJE-TpEBS7-YZ5). The levels of binding between COP1 and 14-3-3 σ increased when cells were irradiated in the presence of ATM but binding was compromised in the absence of ATM (Figure 3-22). Since COP1-S387 is phosphorylated by ATM (Dornan et al., 2006) and binding between COP1 and 14-3-3 σ is phosphorylation-dependent (Figure 3-21), we examine whether phosphorylation of COP1 at Ser 387 is required for binding between 14-3-3 σ and COP1. We mutated serine to alanine at COP1 at S387 and coimmunoprecipitation showed that COP1 (S387A) mutant lost the binding for

14-3-3 σ (Figure 3-23). It indicates that COP1-S387 phosphorylation is required for the binding between 14-3-3 σ and COP1.

A

14-3-3 binding motif	R	S/T	X	S	X	P
Human COP1	R	T	A	S	Q	L
ASK1	R	S	I	S	L	P
Cdc25C	R	S	P	S	M	P
p53	Q	S	T	S	R	H
FKHRL1	R	A	V	S	M	D
KSR	R	T	E	S	V	P

B

14-3-3 binding motif					RS/TX	S	X	P					
Human	381	D	D	S	R	T	A	S	Q	L	D	E	F
Chimpanzee	381	D	D	S	R	T	A	S	Q	L	D	E	F
Dog	383	D	D	S	R	T	A	S	Q	L	D	E	F
Mouse	383	D	D	S	R	T	A	S	Q	L	D	E	F
Cattle	385	D	D	S	R	T	A	S	Q	L	D	E	F

Figure 3-20. COP1 contains 14-3-3 σ consensus binding motif. (A) Sequences of COP1 and other known 14-3-3 substrates are shown for comparison. (B) Sequence alignment of COP1 containing 14-3-3 binding motifs among different species is shown. The consensus 14-3-3 binding motif is highlighted.

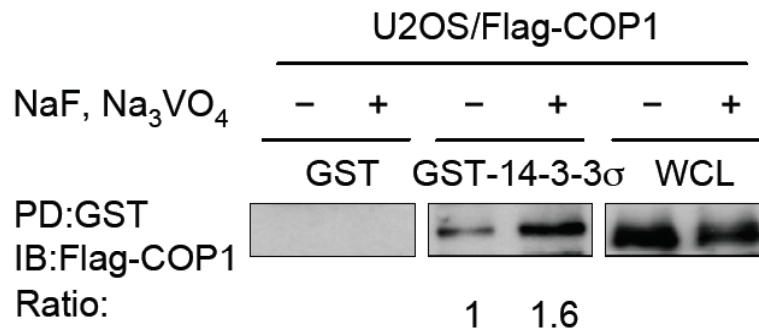


Figure 3-21. Binding between 14-3-3 σ and COP1 is phosphorylation-dependent.

Lysates of U2OS cells stably expressing Flag-COP1 were treated with or without sodium fluoride and sodium orthovanadate. Before harvesting, cells were treated with proteasome inhibitors. Lysates were incubated with purified GST-14-3-3 σ or GST and immunoblotted with anti-Flag. PD: pull down.

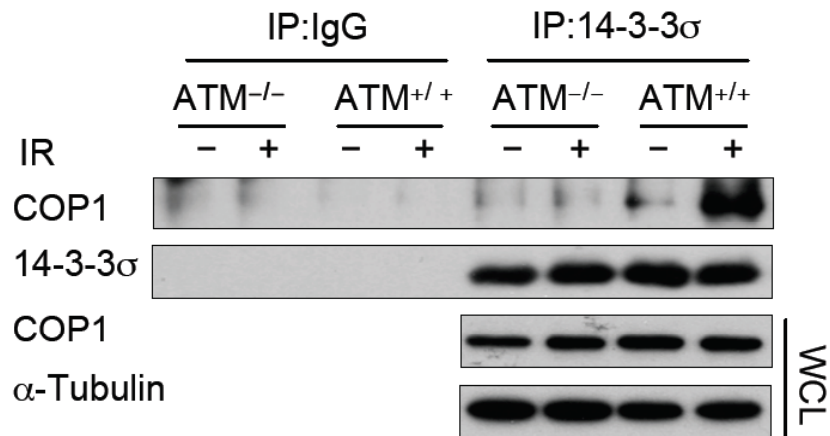


Figure 3-22. ATM facilitates the binding between 14-3-3σ and COP1. AT221JE-T/pEBS7 (ATM^{-/-}) and AT221JE-T/YZ5 (ATM^{+/+}) cells were treated with MG132 for 6 hrs before harvesting and were prepared at 0 (-) and 1 hr (+) after cells were treated with 10 Gy IR. Lysates were immunoprecipitated with anti-14-3-3σ and immunoblotted with anti-COP1.

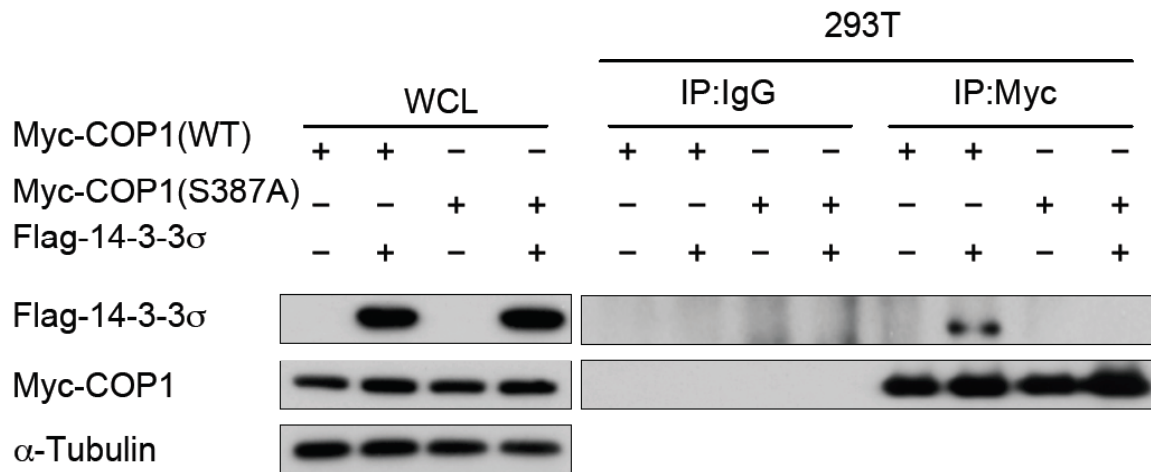


Figure 3-23. COP1 (S387A) abolishes binding to 14-3-3 σ *in vivo*. 293T cells were transfected with Flag-14-3-3 σ , Myc-COP1 (WT), and Myc-COP1 (S387A). Lysates were immunoprecipitated with anti-Myc and then immunoblotted with anti-Flag.

3.7 COP1 S387 phosphorylation is required for 14-3-3 σ -mediated COP1 nuclear export

14-3-3, which functions as an adaptor protein, can bind and change the subcellular localization of its targets (Rittinger et al., 1999). Given that ectopic 14-3-3 σ promotes nuclear export of COP1 (Figure 3-17), COP1 is accumulated in the nucleus in 14-3-3 σ knockout cells, and COP1-S387 phosphorylation is required for 14-3-3 σ binding. We further investigate whether 14-3-3 σ induces nuclear export of COP1 is dependent on S387 phosphorylation. 293T cells were cotransfected with Flag-COP1 (wt) and Flag-COP1 (S387A). We detected nuclear and cytoplasmic COP1 fraction using a fractionation assay and found that cytoplasmic COP1 (wt) fraction was increased when cells were infected with Ad-14-3-3 σ compared to cells infected with control Ad- β -gal. However, the increase of cytoplasmic COP1 (S387A) portion was inhibited when cells were infected by Ad-14-3-3 σ following DNA damage, indicating that 14-3-3 σ -mediated COP1 nuclear export is required for S387 phosphorylation of COP1 (Figure 3-24). We confirmed this result using confocal microscopy. Following DNA damage, GFP-COP1 dynamic shuttling was blocked to the nucleus when cells transfected with 14-3-3 σ . However, GFP-COP1 (S387A) dynamic shuttling was resistant to 14-3-3 σ -mediated nuclear-export effect (Figure 3-25). Together, these results suggest that 14-3-3 σ is required for IR-induced COP1 nuclear exclusion and 14-3-3 σ –mediated nuclear export of COP1 is dependent on phosphorylated COP1 at Ser 387.

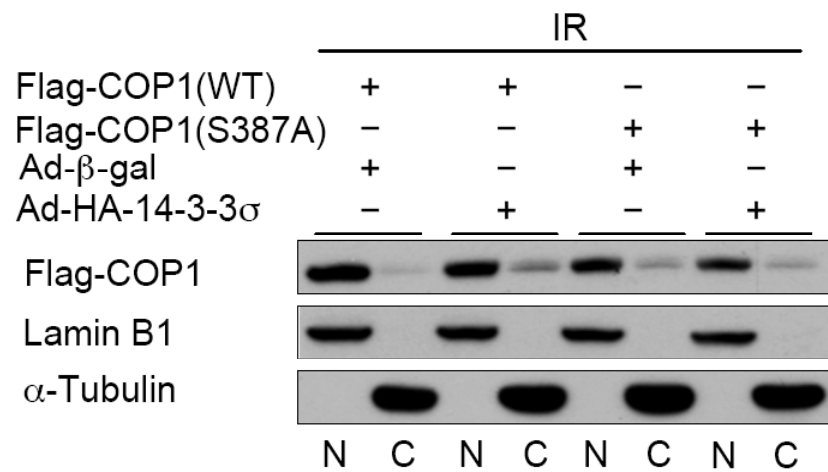


Figure 3-24. 14-3-3 σ -induced COP1 translocation to the cytoplasm is S387 phosphorylation-dependent. 293T cells were transfected with the indicated plasmids. Cytoplasmic and nuclear extracts were prepared 2 hours after 10 Gy IR.

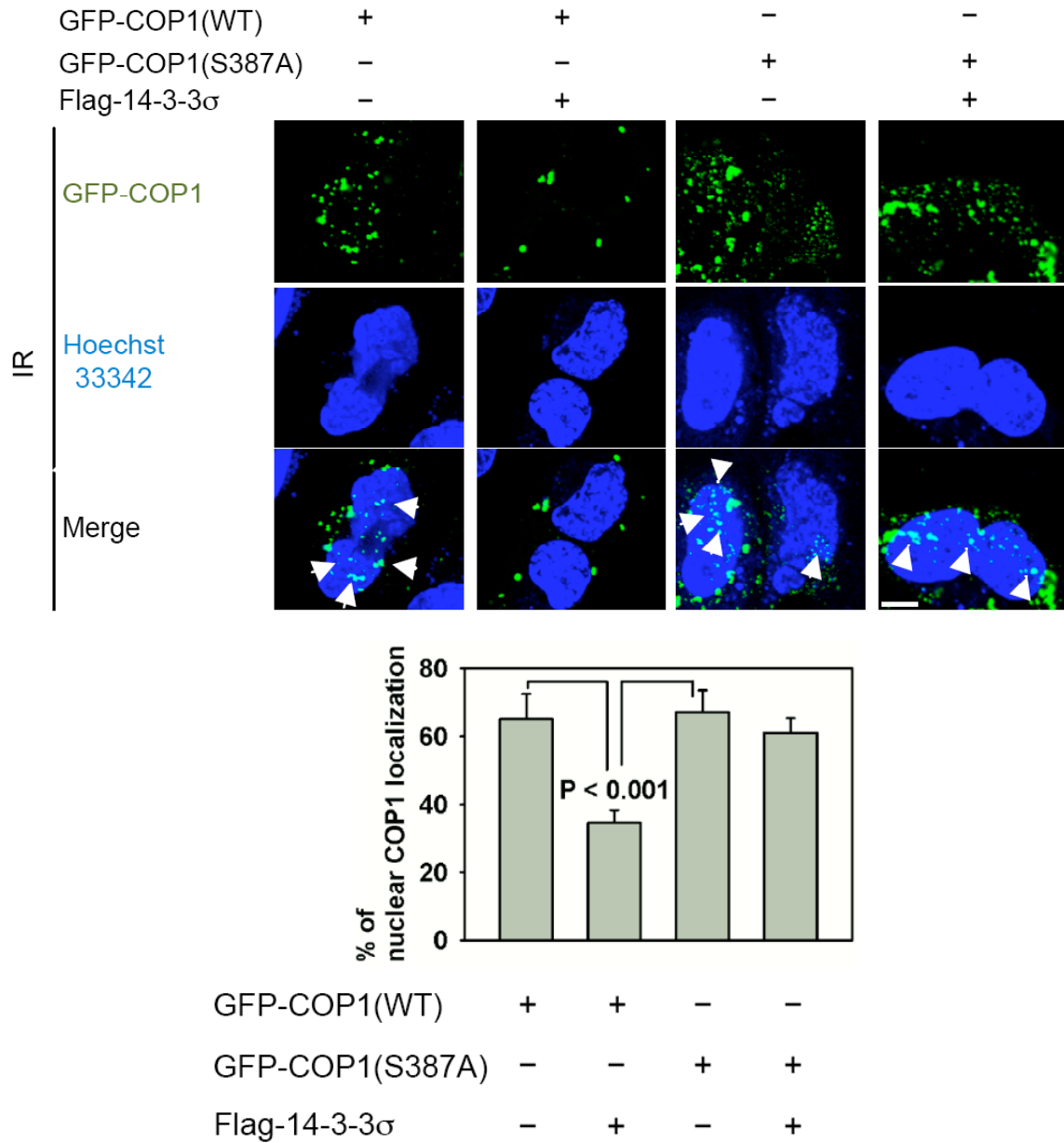


Figure 3-25. 14-3-3 σ -induced COP1 translocation to the cytoplasm is S387 phosphorylation-dependent. U2OS cells were transfected with the indicated plasmids. GFP-COP1 localization of live-cell images were captured using a confocal microscope (top). Cytoplasmic and nuclear extracts were prepared 2 hours after 10 Gy IR. Percentage of COP1 localization in the nucleus is measured and shown as a bar graph at 2 hr after 10 Gy IR (bottom).

3.8 COP1-S387 phosphorylation is important for 14-3-3 σ -mediated COP1 degradation

Since 14-3-3 σ causes the instability of COP1 (Figure 3-4, 3-5, 3-6) and 14-3-3 σ binds to phosphorylated COP1 at S387 (Figure 3-23), we hypothesize that COP1-S387A expression may abolish 14-3-3 σ -mediated COP1 degradation. 293T cells were transfected with either COP1 (wt) or COP1 (S387A). The levels of wild-type COP1 steady-state were decreased in a dose-dependent manner when cells were transfected 14-3-3 σ . However, the steady-state level of COP1 (S387A) was not affected by the expression of 14-3-3 σ (Figure 3-26). We further showed that the turnover rate of COP1 was facilitated by 14-3-3 σ expression; while the turnover rate of COP1 (S387A) was not affected by 14-3-3 σ expression (Figure 3-27). In addition, COP1 ubiquitination was facilitated by 14-3-3 σ while COP1 (S387A) ubiquitination was not affected by 14-3-3 σ (Figure 3-28). Given that 14-3-3 σ is involved in DNA damage-induced COP1 translocation to the cytoplasm and facilitates COP1 ubiquitination, we investigate whether 14-3-3 σ promotes cytoplasmic COP1 ubiquitination in the response to DNA damage. More cytoplasmic COP1 ubiquitination was detected in HCT116 14-3-3 $\sigma^{+/+}$ cells treated with 10 Gy IR compared with no IR treatment (lane 1 and lane 2 in Figure 3-29). At the same time, we found that cytoplasmic COP1 ubiquitination was reduced in HCT116 14-3-3 $\sigma^{-/-}$ cells compared to HCT116 14-3-3 $\sigma^{+/+}$ cells (lane 2 and lane 4 in Figure 3-29). Taken together, ATM-induced COP1 S387 phosphorylation is required for 14-3-3 σ -mediated COP1 nuclear export and ubiquitination in the cytoplasm.

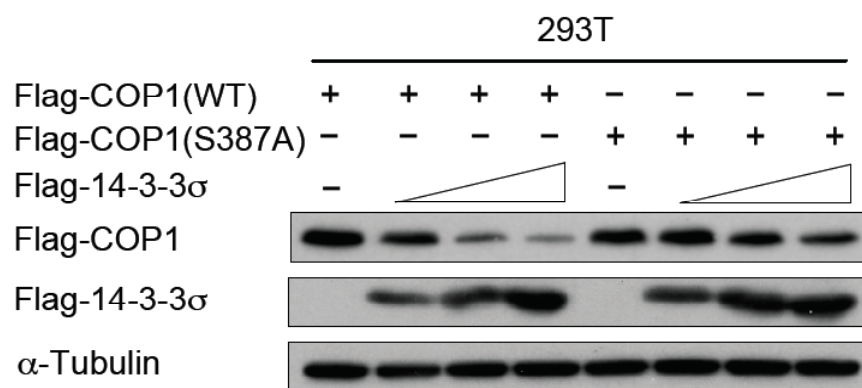


Figure 3-26. 14-3-3 σ downregulates the steady state of COP1 (WT) but not COP1 (S387A). 293T cells were cotransfected with the indicated Flag-COP1 (WT), Flag-COP1 (S387A), and Flag-14-3-3 σ . Cell lysates were immunoblotted with anti-Flag, and anti-tubulin

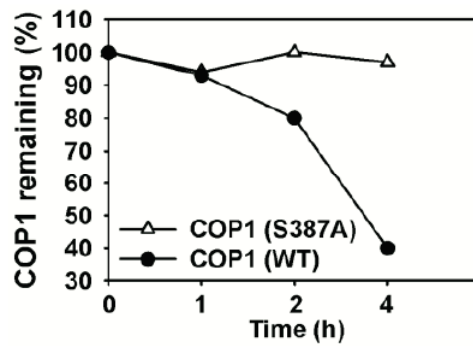
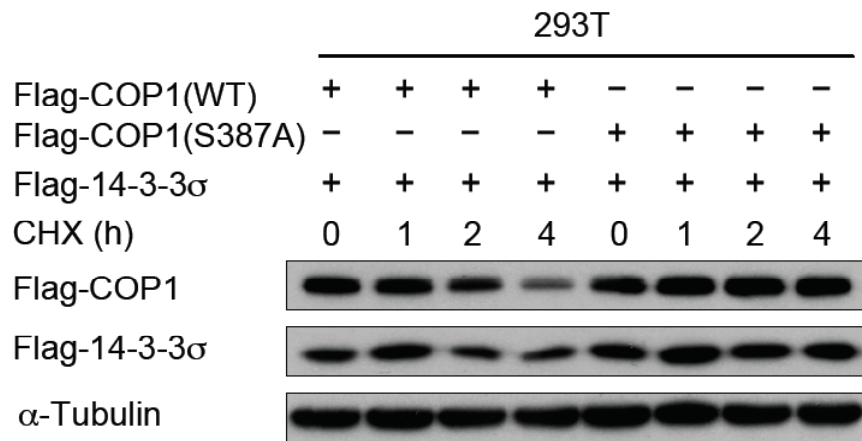


Figure 3-27. 14-3-3 σ facilitates turnover rate of COP1 (WT) but not COP1 (S387A). 293T cells were cotransfected as Figure 3-26. Before harvesting, cells were treated with cycloheximide (CHX) for the indicated times. Cell lysates were immunoblotted with anti-Flag, and anti-tubulin.

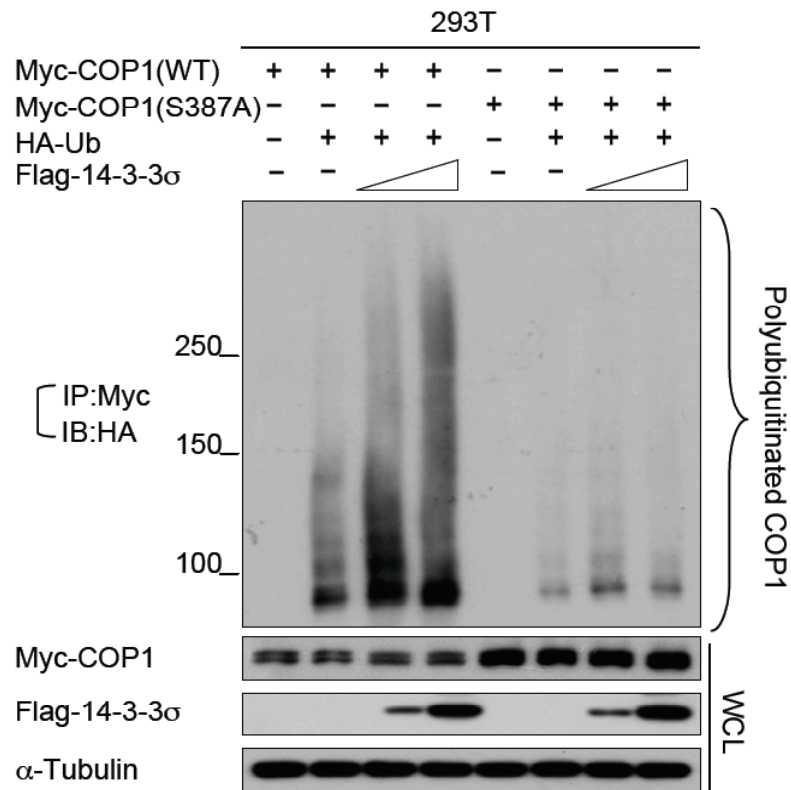


Figure 3-28. 14-3-3 σ promotes COP1 (WT) but not COP1 (S387A) polyubiquitination. 293T cells were cotransfected with indicated Myc-COP1 (WT), Myc-COP1 (S387A), and Flag-14-3-3 σ . The cells were treated with MG132 for 6 h before harvest, and the ubiquitinated COP1 was immunoprecipitated with anti-Myc and immunoblotted with anti-HA. Equal amounts of lysates were immunoblotted with anti-Myc, anti-Flag, or anti-tubulin.

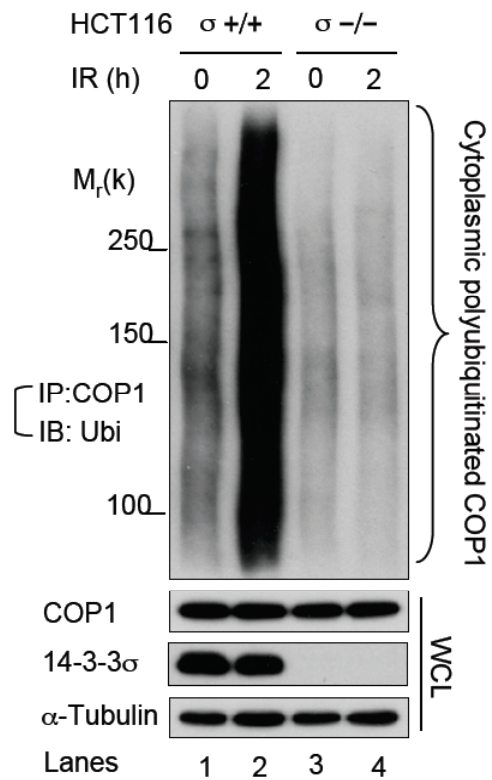


Figure 3-29. 14-3-3 σ promotes cytoplasmic COP1 polyubiquitination in response to DNA damage. HCT116 14-3-3 $\sigma^{+/+}$ (lanes 1 and 2) and HCT116 14-3-3 $\sigma^{-/-}$ (lanes 3 and 4) were treated with MG132 for 6 hrs before harvesting. Cytoplasmic extracts were prepared at 0 and 2 hr after cells were treated with 10 Gy IR. Cytoplasmic polyubiquitinated COP1 was detected by immunoprecipitation with anti-COP1 and immunoblotting with anti-ubiquitin in indicated cells.

3.9 14-3-3 σ blocks COP1-mediated p53 degradation and transcriptional repression

Previous evidence has shown that COP1 is a p53 E3 ligase (Dornan et al., 2004a) and previous data have shown that 14-3-3 σ binds to COP1 and promotes COP1 ubiquitination (Figure 3-7 and 3-11). We further studied whether 14-3-3 σ blocks COP1-mediated p53 degradation. 293T cells were cotransfected with Flag-COP1, GFP-p53, and increasing amount of 14-3-3 σ . As we expected, the steady state levels of p53 was lowered by COP1. At the time, increasing amount of 14-3-3 σ degraded COP1 and blocked COP1-mediated p53 degradation (Figure 3-30). 14-3-3 σ negative impacts on COP1-mediated p53 degradation will be confirmed in endogenous p53 levels. We further transfected p53, Flga-COP1, and Flag-14-3-3 σ in H1299 (p53 null) to detect p53 ubiquitination. We found that increasing amount of 14-3-3 σ blocked COP1-mediated p53 ubiquitination (Figure 3-31). To exclude the contribution of MDM2, a p53 E3 ligase, on p53 ubiquitination, p53^{-/-} MDM2^{-/-} MEF cells were transfected with the same plasmids. We found that 14-3-3 σ still blocked COP1-promoted p53 ubiquitination (Figure 3-32). This suggests that 14-3-3 σ 's negative impact on COP1-mediated p53 ubiquitination is independent of negative impacts on MDM2-mediated p53 ubiquitination.

To study the biological consequence of 14-3-3 σ 's negative impact on COP1-mediated p53 degradation and ubiquitination, we analyze gene expression of p53 target genes in two p53-positive cell lines (colon carcinoma HCT116 and osteosarcoma U2OS) using real-time PCR. We found that mRNA levels of p53 target genes, including *CDKN1A*, *SFN*, *BAX*, and *PUMA*, were reduced in Myc-COP1 or RFP-COP1 overexpressing cell lines. However, mRNA levels of p53 targets were accumulated in COP1 overexpression cells infected with

Ad-14-3-3 σ compared with cells infected Ad- β -gal (Figure 3-33). To further confirm p53 transcriptional activity using a luciferase reporter gene assay, H1299 (p53 null) cells were transfected with a 14-3-3 σ reporter containing a p53-binding element in the promoter, p53, COP1, and/or 14-3-3 σ plasmids. We found that 14-3-3 σ antagonized COP1-mediated p53 transcriptional repression (Figure 3-34). Taken together, the data suggests that 14-3-3 σ negatively regulates COP1, blocks COP1-mediated p53 degradation, and inhibits COP1-mediated p53 transcriptional repression.

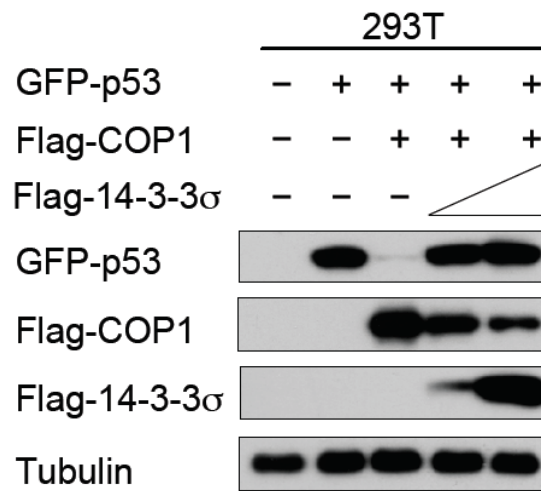


Figure 3-30. 14-3-3 σ antagonizes COP1-mediated p53 degradation. 293T cells were cotransfected with the indicated Flag-COP1, His-p53, and increasing amounts of 14-3-3 σ . Lysates were immunoblotted with anti-His, anti-Flag or tubulin.

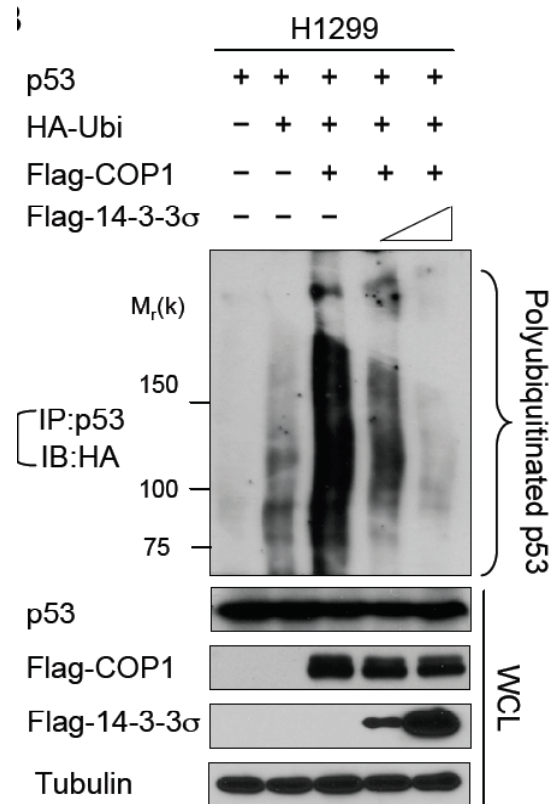


Figure 3-31. 14-3-3 σ inhibits COP1-mediated p53 polyubiquitination. H1299 cells were cotransfected with the indicated HA-ubiquitin, Flag-COP1, p53, and increasing amounts of Flag-14-3-3 σ . Cells were treated with MG132 before harvesting. Lysates were immunoprecipitated with anti-p53 and immunoblotted with anti-HA.

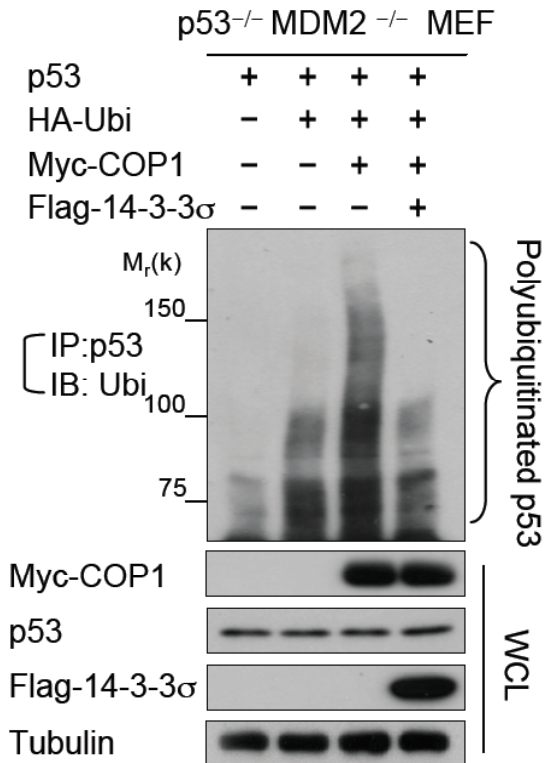


Figure 3-32. 14-3-3 σ reduces COP1-mediated poly-ubiquitination of p53 regardless of the deficiency of MDM2. p53^{-/-}MDM2^{-/-} MEF cells were cotransfected with the indicated Myc-COP1, p53, HA-ubiquitin, and Flag-14-3-3 σ plasmids. Cells were treated with MG132 before harvesting. Poly-ubiquitination of p53 was detected by immunoprecipitation with anti-p53 and immunoblotted with anti-ubiquitin. Lysates were also immunoblotted with indicated antibodies.

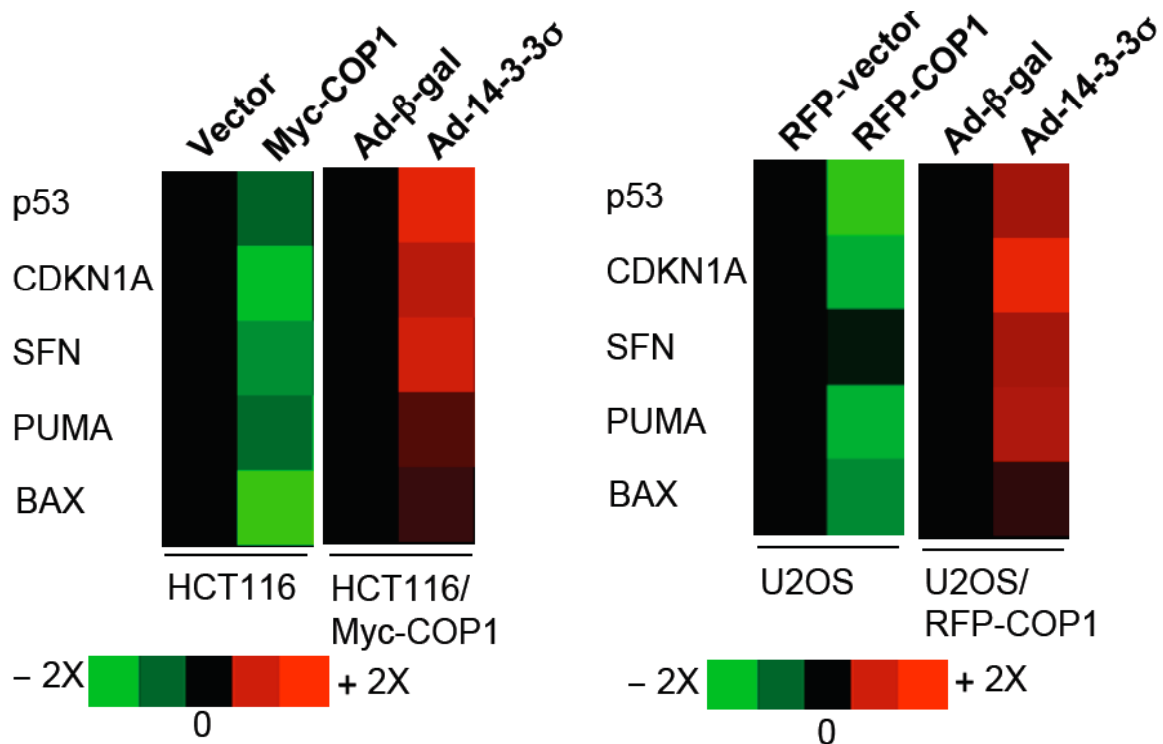


Figure 3-33. 14-3-3σ impairs COP1-mediated p53 transcriptional repression determined by quantitative RT-PCR in cells. The mRNA levels of the indicated p53 target genes, including *CDKN1A*, *SFN*, *PUMA*, and *BAX*, were detected by RT-PCR in indicated cells stably expressing vector, Myc-COP1, or RFP-COP1. Some cells were also infected with the indicated adenovirus expressing β-gal (control) or 14-3-3σ. The expression levels of the indicated p53 target genes were quantitated, and the data are presented as a heat map.

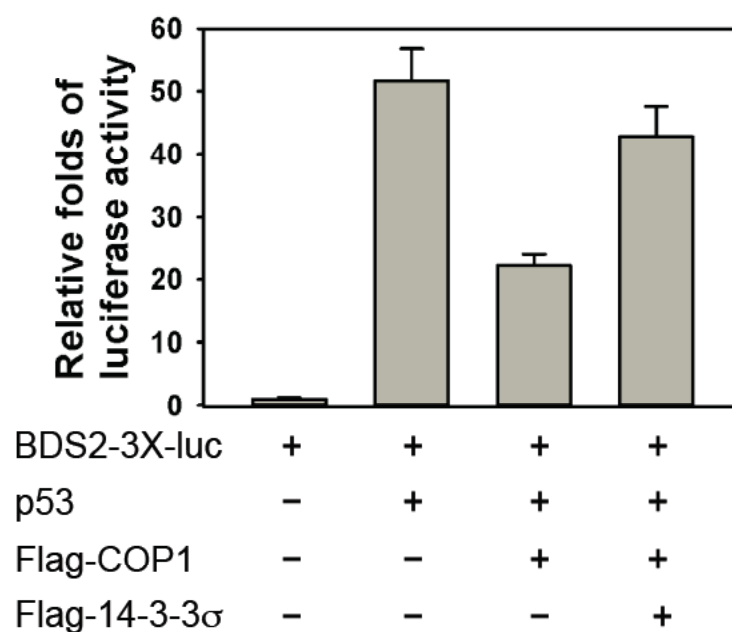


Figure 3-34. 14-3-3 σ antagonizes COP1-suppressed p53 transcriptional activity. The BDS2-3X-luc reporter containing a p53-responsive element was transfected with the indicated p53, Flag-14-3-3 σ , and Flag-COP1 plasmids. Relative luciferase activity was shown in a bar graph.

3.10 14-3-3 σ inhibits COP1-mediated cell proliferation and transformation

Given that COP1 degrades p53(Dornan et al., 2004b), a tumor suppressor, it is possible that COP1 has a negative impact on cell cycle arrest. To prove this possibility, cell growth of COP1 overexpression cells was measured using a MTT assay. We found that stably expressing COP1 promoted cell growth. However, COP1 overexpression cells infected with Ad-14-3-3 σ reduced cell growth compared with cells infected with Ad- β -gal (Figure 3-35).

It has been reported that the knockdown of COP1 sensitizes p53-induced cell death following IR treatment (Dornan et al., 2004b). We examined whether 14-3-3 σ may sensitize COP1 overexpressing cells to IR-induced cell death. We found that cell death were increased when cells were infected with Ad-14-3-3 σ compared with cells infected with Ad- β -gal in response to IR (Figure 3-36). It indicates that 14-3-3 σ facilitates IR-mediated cell death in COP1 overexpressing cells.

Furthermore we studied cell cycle distribution using flow cytometry. We found that COP1 overexpression cells caused S-phase accumulation (28%), while S-phase was reduced to 18% in HCT116 vector controls. Interestingly, the percentage of 14-3-3 σ -infected cells in G2 phase was higher than cells infected Ad- β -gal (Figure 3-37). It indicates that 14-3-3 σ inhibits COP1-mediated cell proliferation through G2 arrest.

Since that COP1 promotes cell growth, we address whether COP1 promotes cell transformation. We found that more numbers of colonies in COP1-overexpressing cells than in control cells using the foci formation assay. However, Ad-14-3-3 σ -infected cells reduced

the numbers of colonies compared with Ad- β -gal-infected cells (Figure 3-38A). We obtained similar results to confirm COP1 has anchorage-independent growth abilities using soft agar formation assay. However, Ad-14-3-3 σ -infected cells reduced the numbers of soft agar colonies compared with Ad- β -gal-infected cells (Figure 3-38B). Together, these functional assays have indicated that COP1 promotes cell proliferation and transformation, and 14-3-3 σ abolishes COP1-promoted cell proliferation and transformation.

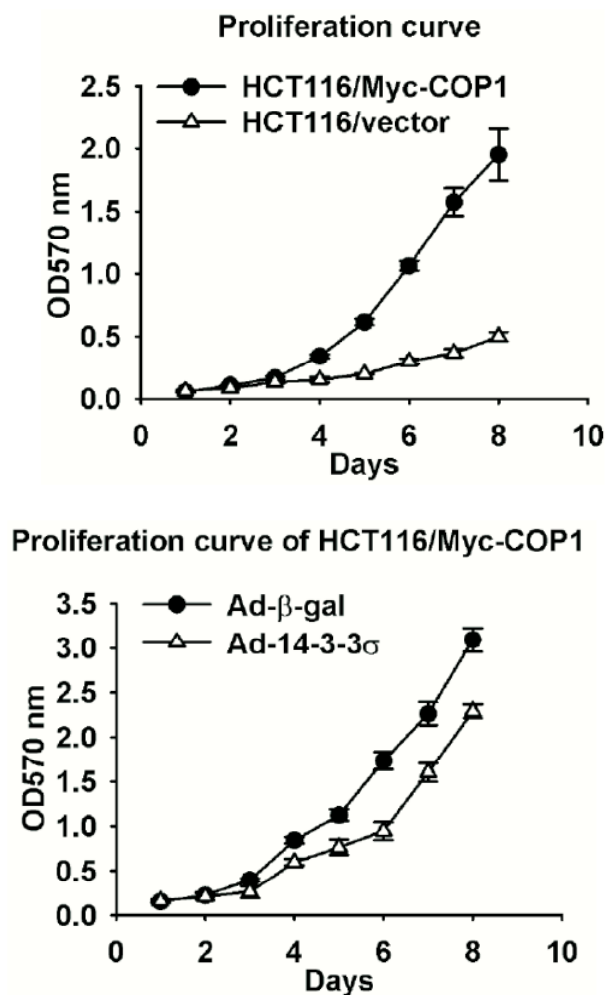


Figure 3-35. 14-3-3 σ inhibits COP1-mediated cell proliferation. The number of live cells of HCT116/Myc-COP1 and HCT116/vector cells was estimated by MTT assay every day for a total of 7 days (top). The results were expressed as the value of OD570 reading. Myc-COP1 expressing cells were infected with Ad- β -gal or Ad-14-3-3 σ (bottom). OD570 absorbance of each group was shown. Error bars represent 95% confidence intervals.

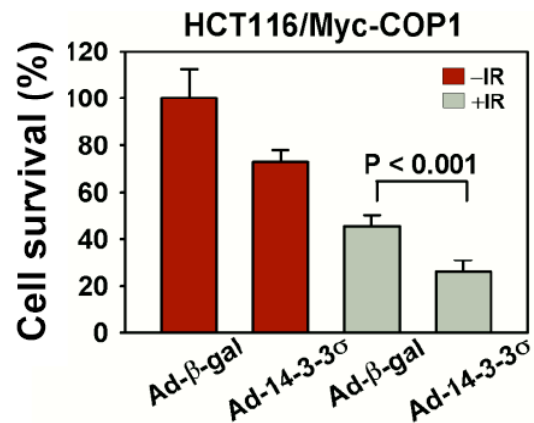


Figure 3-36. 14-3-3 σ can sensitize COP1-expressing HCT116 cells to IR-mediated cell death. HCT116/Myc-COP1 cells were infected with Ad- β -gal or Ad-14-3-3 σ on day 1. Infected cells were treated with or without 10 Gy IR on day 2. Live cells were detected as dye-excluding cells and counted after trypan blue staining on day 4. The bar graph shows the percentage of live cells. Error bars represent 95% confidence intervals.

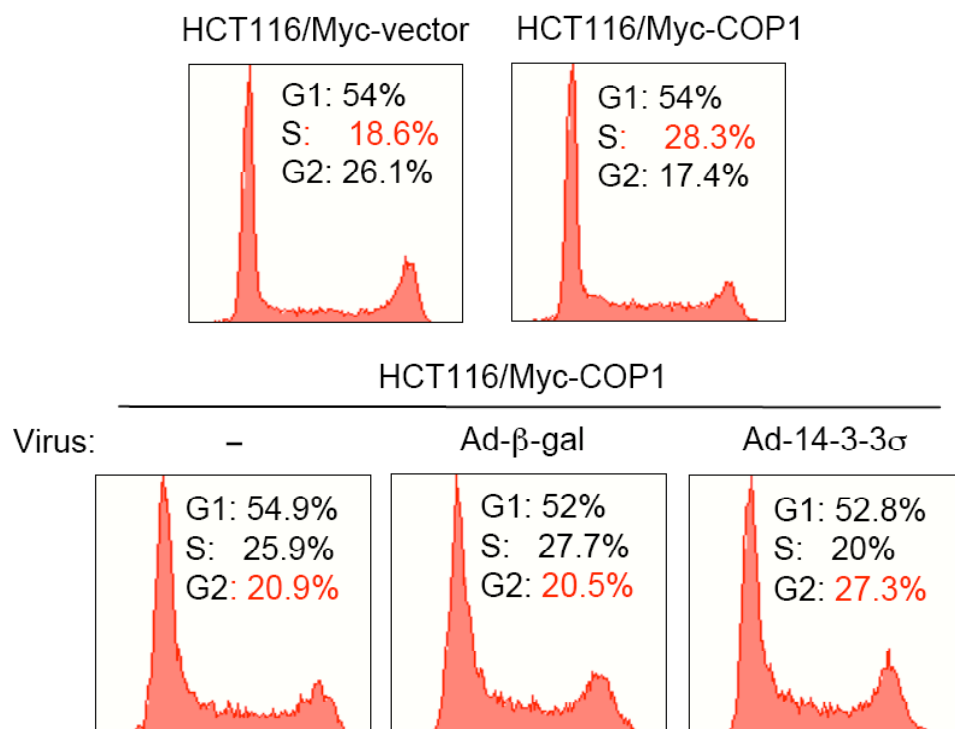


Figure 3-37. 14-3-3 σ inhibits COP1-accumulated S phase population. HCT116/Myc-COP1 and HCT116/vector cells were analyzed for cell cycle distribution using FACS (top). HCT116/Myc-COP1 cells were left uninfected or infected with Ad- β -gal or Ad-HA-14-3-3 σ followed by FACS for cell cycle analysis (bottom). Percentage of each cell cycle phase was indicated. This experiment was done in triplicate.

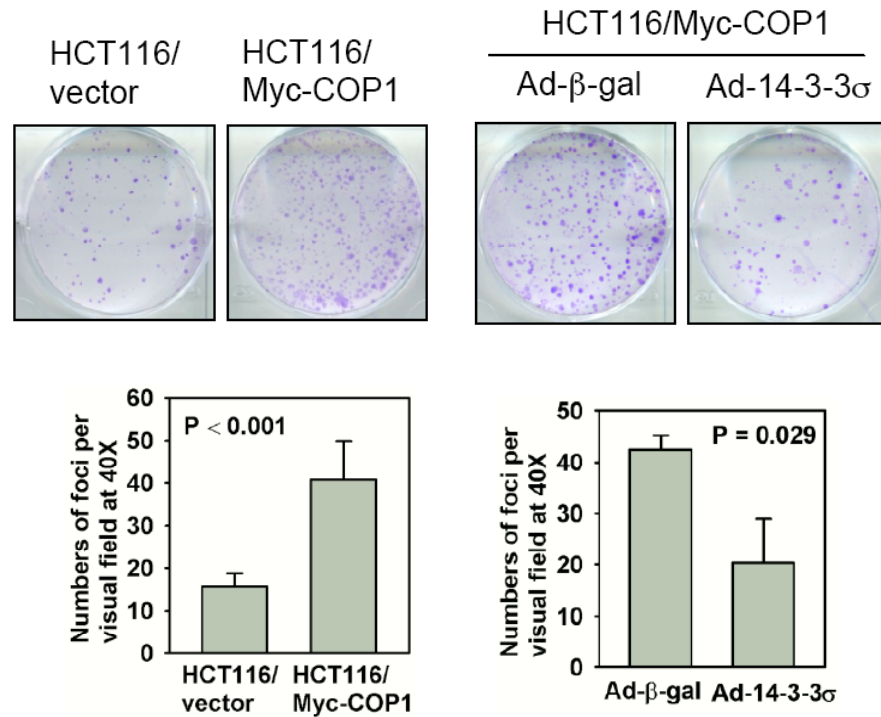


Figure 3-38. 14-3-3 σ antagonizes COP1-mediated foci formation. HCT116/Myc- COP1 and HCT116/vector cells were analyzed for foci formation (top, left panel). HCT116/Myc- COP1 cells infected with Ad- β -gal or Ad-HA-14-3-3 σ were subjected to foci formation (top, right panel). The foci numbers of vector control cells, COP1 overexpression cells, and Ad- β -gal-, and Ad-14-3-3 σ -infected COP1 overexpression cells are presented as bar graphs (bottom). Error bars represent 95% confidence intervals.

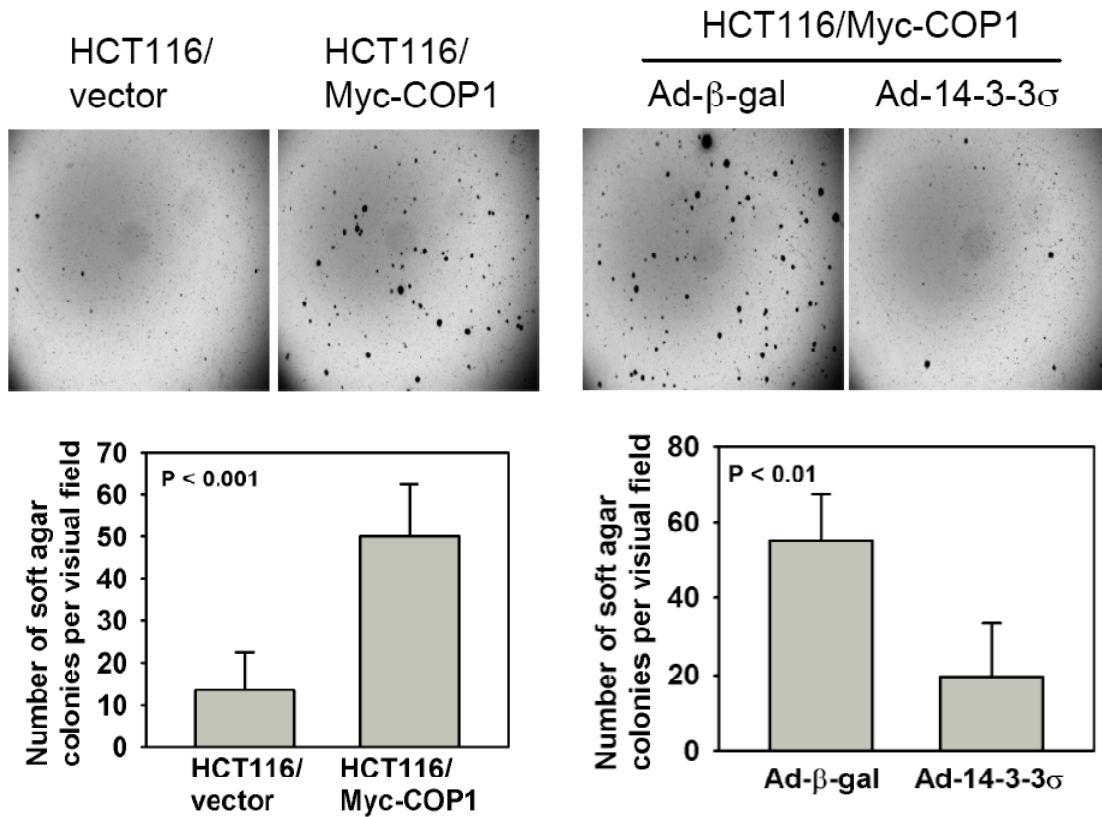


Figure 3-39. 14-3-3 σ antagonizes COP1-promoted soft agar colony formation. HCT116/Myc-COP1 and HCT116/vector cells were analyzed by soft agar assay (top, left panel). HCT116/Myc-COP1 cells infected with Ad- β -gal or Ad-HA-14-3-3 σ were subjected to soft agar assay (top, right panel). The average number of colonies per plate is scored and represented (bottom). Error bars represent 95% confidence intervals.

3.11 14-3-3 σ inhibits COP1-mediated tumor progression

To confirm that 14-3-3 σ blocks COP1 activity *in vivo*, we used a nude mice xenograft model to study the roles of COP1 in tumor progression. Myc-COP1-expressing cells and vector control HCT116 cells were injected into the flanks of nude mice. We found the tumors grew faster in COP1 expressing groups than in vector control groups (Figure 3-40). When mice were scarified and xenografts were measured at the end of experiments, we found that the average of tumor weight and size in COP1 expressing groups was greater than in than HCT116 control cells (Figure 3-40). This indicates that COP1-expressing cells formed the larger tumors than vector control HCT116 cells.

Given that the above results, it is interesting to study whether 14-3-3 σ abolishes COP1 activity in tumor progression. Ad-14-3-3 σ - and Ad- β -gal-infected COP1-expressing cells were injected in nude mice. We found that tumors grew slower in Ad-14-3-3 σ -infected groups than Ad- β -gal groups (Figure 3-41). The average of tumor weight and size in Ad-14-3-3 σ infected groups is smaller than in Ad- β -gal infected groups (Figure 3-41). Xenografts removed from mice were prepared for immunohistochemistry. The levels of cleaved caspase 3, a marker for apoptosis, and p53 were higher and the levels of Ki67, a marker for proliferation, were lower in Ad-14-3-3 σ infected groups than in Ad- β -gal groups (Figure 3-42). Taken together, COP1 overexpression facilitates tumor formation and increases tumor size while 14-3-3 σ compromises COP1-mediated tumor progression.

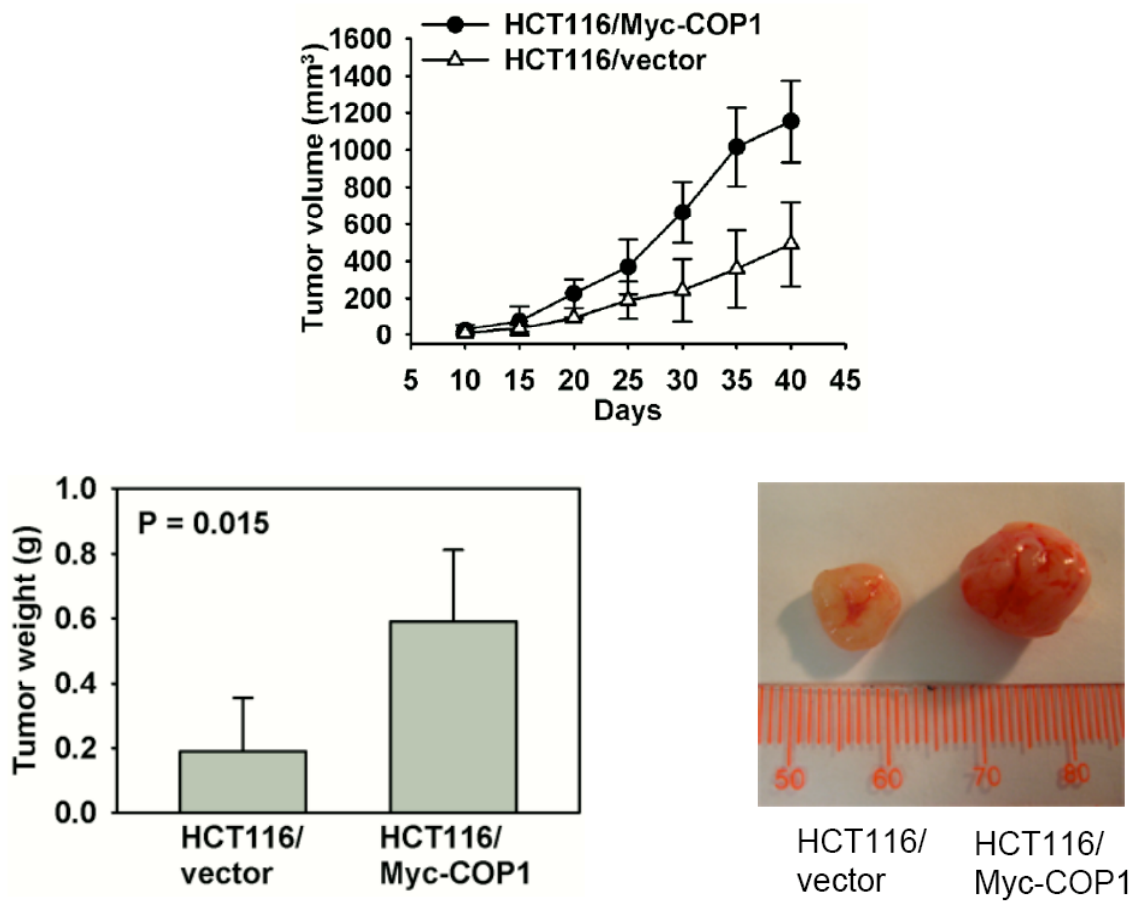


Figure 3-40. Overexpression of COP1 promotes tumor progression. Myc-COP1 overexpressing HCT116 stable transfectants and vector control transfectants were injected subcutaneously into the flank regions of female nude mice. Each group included five mice. Tumor volumes were monitored for 40 days (top). Tumor growth curves are measured at the indicated time points. Error bars represent 95% confidence intervals. Tumors were dissected, and weighed (bar graph) 40 days post-injection (bottom, left panel). Error bars represent 95% confidence intervals. The photograph shows the size of representative tumors obtained (bottom, right panel).

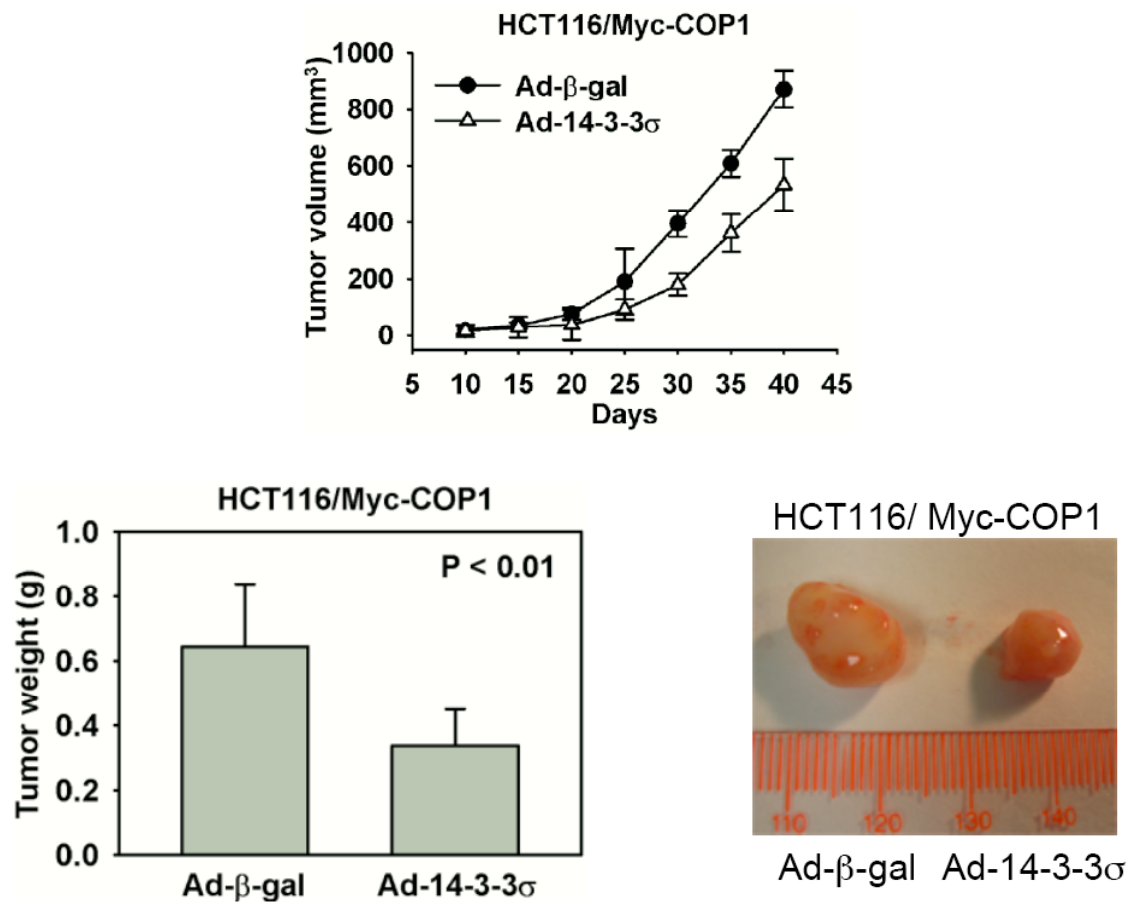


Figure 3-41. 14-3-3 σ suppresses COP1-mediated tumor progression. Myc-COP1 overexpressing HCT116 stable transfectants were infected with Ad-14-3-3 σ and Ad- β -gal. Cells were injected subcutaneously into nude mice. Each group included five mice. Tumor growth curves (top), tumor weight (bottom, left panel), and tumor size (bottom, right panel) were measured. The error bars show 95% confidence.

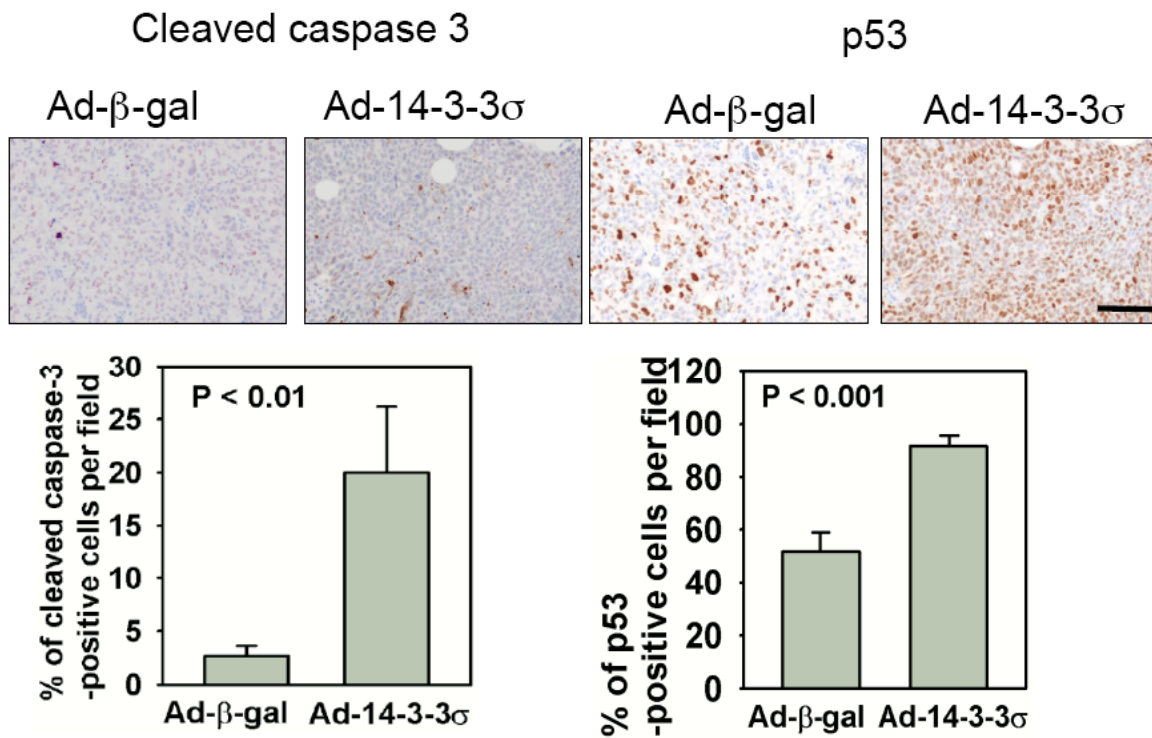


Figure 3-42. Serial tumor sections stained with anti-cleaved Caspase 3 and anti-p53 from experiments in Figure 3-41. Percentage of cells with positive signals from each staining was quantitated and presented as a bar graph. Error bars represent 95% confidence intervals.

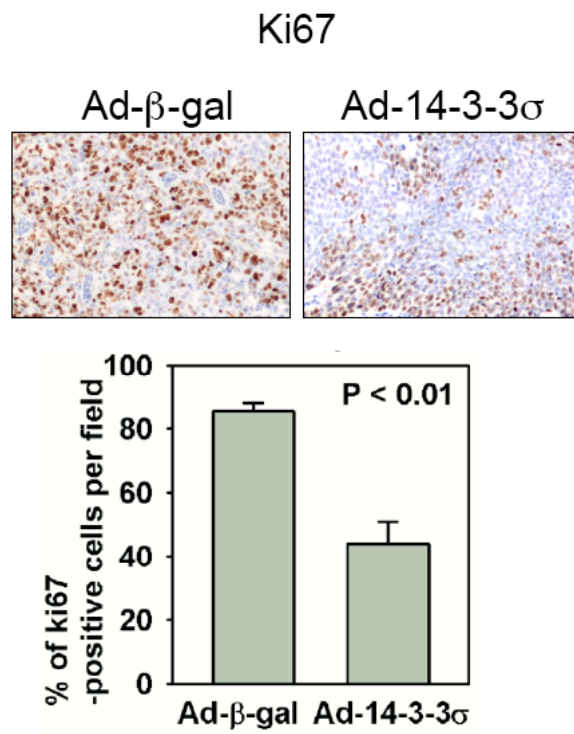


Figure 3-43. Serial tumor sections stained with anti-Ki67 from experiments in **Figure 3-41**. Percentage of cells with positive signals from each staining was quantitated and presented as a bar graph. Error bars represent 95% confidence intervals.

3.12 The expression of COP1 and 14-3-3 σ has an inverse relationship

Our findings show that the 14-3-3 σ inhibits COP1-mediated cell proliferation, cell transformation, and tumor progression. Using immunoblotting assay, we analyzed protein levels of 14-3-3 σ and COP1 in 24 human primary breast cancer specimens. We found that the expression of 14-3-3 σ and COP1 is disproportional (Figure 3-44). Furthermore, we examine 121 human pancreatic cancer specimens to study the inverse relationship between 14-3-3 σ and COP1 using immunohistochemistry (Figure 3-45). Indeed, low 14-3-3 σ expression was detected in 40 (72.2%) of the 55 pancreatic cancer specimens with high COP1 expression ($p < 0.005$) (Table 3-1). Taken together, we have shown that 14-3-3 σ and COP1 have an inverse relationship in breast and pancreatic cancer specimens. This suggests that 14-3-3 σ 's negative impact on COP1 may be clinically useful in the future.

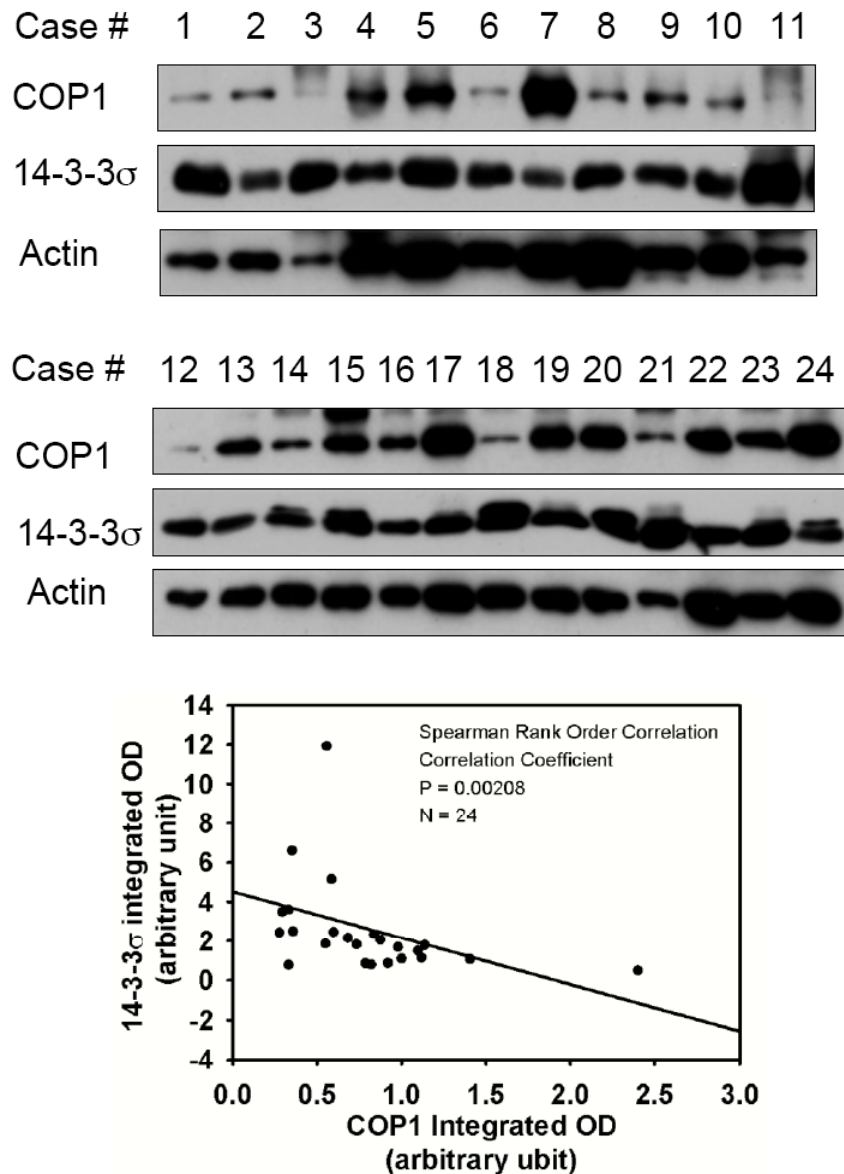


Figure 3-44. 14-3-3 σ and COP1 expression levels are inversely correlated in malignant human breast cancer specimens. Protein levels of COP1 and 14-3-3 σ were analyzed by immunoblotting (top and middle panel). The integrated optical intensity of COP1 was plotted against that of 14-3-3 σ (bottom panel). Spearman rank order correlation was used to demonstrate the inverse correlation between COP1 and 14-3-3 σ protein levels ($p < 0.01$).

Table 3-1. An inverse correlation between 14-3-3 σ and COP1 in pancreatic cancer samples

	COP1 (Low)	COP1 (High)	Total (Number)
14-3-3σ (Low)	32 (48.5%)	40 (72.7%)	72
14-3-3σ (High)	34 (51.5%)	15 (27.3%)	49
Total (Number)	66	55	121

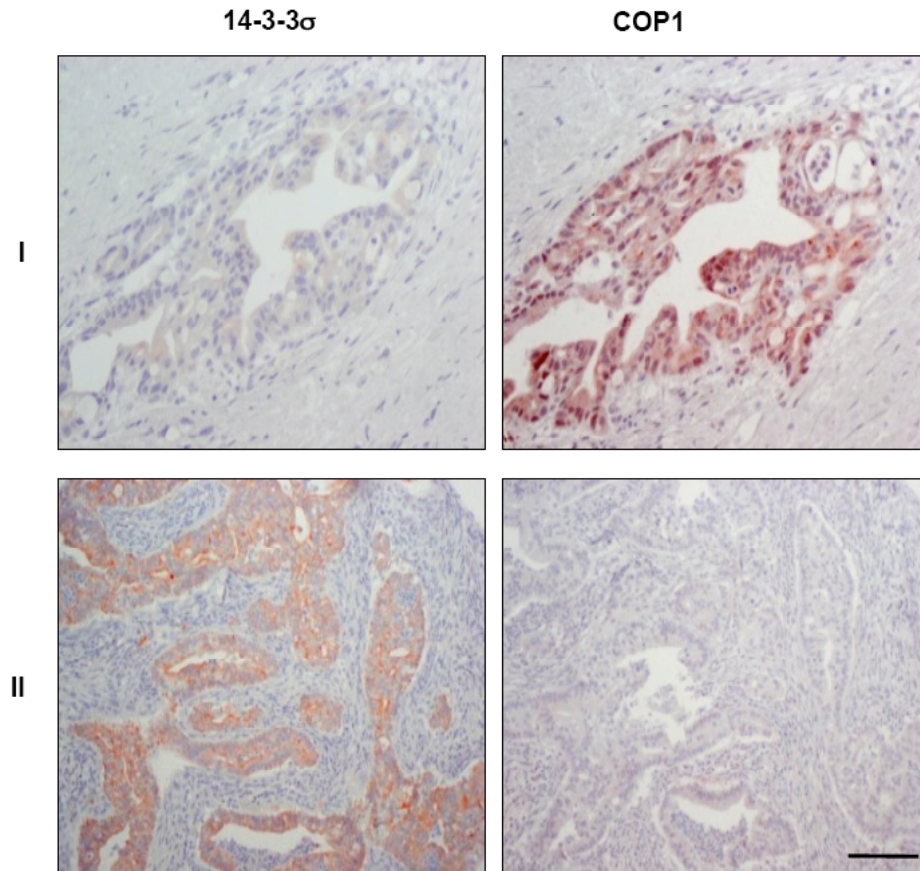


Figure 3-45. There is an inverse correlation between 14-3-3 σ and COP1 in human primary pancreatic cancer specimens. Consecutive tissue sections from tumor case I show a low level of 14-3-3 σ but a high level of COP1. In contrast, consecutive sections from tumor case II show abundant 14-3-3 σ but scanty COP1 (Original magnification, 200 \times). See Table 3-1 for a summary of expression levels of 14-3-3 σ and COP1 expression in these pancreatic carcinoma samples.

CHAPTER 4. Discussion

4-1. The functions of COP1 determined by binding of COP1-interacting proteins on regions of COP1

14-3-3 σ directly binds to COP1 and binds to coiled-coil domain of COP1 using the domain mapping experiment. This binding region is different from other COP1-binding targets such as FOXO1 and c-JUN (Kato et al., 2008; Wertz et al., 2004). These two proteins bind to COP1 within WD-40 repeats. Both of them are degraded by COP1. The domain of WD40 repeats is known for protein-protein interacting regions. Importantly, WD40 repeat containing proteins also have been associated with a diversity of cellular function due to their targets. For example E3 ligase COP1 binds to its substrate FOXO1 within COP1 WD40 repeats suggests that COP1 facilitates FOXO1 degradation and thus inhibits transcriptional activity. Major targets of FOXO1, such as PEPCK and G6Pase (Kato et al., 2008), are critical for glucose production. It indicates that COP1 inhibits glucose production via FOXO1. Taken together, E3 ligase targets of COP1 preferentially bind to its WD40 regions and the interaction provides E3 ligase COP1 for the diversity of function.

In contrast, 14-3-3 σ binds to the coiled-coil domain of COP1 in this study. In this case, 14-3-3 σ is not an E3 ligase substrate of COP1. Coiled-coil domain is known for protein-protein interaction domain and dimerization domain. Indeed, it has been shown that COP1 forms dimerization through its coiled-coil region (Bianchi et al., 2003). However, it is unknown why COP1 forms dimers and whether dimerization of COP1 affects COP1 functions. Our

data suggest that 14-3-3 σ may directly affect self-association of COP1 or have an indirect effect on COP1 self-association through binding to COP1 binding partners. Once COP1 dimerization is abolished, COP1's activity and function may be abrogated. This will be further determined.

4-2. Regulation of COP1 stability in unstressed cells

Mammalian COP1 is mainly localized in the nucleus and regulates targets through proteasome-mediated degradation (Dornan et al., 2006; Dornan et al., 2004b). However, little is known about the detail regulation in COP1 stability and degradation process. Here we have shown that the loss of COP1 is rescued following proteasome inhibitor treatment. It implies that COP1 degradation is mediated by a 26-proteasome pathway. In addition, it is well known that 14-3-3 σ binds to and regulates targets' stability. In these studies, 14-3-3 σ negatively regulates COP1 through direct interaction with COP1. Furthermore, the turnover rate of COP1 in the absence of 14-3-3 σ is comprised compared to the presence of 14-3-3 σ , suggesting that 14-3-3 σ may be involved in the degradation process of COP1. We thereby discover that 14-3-3 σ promotes COP1 ubiquitination *in vivo* and even *in vitro*. It is possible that 14-3-3 σ directly regulates COP1 self-ubiquitination. We confirm this regulation *in vitro*. However 14-3-3 σ is not an E3 ligase and 14-3-3 σ 's major function is as an adaptor in cells. One explanation for 14-3-3 σ -facilitated COP1 ubiquitination *in vitro* is that 14-3-3 σ homo-dimer alters the structure of COP1 and exposes the RING-finger of COP1. This structure of COP1 is unstable and is easily got degraded through self-ubiquitination. The stability and turnover rate of COP1 RING mutant should be addressed in the future.

In vivo 14-3-3 σ may indirectly bind to COP1's negative regulators that ubiquitinate COP1. For example COP1 binds to MDM2 (data not shown) and 14-3-3 σ binds to MDM2 (Yang et al., 2007), since it is possible that COP1 is ubiquitinated by MDM2 and 14-3-3 σ facilitates this process. Therefore, characterizing binding partners of COP1 in 14-3-3 σ -COP1 complexes will confirm the models between COP1 self-ubiquitination and an E3 ligase-mediated COP1 ubiquitination. Taken together, 14-3-3 σ downregulates COP1, thus preventing COP1-mediated p53 degradation, and maintains the basal levels of p53.

4-3. COP1 is 14-3-3 σ phosphorylation binding protein

The identification of COP1 domains for 14-3-3 σ binding shows that 14-3-3 σ preferentially binds to middle part of COP1 (216 aa – 420 aa) which including coiled-coil domain. It is well known that the members of the 14-3-3 family show consensus binding motif, RSXpSXP and RXXXpSXP, on its targets. For this reason, we searched for COP1 sequence using Netphos2.0 program and identified several sites within coiled-coil region of COP1, which is potential for 14-3-3 σ binding. It includes Ser 387, Ser 404, Ser 332, and Thr 311. Thus, I screened all of the COP1 mutants' binding affinity for 14-3-3 σ by mutating either serine or threonine to alanine *in vivo* (data not shown). Interestingly, we found that 14-3-3 σ no longer binds to COP1 (S387A). It suggests that 14-3-3 σ 's binding to COP1 is phosphorylation-dependent. It has been shown that ATM phosphorylates COP1-Ser 387 in response to DNA damage. We also confirm that 14-3-3 σ -COP1 binding is abrogated in ATM null cells after DNA damage. Also, it is interesting to identify kinases for the other potential phosphorylation sites, such as EDST³¹¹VP, TEYS³³²QP, RYNS⁴⁰⁴VR, and study

whether these phosphorylation sites are required for 14-3-3 σ binding. 14-3-3 targets can be phosphorylated by different kinases, such as AKT, PKC and CHK1. These phosphorylation sites suggest that these kinases may compete with each other in regulating COP1 stability. For example ATM-phosphorylated COP1 leads to COP1 self-ubiquitination while AKT may phosphorylate COP1 and mask the phosphorylation site, which is phosphorylated by ATM. Thus AKT-phosphorylated COP1 may lead to COP1 stabilization and COP1 may further trigger cell survival following AKT signaling. These will be further addressed in the future.

4-4. The stability of COP1 in response to DNA damage

It has been demonstrated that DNA damage triggers ATM-phosphorylated COP1 at Ser 387 which in turn promotes COP1 nuclear export and triggers COP1 ubiquitination (Dornan et al., 2006). However, it is unclear regarding the mechanism behind COP1 nuclear export following DNA damage. 14-3-3 σ 's binding to COP1 is phosphorylation-dependent in response to DNA damage in our data. It seems that 14-3-3 σ binds to phosphorylated COP1 and thus is involved in nuclear export of COP1. Importantly, we found that 14-3-3 σ promotes the ubiquitination of COP1 that is Ser 387 phosphorylation dependent. In addition, 14-3-3 σ -mediated COP1 translocation to the cytoplasm leads to enhanced cytoplasmic COP1 ubiquitination after DNA damage here. Here we fill the gap that 14-3-3 σ is involved in ATM-mediated COP1 nuclear export and ubiquitination. Given that 14-3-3 σ plays a role in COP1 ubiquitination, it will be interesting to explore whether 14-3-3 σ -mediated COP1 ubiquitination is through lysine 48 linkage or lysine 63 linkage.

It was reported that ATM interacts to CSN and phosphorylates CSN3 following DNA damage. CSN is an upstream effector of COP in plant. Furthermore, a recent report shows that CSN3 facilitates COP1 downregulation and p53 accumulation after UV irradiation in mammal. Thus it is tempting to speculate that CSN3 may be involved in ATM-triggered COP1 instability after DNA damage. In contrast, CSN6 binds to and stabilizes COP1 in our lab. CSN3 and CSN6 are subunits in COP9 signalosome and show opposite effects on COP1 regulation. CSN6 and CSN3 have different subdomains and they may assemble to different subunits in complex of COP9 signalosome. It will be interesting to further explore the roles of COP9 signalosome on COP1 regulations in mammals.

4-5. 14-3-3 σ is downregulating COP1 and inhibits COP1-mediated cell cycle progression

14-3-3 σ , a p53 target gene, is induced in response to DNA damage. The induction of 14-3-3 σ by the DNA damage causes G2 arrest, indicating 14-3-3 σ is a negative regulator of cell cycle progression. 14-3-3 σ negatively regulates proteins that target cell cycle progression. For example, 14-3-3 σ binds to cyclin-dependent kinases and blocks the activity of CDKs (Chan et al., 1999; Laronga et al., 2000), thereby inhibiting cell growth. Moreover, 14-3-3 σ regulates the stability of oncogenic proteins and leads to the stability of p53. For example, 14-3-3 σ facilitates the turnover rate of MDM2, thereby leading to prevent MDM2-mediated p53 degradation (Yang et al., 2003). Therefore, it is possible that 14-3-3 σ may regulate cell cycle negative regulator COP1 due to the involvement of p53 degradation. Eventually 14-3-3 σ -COP1 regulations lead to the proper cell cycle process. Our data show that DNA

damage-induced 14-3-3 σ caused COP1 downregulation. In addition, cells overexpressing COP1 lead to cell proliferation and S-phase accumulation while ectopic 14-3-3 σ inhibits COP1-mediated cell proliferation through G2 arrest. So far it is unknown about the role of COP1 in cell cycle regulation. The level of COP1 during cell cycle is the first thing that should be addressed. This mechanistic study will help understand how 14-3-3 σ negatively regulates COP1 during cell cycle.

4-6. 14-3-3 σ plays an important role in protecting p53 from E3 ligase

p53 has three major RING-containing E3 ligases, such as COP1, MDM2, and Pirh2. In normal conditions, p53 levels are tightly controlled by these E3 ligases. In our previous study, we show that 14-3-3 σ stabilizes p53 through shortening the turnover rate of MDM2 and facilitating the ubiquitination of MDM2. In this study, we also found that 14-3-3 σ inhibits COP1-mediated p53 ubiquitination and transcriptional repression. It is possible that 14-3-3 σ -COP1 axis regulates p53 via 14-3-3 σ -MDM2 pathway. Our results show that 14-3-3 σ blocks COP1-mediated p53 ubiquitination, and this process is independent of MDM2 although we detect that COP1 binds to MDM2. Moreover, 14-3-3 σ inhibits COP1-mediated p53 nuclear export regardless of MDM2 (data not shown). Therefore MDM2 binding to COP1 is not required for COP1 negative effects on p53. We conclude that 14-3-3 σ blocks COP1-mediated p53 instability, and this process is independent on 14-3-3 σ 's negative impacts on MDM2.

In Figure 3-3, we found that p53 levels are not reduced in 14-3-3 σ null cells compared to 14-3-3 σ wild-type cells upon doxorubicin treatment. It is not what we expected because 14-3-3 σ has a positive feedback on p53 as we mention. We will further confirm this issue by using different cell lines and different DNA damage agent.

4-7. Roles of COP1 in chromosome stability

COP1 overexpression was found in ovarian and breast cancer, indicating that COP1 plays an important role in tumorigenesis. Notably, we found that COP1 overexpression in HCT116 leads to chromosome breaks and fusion, leading to γ -H2AX accumulation (data not shown). It indicates that COP1 overexpression causes a lot of genomic instability. It is interesting to further examine that overexpression of COP1 may either induce checkpoint defects, chromosome aberration, or DNA repair defect, thus promoting tumor progression. One of the possibilities is that COP1 overexpression leads to p53 ubiquitination. The lack of functional p53 pathway leads to the failure of proper G1 checkpoint and centrosome aberrations. There are several examples showing that overexpression of cyclin E contributes to genomic instability through the defect cell cycle checkpoint (Spruck et al., 1999) and overexpression of MDM2 leads to chromosome breaks through binding to Nbs1, thus abolishing the function of Mre11–Rad50–Nbs1 in DNA repair signaling (Alt et al., 2005; Bouska et al., 2008). We found that homologous recombination was reduced in COP1-overexpressing cells (data not shown). It is a piece of strong evidence that COP1 negatively regulates homologous recombination repair. At the same time, we should hypothesize whether COP1 plays a role in DNA repair signaling. Logically COP1 may delay the accumulation of DNA repair protein at double strand breaks or ubiquitinate DNA repair

factors, thereby causing chromosome abnormality and tumor progression. We will further study the mechanism by which COP1 inhibits the DNA repair signaling in the future.

4-8. 14-3-3 σ impacts on an oncoprotein COP1

The oncogenic activities of COP1 are attributed to ubiquitinate p53 and inhibit p53-dependent apoptosis. In addition, COP1 is overexpressed in ovarian and breast adenocarcinomas. In our study, we also found that COP1 is deregulated in pancreatic and breast cancer patient samples. Taken together, it indicates that COP1 may have oncogenic activities and promote tumor progression. However, it remains a question how COP1 executes its oncogenic activities. We showed that COP1 overexpression leads to increased cell proliferation, S-phase accumulation, cell transformation and tumor progression. It has been shown that 14-3-3 σ suppressed the anchorage-independent growth of some breast cancer cell lines and reduced 14-3-3 σ expression in head and neck squamous and keratinocytes. We hypothesize that 14-3-3 σ has its tumor suppressor function to block COP1's oncogenic effect. The result that 14-3-3 σ abrogates COP1 cell proliferation, cell transformation, and tumor progression supports an idea that 14-3-3 σ is one of the mechanism to eliminate COP1 oncogenic activity. At the same time, COP1 is overexpressed in high percentage of pancreatic cancer samples in which 14-3-3 σ expression is low in our clinical samples. Moreover, breast cancer samples demonstrate expressing COP1 and 14-3-3 σ has the inverse correlation. Therefore 14-3-3 σ can be developed as a clinical therapeutic target treating COP1-overexpression cancer patients in the future.

4-9. Possible COP1 upstream positive regulators/kinases

COP1 E3 ligase degrades tumor suppressors including p53 and FOXO1. Here we discovered that COP1 overexpression leads to cell proliferation and tumor progression. Thus it is tempting to address the upstream signals that regulate stability of COP1 and trigger COP1 oncogenic activities. Scanning the COP1 sequence, COP1 contain a lot of serine and threonine residues, suggesting that COP1 is phosphorylated by threonine/serine kinases. These kinases, including AKT, CDK2, PKC, and Pim family, can promote cell growth and survival (Ellwood-Yen et al., 2003; Hammerman et al., 2005; Zippo et al., 2007). For example, Pim-1 has been reported to phosphorylate and stabilize Skp2, thereby leading to Skp2-mediated p27 degradation (Cen et al.2010; Gao et al., 2009; Rodier et al., 2008). Lower p27 levels lead to deregulation in cell cycle. However none of the kinases are found to regulate COP1 activities. The COP1 sequence is analyzed for identifying these kinase-phosphorylated consensus site. Importantly, we found that COP1 contain a potential AKT and Pim-1 phosphorylated consensus site. We will further examine whether COP1 is regulated by AKT and Pim-1, and if they regulate COP1 stability. Therefore, kinases interplay between AKT and ATM may determine the activities of COP1 and affect the cell fate.

4-10. Future directions

To observe the role of COP1 in cell growth, I have generated COP1 overexpression cells. In addition to cell proliferation in COP1 overexpression cells, I accidentally found that more γ -H2AX was detected in COP1 overexpression cells compared to vector control cells. It indicates that COP1 expression enhances DNA double strand breaks. Moreover, more chromosome aberrations were found in COP1 overexpression cells using karyotyping

analysis. It indicates that COP1 overexpression causes the accumulation of DNA double strand breaks, which in turn leads to chromosome instability. If it is true, we can explain that COP1-induced DNA damage causes chromosome aberrations, thereby leading to tumorigenesis. However it is unclear how COP1 negatively regulates DNA repair signaling. Here the preliminary data shows that homologous recombination repair process is inhibited in COP1 overexpression cells after I-SceI-induced double strand breaks. Moreover COP1 expression cells sensitize to IR-induced cell death using cell survival foci formation assay. Technically in addition to the accumulation of DNA damage defect in COP1 overexpression cells, it should be further confirmed that defective DNA repair is reduced in COP1 knockdown cells. Taken together, COP1 may play a role in homologous recombination repair. I hypothesize that COP1 causes defective DNA repair due to the inhibition of homologous recombination repair. Therefore I propose two specific aims for the future study.

(1) To determine whether AKT phosphorylates cytoplasmic COP1 and phosphorylated COP1 translocates to the nucleus upon DNA damage.

Our preliminary data have shown that AKT interacts with COP1 and translocates COP1 to the nucleus. We further address whether COP1 is a substrate of AKT and AKT phosphorylates COP1, thereby translocating phosphorylated COP1 to the nucleus upon DNA damage. It will further distinguish that COP1 shuttling is contributed by ATM and AKT upon DNA damage.

(2) To determine whether COP1 regulates DNA damage and repair proteins following DNA damage.

Given that DNA damage signal regulates COP1 (Dornan et al., 2006), it is unknown whether AKT-phosphorylated COP1 is localized at DNA double strand breaks. To observe whether COP1 is accumulated at ionizing radiation-induced foci formation (IRIF), the interactions between COP1 and γ H2AX need to be addressed using co-immunoprecipitation and live-cell image assays. If COP1 is localized at the foci, I will further investigate whether COP1 abrogates downstream proteins accumulation in IRIF. COP1-knockdown cells and COP1-knockdown cells reconstituted with wild-type COP1 can be addressed in DNA damage-induced foci, including MDC1, RNF8, and 53BP1 foci etc. If COP1 knockdown causes the accumulation of MDC1, RNF8, and 53BP1 foci, the mechanism behind COP1's negative impacts on DNA repair proteins will be further identified.

(3) To determine whether COP1 regulates DNA damage and repair proteins following DNA damage.

Given that MDC1 and 53BP1 contain COP1 consensus binding motif, it is tempting to further address whether COP1 negatively regulates MDC1 and 53BP1 in response to DNA damage.

Taken together, COP1 is overexpressed in ovarian and breast cancer. However, how COP1 causes tumor progression is poorly understood in addition to degrade functional p53 proteins. Studying whether COP1 causes defective DNA and reduce DNA repair process

and in turn too many damage DNA lead to cancer formation will help the designation of therapeutic agents that target on COP1.

In summary, 14-3-3 σ is induced by p53 transcriptional factor following DNA damage and 14-3-3 σ is shown to positively regulate p53. COP1 is an E3 ligase for p53. Following DNA damage, COP1 is phosphorylated by ATM and translocated to the cytoplasm. However, the mechanism of COP1 translocation to the cytoplasm is still unclear. Here the study shows that doxorubicin-induced DNA damage causes COP1 downregulation, which is dependent on 14-3-3 σ . However 14-3-3 σ only reduces protein levels not mRNA levels of COP1, indicating that 14-3-3 σ negatively regulates COP1 through post-translational modification, such as ubiquitination and phosphorylation. To further address specific roles of 14-3-3 σ on the levels of COP1, we found that 14-3-3 σ decreases the steady-state levels of COP1, facilitates the turnover rate of COP1, and promotes ubiquitination of COP1. This indicates that 14-3-3 σ negatively regulates COP1 through facilitating COP1 ubiquitinating process. To examine the mechanism which 14-3-3 σ negatively regulates COP1, we identify that 14-3-3 σ functions as an adaptor and binds to phosphorylated COP1 at Ser 387 after DNA damage, thereby leading to the nuclear export of COP1. Cytoplasmic COP1 ubiquitination is increased in the presence of 14-3-3 σ compared to those in the absence of 14-3-3 σ . In contrast, COP1 (S387A) loses the binding site for 14-3-3 σ . In turn, 14-3-3 σ loses the ability to promote the nuclear export, the turnover rate and ubiquitination of S387A mutant (Figure 4-1). Importantly, to study biological significance of 14-3-3 σ 's negative impact on COP1-mediated p53 instability, we have shown that 14-3-3 σ blocks COP1-mediated p53

degradation, and COP1-suppressed p53 transcriptional activity. Furthermore, 14-3-3 σ abolishes COP1-promoted cell growth, cell transformation, and tumor progression. Taken together, 14-3-3 σ can be developed as a clinical therapy treat COP1-overexpressison cancer patients in the future.

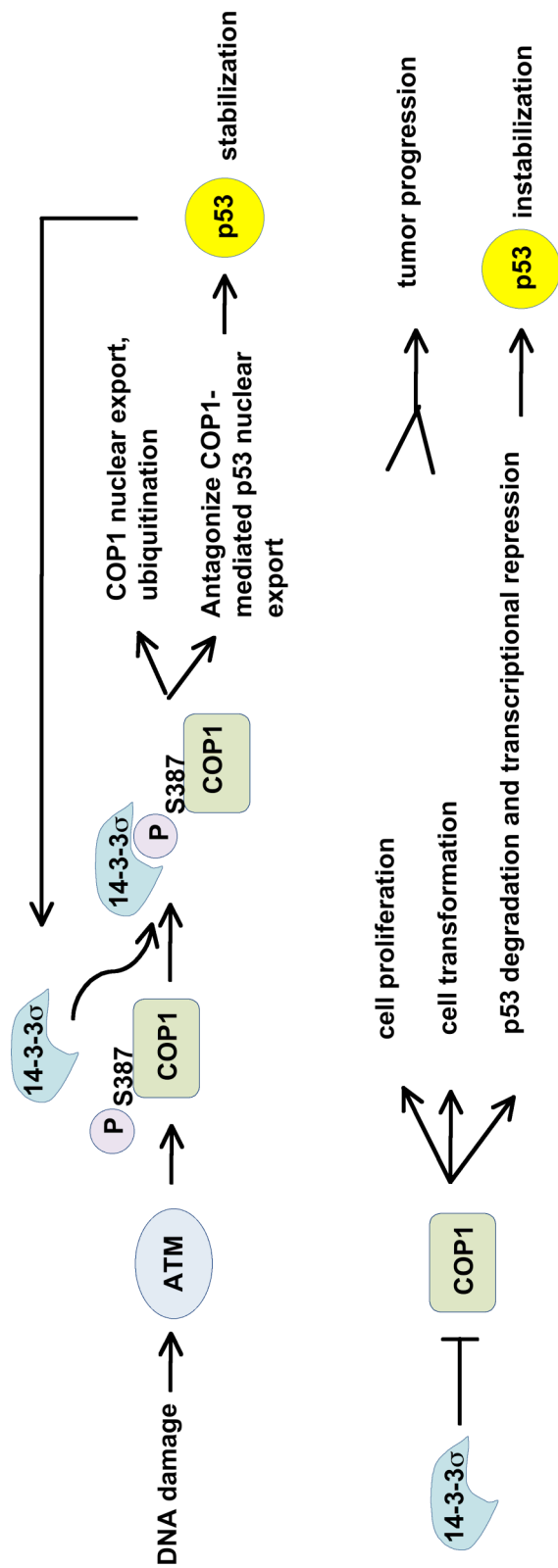


Figure 4-1. Working model. Once DNA damage occurs and ATM is activated, ATM phosphorylates COP1 at Ser 387. This phosphorylation event enables 14-3-3σ to recognize and bind to COP1, resulting in COP1 translocation to the cytoplasm, and COP1 ubiquitination, and in turn the stabilization of p53 (top). 14-3-3σ blocks COP1-mediated cell proliferation, cell transformation, and tumor progression. In addition, 14-3-3σ protects p53 from COP1-mediated p53 degradation and p53 transcriptional repression (bottom).

CHAPTER 5. References

- Aitken, A., Amess, B., Howell, S., Jones, D., Martin, H., Patel, Y., Robinson, K., and Toker, A. (1992). The role of specific isoforms of 14-3-3 protein in regulating protein kinase activity in the brain. *Biochem Soc Trans* 20, 607-611.
- Alt, J.R., Bouska, A., Fernandez, M.R., Cerny, R.L., Xiao, H., and Eischen, C.M. (2005). Mdm2 binds to Nbs1 at sites of DNA damage and regulates double strand break repair. *J Biol Chem* 280, 18771-18781.
- Baert, J.L., Monte, D., Verreman, K., Degerny, C., Coutte, L., and de Launoit, Y. (2010). The E3 ubiquitin ligase complex component COP1 regulates PEA3 group member stability and transcriptional activity. *Oncogene* 29, 1810-1820.
- Banin, S., Moyal, L., Shieh, S., Taya, Y., Anderson, C.W., Chessa, L., Smorodinsky, N.I., Prives, C., Reiss, Y., Shiloh, Y., *et al.* (1998). Enhanced phosphorylation of p53 by ATM in response to DNA damage. *Science* 281, 1674-1677.
- Benzinger, A., Muster, N., Koch, H.B., Yates, J.R., 3rd, and Hermeking, H. (2005). Targeted proteomic analysis of 14-3-3 sigma, a p53 effector commonly silenced in cancer. *Mol Cell Proteomics* 4, 785-795.
- Bianchi, E., Denti, S., Catena, R., Rossetti, G., Polo, S., Gasparian, S., Putignano, S., Rogge, L., and Pardi, R. (2003). Characterization of human constitutive photomorphogenesis protein 1, a RING finger ubiquitin ligase that interacts with Jun transcription factors and modulates their transcriptional activity. *J Biol Chem* 278, 19682-19690.
- Boston, P., and Jackson, P. (1980). Purification and properties of a brain-specific protein, human 14-3-3 protein. *Biochem Soc Trans* 8, 617-618.

- Bouska, A., Lushnikova, T., Plaza, S., and Eischen, C.M. (2008). Mdm2 promotes genetic instability and transformation independent of p53. *Mol Cell Biol* 28, 4862-4874.
- Boyd, S.D., Tsai, K.Y., and Jacks, T. (2000). An intact HDM2 RING-finger domain is required for nuclear exclusion of p53. *Nat Cell Biol* 2, 563-568.
- Brasemann, S., and McCormick, F. (1995). Bcr and Raf form a complex in vivo via 14-3-3 proteins. *Embo J* 14, 4839-4848.
- Bridges, D., and Moorhead, G.B. (2005). 14-3-3 proteins: a number of functions for a numbered protein. *Sci STKE* 2005, re10.
- Broadie, K., Rushton, E., Skoulakis, E.M., and Davis, R.L. (1997). Leonardo, a Drosophila 14-3-3 protein involved in learning, regulates presynaptic function. *Neuron* 19, 391-402.
- Canman, C.E., Lim, D.S., Cimprich, K.A., Taya, Y., Tamai, K., Sakaguchi, K., Appella, E., Kastan, M.B., and Siliciano, J.D. (1998). Activation of the ATM kinase by ionizing radiation and phosphorylation of p53. *Science* 281, 1677-1679.
- Castle, L.A., and Meinke, D.W. (1994). A FUSCA gene of Arabidopsis encodes a novel protein essential for plant development. *Plant Cell* 6, 25-41.
- Cen, B., Mahajan, S., Zemskova, M., Beharry, Z., Lin, Y.W., Cramer, S.D., Lilly, M.B., and Kraft, A.S. (2010). Regulation of Skp2 levels by the Pim-1 protein kinase. *J Biol Chem* 285, 29128-29137.
- Chamovitz, D.A., Wei, N., Osterlund, M.T., von Arnim, A.G., Staub, J.M., Matsui, M., and Deng, X.W. (1996). The COP9 complex, a novel multisubunit nuclear regulator involved in light control of a plant developmental switch. *Cell* 86, 115-121.

- Chan, T.A., Hermeking, H., Lengauer, C., Kinzler, K.W., and Vogelstein, B. (1999). 14-3-3Sigma is required to prevent mitotic catastrophe after DNA damage. *Nature* *401*, 616-620.
- Chehab, N.H., Malikzay, A., Appel, M., and Halazonetis, T.D. (2000). Chk2/hCds1 functions as a DNA damage checkpoint in G(1) by stabilizing p53. *Genes Dev* *14*, 278-288.
- Chehab, N.H., Malikzay, A., Stavridi, E.S., and Halazonetis, T.D. (1999). Phosphorylation of Ser-20 mediates stabilization of human p53 in response to DNA damage. *Proc Natl Acad Sci U S A* *96*, 13777-13782.
- Chen, J., Marechal, V., and Levine, A.J. (1993). Mapping of the p53 and mdm-2 interaction domains. *Mol Cell Biol* *13*, 4107-4114.
- Chiang, C.W., Harris, G., Ellig, C., Masters, S.C., Subramanian, R., Shenolikar, S., Wadzinski, B.E., and Yang, E. (2001). Protein phosphatase 2A activates the proapoptotic function of BAD in interleukin- 3-dependent lymphoid cells by a mechanism requiring 14-3-3 dissociation. *Blood* *97*, 1289-1297.
- Cotelle, V., Meek, S.E., Provan, F., Milne, F.C., Morrice, N., and MacKintosh, C. (2000). 14-3-3s regulate global cleavage of their diverse binding partners in sugar-starved *Arabidopsis* cells. *Embo J* *19*, 2869-2876.
- Datta, S.R., Katsov, A., Hu, L., Petros, A., Fesik, S.W., Yaffe, M.B., and Greenberg, M.E. (2000). 14-3-3 proteins and survival kinases cooperate to inactivate BAD by BH3 domain phosphorylation. *Mol Cell* *6*, 41-51.
- Deb, S.P. (2002). Function and dysfunction of the human oncoprotein MDM2. *Front Biosci* *7*, d235-243.

- Deng, X.W., Caspar, T., and Quail, P.H. (1991). *cop1*: a regulatory locus involved in light-controlled development and gene expression in Arabidopsis. *Genes Dev* 5, 1172-1182.
- Dent, P., Jelinek, T., Morrison, D.K., Weber, M.J., and Sturgill, T.W. (1995). Reversal of Raf-1 activation by purified and membrane-associated protein phosphatases. *Science* 268, 1902-1906.
- Dentin, R., Liu, Y., Koo, S.H., Hedrick, S., Vargas, T., Heredia, J., Yates, J., 3rd, and Montminy, M. (2007). Insulin modulates gluconeogenesis by inhibition of the coactivator TORC2. *Nature* 449, 366-369.
- Dhar, S., Squire, J.A., Hande, M.P., Wellinger, R.J., and Pandita, T.K. (2000). Inactivation of 14-3-3sigma influences telomere behavior and ionizing radiation-induced chromosomal instability. *Mol Cell Biol* 20, 7764-7772.
- Dornan, D., Bheddah, S., Newton, K., Ince, W., Frantz, G.D., Dowd, P., Koeppen, H., Dixit, V.M., and French, D.M. (2004a). COP1, the negative regulator of p53, is overexpressed in breast and ovarian adenocarcinomas. *Cancer Res* 64, 7226-7230.
- Dornan, D., Shimizu, H., Mah, A., Dudhela, T., Eby, M., O'Rourke, K., Seshagiri, S., and Dixit, V.M. (2006). ATM engages autodegradation of the E3 ubiquitin ligase COP1 after DNA damage. *Science* 313, 1122-1126.
- Dornan, D., Wertz, I., Shimizu, H., Arnott, D., Frantz, G.D., Dowd, P., O'Rourke, K., Koeppen, H., and Dixit, V.M. (2004b). The ubiquitin ligase COP1 is a critical negative regulator of p53. *Nature* 429, 86-92.

- Ellwood-Yen, K., Graeber, T.G., Wongvipat, J., Iruela-Arispe, M.L., Zhang, J., Matusik, R., Thomas, G.V., and Sawyers, C.L. (2003). Myc-driven murine prostate cancer shares molecular features with human prostate tumors. *Cancer Cell* 4, 223-238.
- Ferguson, A.T., Evron, E., Umbricht, C.B., Pandita, T.K., Chan, T.A., Hermeking, H., Marks, J.R., Lambers, A.R., Futreal, P.A., Stampfer, M.R., *et al.* (2000). High frequency of hypermethylation at the 14-3-3 sigma locus leads to gene silencing in breast cancer. *Proc Natl Acad Sci U S A* 97, 6049-6054.
- Freedman, D.A., Wu, L., and Levine, A.J. (1999). Functions of the MDM2 oncoprotein. *Cell Mol Life Sci* 55, 96-107.
- Furlanetto, R.W., Dey, B.R., Lopaczynski, W., and Nissley, S.P. (1997). 14-3-3 proteins interact with the insulin-like growth factor receptor but not the insulin receptor. *Biochem J* 327 (Pt 3), 765-771.
- Gao, D., Inuzuka, H., Tseng, A., Chin, R.Y., Toker, A., and Wei, W. (2009). Phosphorylation by Akt1 promotes cytoplasmic localization of Skp2 and impairs APCCdh1-mediated Skp2 destruction. *Nat Cell Biol* 11, 397-408.
- Gautier, J., Solomon, M.J., Booher, R.N., Bazan, J.F., and Kirschner, M.W. (1991). cdc25 is a specific tyrosine phosphatase that directly activates p34cdc2. *Cell* 67, 197-211.
- Geyer, R.K., Yu, Z.K., and Maki, C.G. (2000). The MDM2 RING-finger domain is required to promote p53 nuclear export. *Nat Cell Biol* 2, 569-573.
- Graves, P.R., Lovly, C.M., Uy, G.L., and Piwnica-Worms, H. (2001). Localization of human Cdc25C is regulated both by nuclear export and 14-3-3 protein binding. *Oncogene* 20, 1839-1851.

- Groisman, R., Polanowska, J., Kuraoka, I., Sawada, J., Saijo, M., Drapkin, R., Kisselev, A.F., Tanaka, K., and Nakatani, Y. (2003). The ubiquitin ligase activity in the DDB2 and CSA complexes is differentially regulated by the COP9 signalosome in response to DNA damage. *Cell* 113, 357-367.
- Hammerman, P.S., Fox, C.J., Birnbaum, M.J., and Thompson, C.B. (2005). Pim and Akt oncogenes are independent regulators of hematopoietic cell growth and survival. *Blood* 105, 4477-4483.
- Hardtke, C.S., Gohda, K., Osterlund, M.T., Oyama, T., Okada, K., and Deng, X.W. (2000). HY5 stability and activity in arabidopsis is regulated by phosphorylation in its COP1 binding domain. *Embo J* 19, 4997-5006.
- Haupt, Y., Maya, R., Kazaz, A., and Oren, M. (1997). Mdm2 promotes the rapid degradation of p53. *Nature* 387, 296-299.
- Henriksson, M.L., Francis, M.S., Peden, A., Aili, M., Stefansson, K., Palmer, R., Aitken, A., and Hallberg, B. (2002). A nonphosphorylated 14-3-3 binding motif on exoenzyme S that is functional in vivo. *Eur J Biochem* 269, 4921-4929.
- Hermeking, H., Lengauer, C., Polyak, K., He, T.C., Zhang, L., Thiagalingam, S., Kinzler, K.W., and Vogelstein, B. (1997). 14-3-3 sigma is a p53-regulated inhibitor of G2/M progression. *Mol Cell* 1, 3-11.
- Higa, L.A., Mihaylov, I.S., Banks, D.P., Zheng, J., and Zhang, H. (2003). Radiation-mediated proteolysis of CDT1 by CUL4-ROC1 and CSN complexes constitutes a new checkpoint. *Nat Cell Biol* 5, 1008-1015.

- Hirao, A., Kong, Y.Y., Matsuoka, S., Wakeham, A., Ruland, J., Yoshida, H., Liu, D., Elledge, S.J., and Mak, T.W. (2000). DNA damage-induced activation of p53 by the checkpoint kinase Chk2. *Science* *287*, 1824-1827.
- Holm, M., and Deng, X.W. (1999). Structural organization and interactions of COP1, a light-regulated developmental switch. *Plant Mol Biol* *41*, 151-158.
- Honda, R., Ohba, Y., and Yasuda, H. (1997a). 14-3-3 zeta protein binds to the carboxyl half of mouse weel kinase. *Biochem Biophys Res Commun* *230*, 262-265.
- Honda, R., Tanaka, H., and Yasuda, H. (1997b). Oncoprotein MDM2 is a ubiquitin ligase E3 for tumor suppressor p53. *FEBS Lett* *420*, 25-27.
- Hsu, S.Y., Kaipia, A., Zhu, L., and Hsueh, A.J. (1997). Interference of BAD (Bcl-xL/Bcl-2-associated death promoter)-induced apoptosis in mammalian cells by 14-3-3 isoforms and P11. *Mol Endocrinol* *11*, 1858-1867.
- Ikeda, K., Inoue, S., Orimo, A., Sano, M., Watanabe, T., Tsutsumi, K., and Muramatsu, M. (1997). Multiple regulatory elements and binding proteins of the 5'-flanking region of the human estrogen-responsive finger protein (efp) gene. *Biochem Biophys Res Commun* *236*, 765-771.
- Ikeda, K., Inoue, S., Orimo, A., Tsutsumi, K., and Muramatsu, M. (1998). Promoter analysis of mouse estrogen-responsive finger protein (efp) gene: mouse efp promoter contains an E-box that is also conserved in human. *Gene* *216*, 155-162.
- Inoue, S., Orimo, A., Hosoi, T., Kondo, S., Toyoshima, H., Kondo, T., Ikegami, A., Ouchi, Y., Orimo, H., and Muramatsu, M. (1993). Genomic binding-site cloning reveals an estrogen-responsive gene that encodes a RING finger protein. *Proc Natl Acad Sci U S A* *90*, 11117-11121.

- Iwata, N., Yamamoto, H., Sasaki, S., Itoh, F., Suzuki, H., Kikuchi, T., Kaneto, H., Iku, S., Ozeki, I., Karino, Y., *et al.* (2000). Frequent hypermethylation of CpG islands and loss of expression of the 14-3-3 sigma gene in human hepatocellular carcinoma. *Oncogene* 19, 5298-5302.
- Jones, D.H., Ley, S., and Aitken, A. (1995). Isoforms of 14-3-3 protein can form homo- and heterodimers in vivo and in vitro: implications for function as adapter proteins. *FEBS Lett* 368, 55-58.
- Kato, S., Ding, J., Pisch, E., Jhala, U.S., and Du, K. (2008). COP1 functions as a FoxO1 ubiquitin E3 ligase to regulate FoxO1-mediated gene expression. *J Biol Chem* 283, 35464-35473.
- Kubbutat, M.H., Jones, S.N., and Vousden, K.H. (1997). Regulation of p53 stability by Mdm2. *Nature* 387, 299-303.
- Laronga, C., Yang, H.Y., Neal, C., and Lee, M.H. (2000). Association of the cyclin-dependent kinases and 14-3-3 sigma negatively regulates cell cycle progression. *J Biol Chem* 275, 23106-23112.
- Lee, Y.H., Andersen, J.B., Song, H.T., Judge, A.D., Seo, D., Ishikawa, T., Marquardt, J.U., Kitade, M., Durkin, M.E., Raggi, C., *et al.* (2010). Definition of Ubiquitination Modulator COP1 as a Novel Therapeutic Target in Human Hepatocellular Carcinoma. *Cancer Res.*
- Leffers, H., Madsen, P., Rasmussen, H.H., Honore, B., Andersen, A.H., Walbum, E., Vandekerckhove, J., and Celis, J.E. (1993). Molecular cloning and expression of the transformation sensitive epithelial marker stratifin. A member of a protein family

- that has been involved in the protein kinase C signalling pathway. *J Mol Biol* 231, 982-998.
- Ljungman, M., and Lane, D.P. (2004). Transcription - guarding the genome by sensing DNA damage. *Nat Rev Cancer* 4, 727-737.
- Lodygin, D., Diebold, J., and Hermeking, H. (2004). Prostate cancer is characterized by epigenetic silencing of 14-3-3sigma expression. *Oncogene* 23, 9034-9041.
- Lodygin, D., Yazdi, A.S., Sander, C.A., Herzinger, T., and Hermeking, H. (2003). Analysis of 14-3-3sigma expression in hyperproliferative skin diseases reveals selective loss associated with CpG-methylation in basal cell carcinoma. *Oncogene* 22, 5519-5524.
- Martens, G.J., Piosik, P.A., and Danen, E.H. (1992). Evolutionary conservation of the 14-3-3 protein. *Biochem Biophys Res Commun* 184, 1456-1459.
- Matsuoka, S., Ballif, B.A., Smogorzewska, A., McDonald, E.R., 3rd, Hurov, K.E., Luo, J., Bakalarski, C.E., Zhao, Z., Solimini, N., Lerenthal, Y., *et al.* (2007). ATM and ATR substrate analysis reveals extensive protein networks responsive to DNA damage. *Science* 316, 1160-1166.
- McNellis, T.W., von Arnim, A.G., Araki, T., Komeda, Y., Misera, S., and Deng, X.W. (1994). Genetic and molecular analysis of an allelic series of cop1 mutants suggests functional roles for the multiple protein domains. *Plant Cell* 6, 487-500.
- Mhaweche, P., Benz, A., Cerato, C., Greloz, V., Assaly, M., Desmond, J.C., Koeffler, H.P., Lodygin, D., Hermeking, H., Herrmann, F., *et al.* (2005). Downregulation of 14-3-3sigma in ovary, prostate and endometrial carcinomas is associated with CpG island methylation. *Mod Pathol* 18, 340-348.

- Misera, S., Muller, A.J., Weiland-Heidecker, U., and Jurgens, G. (1994). The FUSCA genes of Arabidopsis: negative regulators of light responses. *Mol Gen Genet* 244, 242-252.
- Momand, J., Jung, D., Wilczynski, S., and Niland, J. (1998). The MDM2 gene amplification database. *Nucleic Acids Res* 26, 3453-3459.
- Moore, B.W., and McGregor, D. (1965). Chromatographic and Electrophoretic Fractionation of Soluble Proteins of Brain and Liver. *J Biol Chem* 240, 1647-1653.
- Nakagawa, K., Taya, Y., Tamai, K., and Yamaizumi, M. (1999). Requirement of ATM in phosphorylation of the human p53 protein at serine 15 following DNA double-strand breaks. *Mol Cell Biol* 19, 2828-2834.
- Oliner, J.D., Kinzler, K.W., Meltzer, P.S., George, D.L., and Vogelstein, B. (1992). Amplification of a gene encoding a p53-associated protein in human sarcomas. *Nature* 358, 80-83.
- Orimo, A., Inoue, S., Ikeda, K., Noji, S., and Muramatsu, M. (1995). Molecular cloning, structure, and expression of mouse estrogen-responsive finger protein Efp. Co-localization with estrogen receptor mRNA in target organs. *J Biol Chem* 270, 24406-24413.
- Orimo, A., Inoue, S., Minowa, O., Tominaga, N., Tomioka, Y., Sato, M., Kuno, J., Hiroi, H., Shimizu, Y., Suzuki, M., *et al.* (1999). Underdeveloped uterus and reduced estrogen responsiveness in mice with disruption of the estrogen-responsive finger protein gene, which is a direct target of estrogen receptor alpha. *Proc Natl Acad Sci U S A* 96, 12027-12032.

- Osada, H., Tatematsu, Y., Yatabe, Y., Nakagawa, T., Konishi, H., Harano, T., Tezel, E., Takada, M., and Takahashi, T. (2002). Frequent and histological type-specific inactivation of 14-3-3sigma in human lung cancers. *Oncogene* 21, 2418-2424.
- Osterlund, M.T., Hardtke, C.S., Wei, N., and Deng, X.W. (2000). Targeted destabilization of HY5 during light-regulated development of Arabidopsis. *Nature* 405, 462-466.
- Prasad, G.L., Valverius, E.M., McDuffie, E., and Cooper, H.L. (1992). Complementary DNA cloning of a novel epithelial cell marker protein, HME1, that may be down-regulated in neoplastic mammary cells. *Cell Growth Differ* 3, 507-513.
- Qi, L., Heredia, J.E., Altarejos, J.Y., Screaton, R., Goebel, N., Niessen, S., Macleod, I.X., Liew, C.W., Kulkarni, R.N., Bain, J., *et al.* (2006). TRB3 links the E3 ubiquitin ligase COP1 to lipid metabolism. *Science* 312, 1763-1766.
- Rittinger, K., Budman, J., Xu, J., Volinia, S., Cantley, L.C., Smerdon, S.J., Gamblin, S.J., and Yaffe, M.B. (1999). Structural analysis of 14-3-3 phosphopeptide complexes identifies a dual role for the nuclear export signal of 14-3-3 in ligand binding. *Mol Cell* 4, 153-166.
- Rodier, G., Coulombe, P., Tanguay, P.L., Boutonnet, C., and Meloche, S. (2008). Phosphorylation of Skp2 regulated by CDK2 and Cdc14B protects it from degradation by APC(Cdh1) in G1 phase. *Embo J* 27, 679-691.
- Samuel, T., Weber, H.O., Rauch, P., Verdoodt, B., Eppel, J.T., McShea, A., Hermeking, H., and Funk, J.O. (2001). The G2/M regulator 14-3-3sigma prevents apoptosis through sequestration of Bax. *J Biol Chem* 276, 45201-45206.

- Sanchez, Y., Wong, C., Thoma, R.S., Richman, R., Wu, Z., Piwnica-Worms, H., and Elledge, S.J. (1997). Conservation of the Chk1 checkpoint pathway in mammals: linkage of DNA damage to Cdk regulation through Cdc25. *Science* 277, 1497-1501.
- Schwechheimer, C., and Deng, X.W. (2000). The COP/DET/FUS proteins-regulators of eukaryotic growth and development. *Semin Cell Dev Biol* 11, 495-503.
- Serino, G., Tsuge, T., Kwok, S., Matsui, M., Wei, N., and Deng, X.W. (1999). Arabidopsis cop8 and fus4 mutations define the same gene that encodes subunit 4 of the COP9 signalosome. *Plant Cell* 11, 1967-1980.
- Shiloh, Y. (2006). The ATM-mediated DNA-damage response: taking shape. *Trends Biochem Sci* 31, 402-410.
- Skoulakis, E.M., and Davis, R.L. (1996). Olfactory learning deficits in mutants for leonardo, a *Drosophila* gene encoding a 14-3-3 protein. *Neuron* 17, 931-944.
- Spruck, C.H., Won, K.A., and Reed, S.I. (1999). Deregulated cyclin E induces chromosome instability. *Nature* 401, 297-300.
- Takahashi, Y. (2003). The 14-3-3 proteins: gene, gene expression, and function. *Neurochem Res* 28, 1265-1273.
- Thomson, S.D., Ali, S., Pickles, L., Taylor, J., Pace, P.E., Lymboura, M., Shousha, S., and Coombes, R.C. (2001). Analysis of estrogen-responsive finger protein expression in benign and malignant human breast. *Int J Cancer* 91, 152-158.
- Thorson, J.A., Yu, L.W., Hsu, A.L., Shih, N.Y., Graves, P.R., Tanner, J.W., Allen, P.M., Piwnica-Worms, H., and Shaw, A.S. (1998). 14-3-3 proteins are required for maintenance of Raf-1 phosphorylation and kinase activity. *Mol Cell Biol* 18, 5229-5238.

- Tzivion, G., Luo, Z., and Avruch, J. (1998). A dimeric 14-3-3 protein is an essential cofactor for Raf kinase activity. *Nature* 394, 88-92.
- Urano, T., Saito, T., Tsukui, T., Fujita, M., Hosoi, T., Muramatsu, M., Ouchi, Y., and Inoue, S. (2002). Efp targets 14-3-3 sigma for proteolysis and promotes breast tumour growth. *Nature* 417, 871-875.
- Van Der Hoeven, P.C., Van Der Wal, J.C., Ruurs, P., Van Dijk, M.C., and Van Blitterswijk, J. (2000). 14-3-3 isotypes facilitate coupling of protein kinase C-zeta to Raf-1: negative regulation by 14-3-3 phosphorylation. *Biochem J* 345 Pt 2, 297-306.
- van Heusden, G.P., Griffiths, D.J., Ford, J.C., Chin, A.W.T.F., Schrader, P.A., Carr, A.M., and Steensma, H.Y. (1995). The 14-3-3 proteins encoded by the BMH1 and BMH2 genes are essential in the yeast *Saccharomyces cerevisiae* and can be replaced by a plant homologue. *Eur J Biochem* 229, 45-53.
- von Arnim, A.G., and Deng, X.W. (1994). Light inactivation of Arabidopsis photomorphogenic repressor COP1 involves a cell-specific regulation of its nucleocytoplasmic partitioning. *Cell* 79, 1035-1045.
- Wang, H., Kang, D., Deng, X.W., and Wei, N. (1999). Evidence for functional conservation of a mammalian homologue of the light-responsive plant protein COP1. *Curr Biol* 9, 711-714.
- Wang, Y., Jacobs, C., Hook, K.E., Duan, H., Booher, R.N., and Sun, Y. (2000). Binding of 14-3-3beta to the carboxyl terminus of Wee1 increases Wee1 stability, kinase activity, and G2-M cell population. *Cell Growth Differ* 11, 211-219.

- Waterman, M.J., Stavridi, E.S., Waterman, J.L., and Halazonetis, T.D. (1998). ATM-dependent activation of p53 involves dephosphorylation and association with 14-3-3 proteins. *Nat Genet* 19, 175-178.
- Wei, N., Chamovitz, D.A., and Deng, X.W. (1994). Arabidopsis COP9 is a component of a novel signaling complex mediating light control of development. *Cell* 78, 117-124.
- Wei, N., and Deng, X.W. (1998). Characterization and purification of the mammalian COP9 complex, a conserved nuclear regulator initially identified as a repressor of photomorphogenesis in higher plants. *Photochem Photobiol* 68, 237-241.
- Wei, N., and Deng, X.W. (1999). Making sense of the COP9 signalosome. A regulatory protein complex conserved from Arabidopsis to human. *Trends Genet* 15, 98-103.
- Wei, N., Tsuge, T., Serino, G., Dohmae, N., Takio, K., Matsui, M., and Deng, X.W. (1998). The COP9 complex is conserved between plants and mammals and is related to the 26S proteasome regulatory complex. *Curr Biol* 8, 919-922.
- Wertz, I.E., O'Rourke, K.M., Zhang, Z., Dornan, D., Arnott, D., Deshaies, R.J., and Dixit, V.M. (2004). Human De-etiolated-1 regulates c-Jun by assembling a CUL4A ubiquitin ligase. *Science* 303, 1371-1374.
- Wilker, E.W., Grant, R.A., Artim, S.C., and Yaffe, M.B. (2005). A structural basis for 14-3-3sigma functional specificity. *J Biol Chem* 280, 18891-18898.
- Yaffe, M.B., Rittinger, K., Volinia, S., Caron, P.R., Aitken, A., Leffers, H., Gamblin, S.J., Smerdon, S.J., and Cantley, L.C. (1997). The structural basis for 14-3-3:phosphopeptide binding specificity. *Cell* 91, 961-971.
- Yang, H.Y., Wen, Y.Y., Chen, C.H., Lozano, G., and Lee, M.H. (2003). 14-3-3 sigma positively regulates p53 and suppresses tumor growth. *Mol Cell Biol* 23, 7096-7107.

- Yang, H.Y., Wen, Y.Y., Lin, Y.I., Pham, L., Su, C.H., Yang, H., Chen, J., and Lee, M.H. (2007). Roles for negative cell regulator 14-3-3sigma in control of MDM2 activities. *Oncogene* 26, 7355-7362.
- Yang, J., Xu, Z.P., Huang, Y., Hamrick, H.E., Duerksen-Hughes, P.J., and Yu, Y.N. (2004). ATM and ATR: sensing DNA damage. *World J Gastroenterol* 10, 155-160.
- Yi, C., Wang, H., Wei, N., and Deng, X.W. (2002). An initial biochemical and cell biological characterization of the mammalian homologue of a central plant developmental switch, COP1. *BMC Cell Biol* 3, 30.
- Yoneda-Kato, N., Tomoda, K., Umehara, M., Arata, Y., and Kato, J.Y. (2005). Myeloid leukemia factor 1 regulates p53 by suppressing COP1 via COP9 signalosome subunit 3. *Embo J* 24, 1739-1749.
- Zha, J., Harada, H., Yang, E., Jockel, J., and Korsmeyer, S.J. (1996). Serine phosphorylation of death agonist BAD in response to survival factor results in binding to 14-3-3 not BCL-X(L). *Cell* 87, 619-628.
- Zhang, L., Wang, H., Liu, D., Liddington, R., and Fu, H. (1997). Raf-1 kinase and exoenzyme S interact with 14-3-3zeta through a common site involving lysine 49. *J Biol Chem* 272, 13717-13724.
- Zippo, A., De Robertis, A., Serafini, R., and Oliviero, S. (2007). PIM1-dependent phosphorylation of histone H3 at serine 10 is required for MYC-dependent transcriptional activation and oncogenic transformation. *Nat Cell Biol* 9, 932-944.

VITA

Chun-Hui Su was born in Hsinchu, Taiwan on February 26th, 1979, the daughter of Shein-Rong Su and Shan-Hsiu Liu. She received her Bachelor in Agriculture Chemistry from the National Taiwan University in June 2001. She worked as a research assistant under Dr. Che-Kun James, Shen in the Institute of Molecular Biology, Academia Sinica from August 2001 to August 2002. In September 2002, she was enrolled in the National Chiao Tung University, Department of Biological Science and Technology, where she majored in Biomedical Science under Dr. Chih-Sheng Lin and received the degree of Master in June 2004. She worked as a research assistant under Dr. Wei-Yuan Chow in the National Tsing Hua University, Institute of Molecular and Cellular Biology from July 2004 to July 2005. In August 2005 she entered the University of Texas Health Science Center at Houston, Graduate School of Biomedical Sciences and completed her thesis at Dr. Mong-Hong Lee's laboratory in the Department of Molecular and Cellular Oncology at the M.D. Anderson Cancer Center, Houston, Texas.